Proceedings of the Institute of Acoustics

IDENTIFICATION OF REVERBERATION AUTOREGRESSIVE MODEL AND PREDICTOR BASED ON HYDROACOUSTIC SIGNAL ENVELOPE

E. Hermanowicz and M. Rojewski

Telecommunication Institute, Technical University of Gdańsk
Majakowskiego 11/12, PL 80-952 Gdańsk

ABSTRACT - The paper concerns the identification problem of autoregressive (AR) model as well as the linear prediction and fast start-up equalization of reverberations in specific situation when only the envelope of the echo signal is at disposal. Such a necessity often occurs in underwater communication and location by sonar. The method of phase recovering is developed based on the idea of Hilbert's minimum-phase demodulate as a complex representation of narrowband signal. The discussion of estimating the AR parameters by covariance matrix approach is also given, namely: Cholesky factorization and Makhoul covariance-lattice method.

INTRODUCTION

This paper concerns the identification problem of autoregressive (AR) modelling of reverberations i.e. a special kind of interferences caused by multipath scattering or undesirable multiple reflections occuring in underwater communication and location. Our research refers to particular situation when only the envelope of echo-signal is at disposal. It is assumed that the features of the reverberation process are varying slowly. Thus the possibility of prediction results, which in turn allows to advance the intelligibility and reliability of underwater communication and the performance of location and target recognition as well.

The AR model identification is equivalent to optimal prediction error filter (PEF) or linear predictor synthesis [1,2,3,9]. The linear predictor is used with the aim of reverberation rejection / suppression. On the PEF basis the fast start-up equalizer [4] for received signal enhancement is obtained.

The concept of phase reconstruction is deduced from the idea of Hilberts so called minimum-phase demodulate as complex representation of narrowband signal. The minimum-phase demodulate is unique among all Hilbertian signals of the same bandwidth and identical envelope shape. The properties of such a demodulate are: i/ fastest increase of energy density spectrum integral, ii/ univocal envelope-phase relationship, iii/ improvement possibility of numerical ill-conditioning caused by oversampling.

The paper organization is as follows. First, phase recovery method refering to the complex minimum sampling rate representation of narrowband signal is advanced. Second, on the basis of minimum-phase demodulate digital filter parameters, namely prediction and reflection coefficients of both: transversal and lattice PEF structures are estimated by the covariance matrix approach aimed at nonstationarity. Later on, prediction coefficients are exploited to estimate high-resolution (maximum entropy) power density spectrum [7] of reverberations, while reflection coefficients are treated as distinctive features [8] for different kinds of reverberations. Finally, both PEF structures are used to set the above mentioned equalizer, which effects in deconvolution of useful signal and reverberation.

MOTIVATION

The majority of modern underwater systems tend towards "complex digitization" of signal as close to the receiver input as possible. Precise complex representation of a real bandpass signal is obtained usually by sampling both of real components of complex envelope. A complex series $\{w(n)\}$ produced in such a manner is, after [5] called demodulate. Demodulate contains complete information about the real signal represented by it&constitutes the data for sonar digital signal processing. On the contrary, the signal proportional to the instantaneous target strength is used as the input data in the former generation analog system processing. Such a representation generally apears to be nonunivocal and the instant phase is needed for both demodulate components recovery.

MINIMUM-PHASE DEMODULATE RECONSTRUCTION- -GENERAL OUTLINE AND IMPLEMENTATION APPROACH

Conventionally, a real bandpass signal $\{x(n)\}$ can be treated as the real component of a complex signal $\{u(n)\}$

$$x(n)=\mathrm{Re}\,u(n) \tag{1}$$

$$u(n)\triangleq|u(n)|\exp[j\arg u(n)]=\mathrm{Re}u(n)+j\mathrm{Im}u(n). \tag{2}$$

If the Cartesian components of $\{u(n)\}$ constitute the pair of Hilbert transforms

$$\{\mathrm{Re}u(n)\}\underset{H^{-1}}{\overset{H}{\rightleftharpoons}}\{\mathrm{Im}u(n)\} \tag{3}$$

then (2) is named Hilbertian signal. Its polar components: $\{v(n)\}$ and $\{\psi(n)\}$, where

$$v(n)\triangleq|u(n)|=\left\{[\mathrm{Re}u(n)]^2+[\mathrm{Im}u(n)]^2\right\}^{1/2} \tag{4}$$

$$\psi(n)\triangleq\arg u(n)=\mathrm{arccot}[\mathrm{Re}u(n)/\mathrm{Im}u(n)]+k\pi\,;\quad k=0,\pm1,\pm2,\ldots \tag{5}$$

are named: envelope and instantaneous phase of $\{x(n)\}$ or $\{u(n)\}$, respectively. H and H^{-1} in (3) denote forward and inverse Hilbert transforms of corresponding impulse responses

$$h(n)\triangleq[1-(-1)^n]/(\pi n);\quad n=0,\pm1,\pm2,\ldots \tag{6}$$

$$h^{(-1)}=h(-n)=-h(n);\quad n=0,\pm1,\pm2,\ldots \tag{7}$$

and freguency responses

$$H(e^{j\omega})=\begin{cases} j, & 0<\omega<\pi \\ -j, & -\pi<\omega<0 \\ 0, & \omega=0 \text{ and } \omega=\pi \end{cases} \tag{8}$$

$$H^{-1}(e^{j\omega})=H^*(e^{j\omega})=-H(e^{j\omega}) \tag{9}$$

where asterrisk denotes complex conjugate. If Hilbertian signal polar components i.e. logenvelope $\{\ln v(n)\}$ and instantaneous phase $\{\psi(n)\}$ are the Hilbert transform pair, with the accuracy to an additive constant,

$$\{\ln v(n)\}\underset{H^{-1}}{\overset{H}{\rightleftharpoons}}\{\psi(n)\} \tag{10}$$

then the signal can be called minimum-phase demodulate and denoted as $\{w_{mp}(n)\}$, where

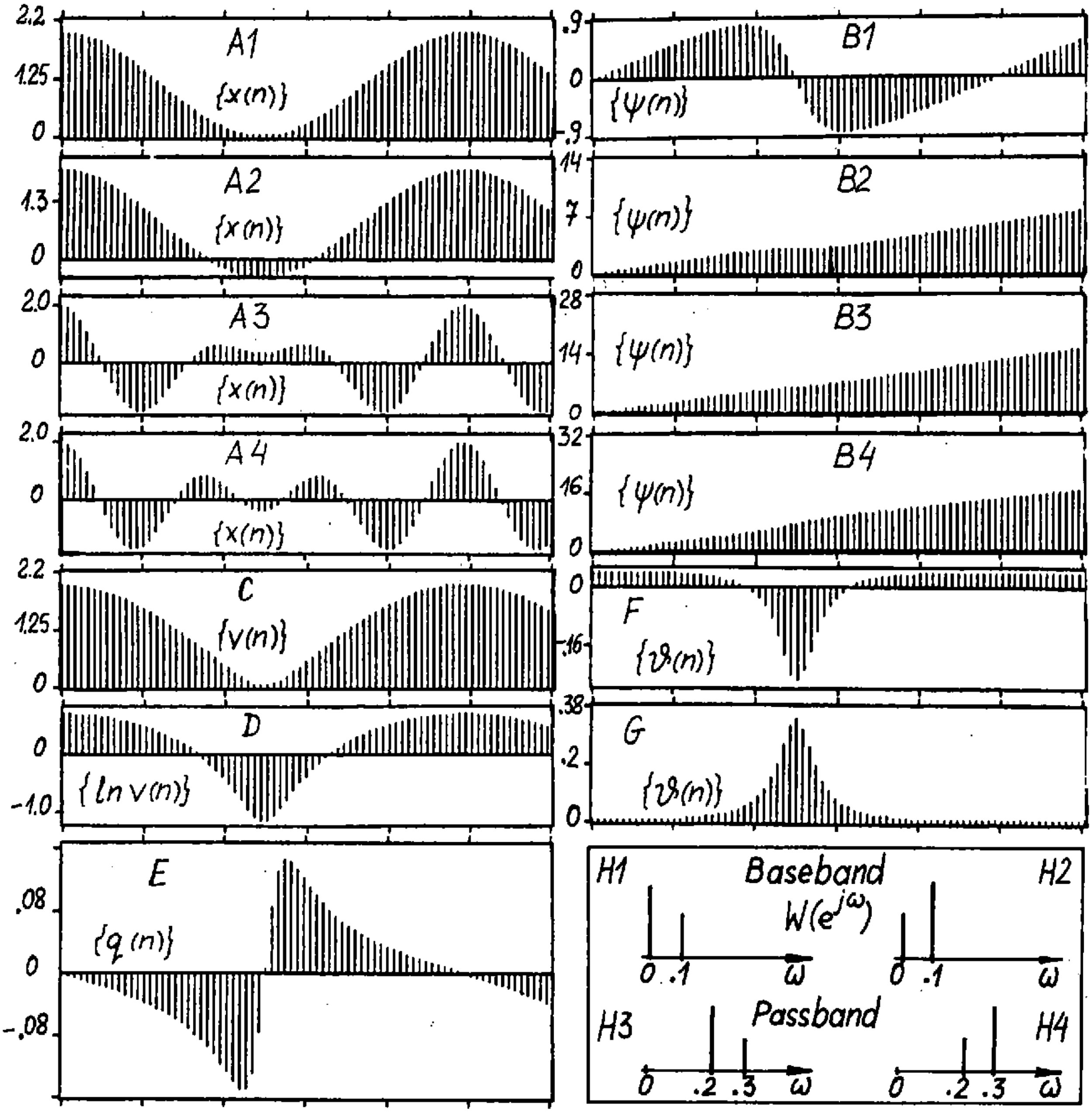

Fig.1. Four examples (A) of biharmonic signal $\{x(n)\} = \{(1+\alpha)\cos\omega_1 n + (1-\alpha)\cos\omega_2 n\}$; $\alpha \in (0,1)$, $0 \leq \omega_1 < \omega_2 < \pi$ with $\alpha = 0.116$ (A1,A3); $\alpha = -0.116$ (A2,A4), its instantaneous phase $\{\psi(n)\}$ (B), common: envelope $\{v(n)\}$)C), logenvelope $\{\ln v(n)\}$ (D) and difference derivative $\{q(n)\}$ (E), instantaneous frequency $\{\vartheta(n)\}$ for minimum - (F) and nonminimum-phase (G), spectra of above signals $W(e^{j\omega})$ (H). Numerical indices depict the correspondence between waveforms and spectra. Note, B1& D as well as E&F are the pairs of (10) or (12) type, hence B1 is $\{\varphi_{mp}(n)\}$ and A1 & A3 are minimum-phase signals.

$$w_{mp}(n) \triangleq v(n)\exp\left[j\,\varphi_{mp}(n)\right] \tag{11}$$

The average component of instantaneous phase $\{\varphi_{mp}(n)\}$ is zero implying the minimum-phase demodulate to be baseband as well as Hilbertian right-singleband waveform. Spectrum $W_{mp}(e^{j\omega})$ of such a demodulate adhers to the right side of coordinate origin. Energetically dominating "components" of $W_{mp}(e^{j\omega})$ group themselves at frequencies as low as it is permitted by envelope shape invariability. These properties are illustrated by Fig.1. Worth noting, that the minimum-phase demodulate is the unique and distinctive for the whole class of equiband and common envelope $\{v(n)\}$ signals. Each minimum-phase signal having the envelope $\{v(n)\}$ i.e. such a signal for which the difference derivative $\{q(n)\}$ of logenvelope and the instantaneous frequency variable component $\{\vartheta(n)\}$ are the Hilbert transform pair

$$\{q(n)\} \underset{H^{-1}}{\overset{H}{\rightleftharpoons}} \{\vartheta(n)\}, \tag{12}$$

can be expressed by the minimum-phase demodulate as

$$u_{mp}(n;\alpha_0,\varphi_0,\bar{\omega}) \triangleq \alpha_0 w_{mp}(n)\exp j(\varphi_0+n\bar{\omega}) = \alpha_0 v(n)\exp\left\{j\left[\varphi_0+n\bar{\omega}+\varphi_{mp}(n)\right]\right\} \tag{13}$$

where

$$q(n) \triangleq \ln v(n)-\ln v(n-1) \tag{14}$$

$$\vartheta(n) \triangleq \omega(n)-\bar{\omega} \tag{15}$$

$$\omega(n) \triangleq \psi(n)-\psi(n-1) = \vartheta(n)+\bar{\omega} \tag{16}$$

and $\bar{\omega}\in[0,\pi)$ is the average component of instantaneous frequency, $\varphi_0\in(-\pi,\pi)$ - the initial phase and $\alpha_0\in(0,\infty)$ - the constant gain.

Now, the rules of minimum-phase signal reconstruction on the basis of real envelope $\{v(n)\}$ can be formed as follows. The instantaneous phase $\{\varphi_{mp}(n)\}$ of minimum-phase demodulate can be obtained via convolution of logenvelope $\{\ln v(n)\}$ and impulse response $\{h(n)\}$ (6)

$$\varphi_{mp}(n) = \sum_{m=-\infty}^{\infty} h(n-m)\ln v(m) = \frac{1}{\pi}\sum_{\substack{m=-\infty \\ m\neq n}}^{\infty} \frac{1-(-1)^{n-m}}{n-m}\ln v(n) \tag{17}$$

Similarly, the instantaneous frequency variable component $\{\vartheta_{mp}(n)\}$ for optional minimum-phase signal reconstruction i.e.

$$\vartheta_{mp}(n) \triangleq \varphi_{mp}(n)-\varphi_{mp}(n-1) \tag{18}$$

can be computed as the convolution sum of $\{\ln v(n)\}$ and $\{k(n)\}$

$$\vartheta_{mp}(n) = \sum_{m=-\infty}^{\infty} k(n-m)\ln v(m) = \sum_{\substack{m=-\infty \\ n\neq m,m+1}}^{\infty}\left[\frac{1(-1)^{n-m}}{n-m} - \frac{1-(-1)^{n-m-1}}{n-m-1}\right]\ln v(n) \tag{19}$$

where

$$k(n) \triangleq \frac{1}{\pi}\left[\frac{1-(-1)^n}{n}\ \frac{1-(-1)^{n-1}}{n-1}\right] \ ; \ n=0,\pm1,\pm2,\ldots \tag{20}$$

is the impulse response of cascade: differenting block and Hilbert transformer. The frequency response of such a cascade is

$$K(e^{j\omega}) = \begin{cases} j(1-\exp(-j\omega)), & -\pi<\omega<0 \\ 0, & \omega=0, \omega=\pi \\ -j(1-\exp(\quad j\omega)), & 0<\omega<\pi \end{cases} \tag{21}$$

Block-schemes for minimum-phase demodulate and for optional minimum-phase signal recovery are presented in Fig.2 and Fig.3.

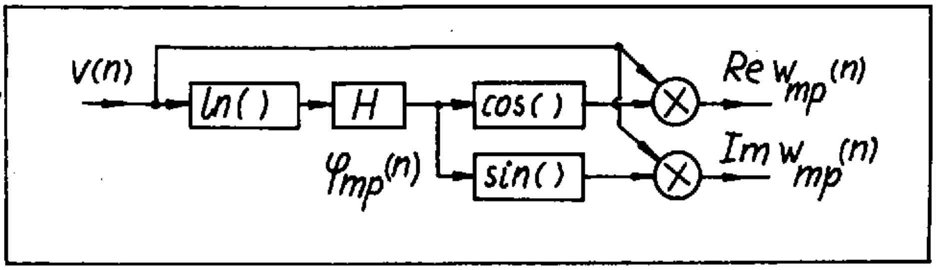

Fig.2. Functional block-scheme for the recovery of minimum-phase demodulate; H-Hilbert transformer.

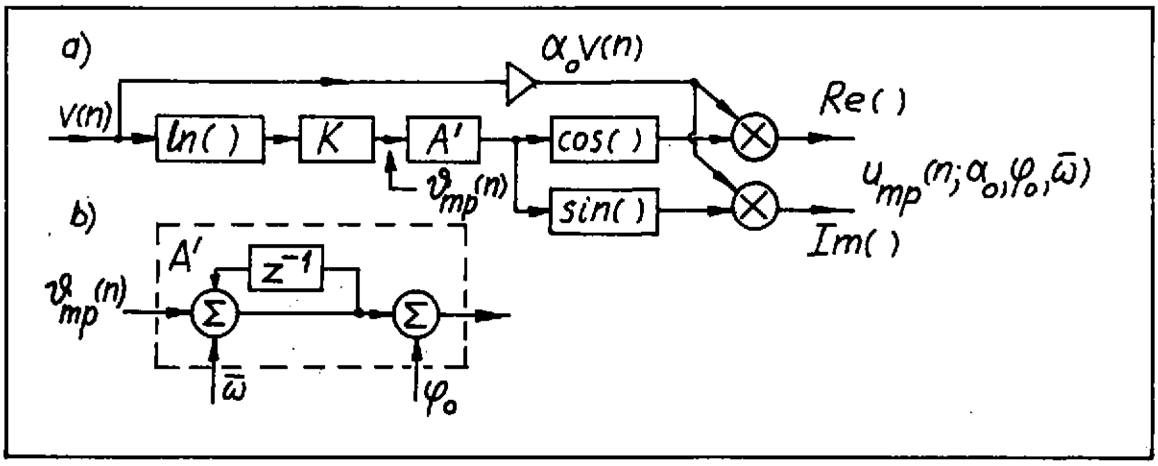

Fig.3. Functional block-scheme for the recovery of optional minimum-phase signal (a); K-cascade of differenting system and Hilbert transformer, A'- phase accumulator (b).

Two methods of processing are at disposal. Blocks H and K shown in Fig.2 and 3 can operate in frequency domain via FFT or in time domain. By the first method especially suitable to batch/ block processing, an N-element train of instantaneous phase $\{\varphi_{mp}(n)\}_0^{N-1}$ or frequency $\{\vartheta_{mp}(n)\}_0^{N-1}$ is obtained as an N-point inverse FFT of product: $H(\exp(j\omega))$ (8) with FFT of $\{\ln v(n)\}_0^{N-1}$ or $K(\exp(j\omega))$ (21) with FFT of $\{q(n)\}_0^{N-1}$ respectively

$$\{\varphi_{mp}(n)\}_0^{N-1} = FFT^{-1}\{H(e^{j2\pi k/N})FFT\{\ln v(n)\}_0^{N-1}\} \tag{22}$$

$$\{\vartheta_{mp}(n)\}_0^{N-1} = FFT^{-1}\{K(e^{j2\pi k/N})FFT\{q(n)\}_0^{N-1}\} \qquad (23)$$

In the second method suitable for on-line processing, the noncausal filters H and K posessing infinite double-sided impulse response (6) and (20) should be replaced by causal, realizable filters with finite impulse response e.g. [10]. The reconstruction of instantaneous phase for optional minimum-phase signal (13) is attained by accumulation of signal (23) or its counterpart given from time-domain filtering approach in the phase accumulator from Fig.3b. This gives the possibility of fixing the initial phase φ_0 and average frequency $\bar{\omega}$.

AR MODEL AND PREDICTION ERROR FILTER

Reverberations, as well as some other additive impairments contributed by propagational media, are frequently treated as locally stationary autoregressive process AR(M) of order M [8]. Each sample w(n) of process AR(M) is, with the accuracy $\mathcal{E}(n)$, the linear combination of M previous samples, within stationarity interval. The differential equation for AR(M) model

$$w(n)+\sum_{m=1}^{M} a_{Mm}w(n-m) = \mathcal{E}(n) \qquad (24)$$

describes the recursive transversal digital filter of taps a_{Mm}; m=1,2,...,M named linear prediction coefficients. The sequence of modelling errors $\{\mathcal{E}(n)\}$, or innovation sequence, constitutes the realization of white Gaussian noise with zero dc component. In the Fig.4 such a model is presented, also in the structure of lattice. Stages of lattice are described by complex parameters - reflection coefficients k_m; m=1,2,...,M (one reflection coefficient per one stage) with $k_M=a_{MM}$. The necessary and sufficient absolute stability constraint $|k_m| < 1$; m=1,2,...,M implies excellent numerical conditioning of the latter structure [9].

For the task of reflection coefficients estimation, the foregoing estimation of autocorrelation matrix corresponding to the actually modelled demodulate is needed. Among the well known autocorrelation matrix estimates, the covariance matrix R has been exploited. Entries of R are stated on the basis of recovered demodulate by formula [2]

$$[R]_{ki} = \sum_{n=M}^{N-1} w_{mp}(n-k)w^*_{mp}(n-i). \qquad (25)$$

This approach does not require sophisticated assumptions of stationarity inside and setting the process to zero outside the observation time. The proper adjustment to the short observation data record typical to nonstationary conditions of e.g. echo is assured in this way.

Further on, the authors attention was concentrated on two methods of reflection coefficients estimation. From among batch nonadaptive algorithms taking into consideration the nonstationarity of data, Cholesky factorization [1] and covariance-lattice method [3] were examined.

The idea of Cholesky factorization method relies on the unique decomposition of covariance matrix (25) with the object of achieving an upper triangular matrix

$$L^{-1} \triangleq \begin{bmatrix} 1 & a_{M1} & \cdots & a_{MM} \\ & 1 & \cdots & a_{M-1,M-1} \\ & & \ddots & \vdots \\ & 0 & 1 & a_{11} \\ & & & 1 \end{bmatrix} \qquad (26)$$

constructed in individual rows from the parametrs of transversal AR(m) models of all orders m=1,2,...,M. The last column in (26) encloses reflection coefficients of lattice AR(M) model: $k_1=a_{11}, k_2=a_{22}, \ldots, k_M=a_{MM}$. Moreover, the first row of (26) supplies the parametrs for the high resolution (maximum entropy) spectrum estimate [7] for the demodulate of the echo signal under examination

$$\hat{s}_w(e^{j\omega}) = \varepsilon_o^2 \left| 1 + \sum_{m=1}^{M} a_{mM} \exp(-j\omega \cdot m) \right|^{-2}; \quad \varepsilon_o^2 \triangleq [R]_{11} \qquad (27)$$

The Makhoul's covariance-lattice method is different, based on covariances (25) method to derive all the above mentioned parameters for AR(m) modelling. Its specific features are low numerical burden of model identification and lack of matrix inversion.

Reflection coefficients $\{k_m\}$ and spectrum (27) of the process being investigated are not the only aim of AR(M) model estimation. Active reverberation suppression imposes further processing including prediction and equalizing for maximization of signal to noise ratio together with useful signal deconvolution from interferences caused by hydroacoustical channel. Fig.5 represents two basic prediction error filtering structures: transversal and lattice. Noting that PEF is an inverse filter to AR model, identification of models shown in Fig.4 is equivalent to the sythesis of optimal PEF. Making a comparision between the two structures in Fig.5, the important decoupling properties of lattice-PEF should be stressed resulting in ortogonalization of backward prediction errors $\beta_m(n)$; m=0,1,...,M, as opposed to lack of such properties in transversal. In effect, the former can be extended to form

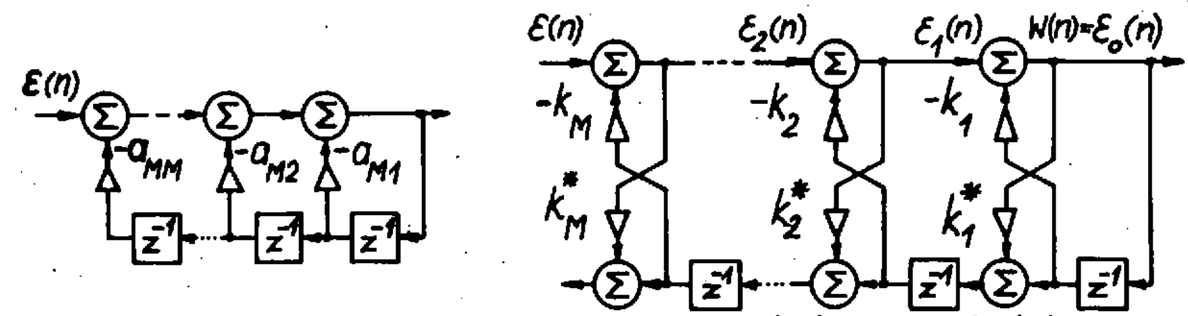

Fig.4. Transversal and lattice structures of AR(M) model; $\varepsilon_m(n)$; m=0, 1,...,M denotes m-order modelling residuals (innovations).

an optimal fast start-up equalizer [4] with additional tap coefficients $\{c_m\}$ adjusted in such a manner that the energy od error between the output $\{y(n)\}$ where

$$y(n) \triangleq \sum_{m=0}^{M} c_m \hat{\beta}_m(n) \tag{28}$$

and some finite reference signal $\{r(n)\}$ of length L; $L \leqslant M+1$ is minimized. The fast convergence of the equalizer spanned on lattice-PEF ought to be underlined owing to the possibility of tap coefficients adjustment to their optimum value in one iteration step.

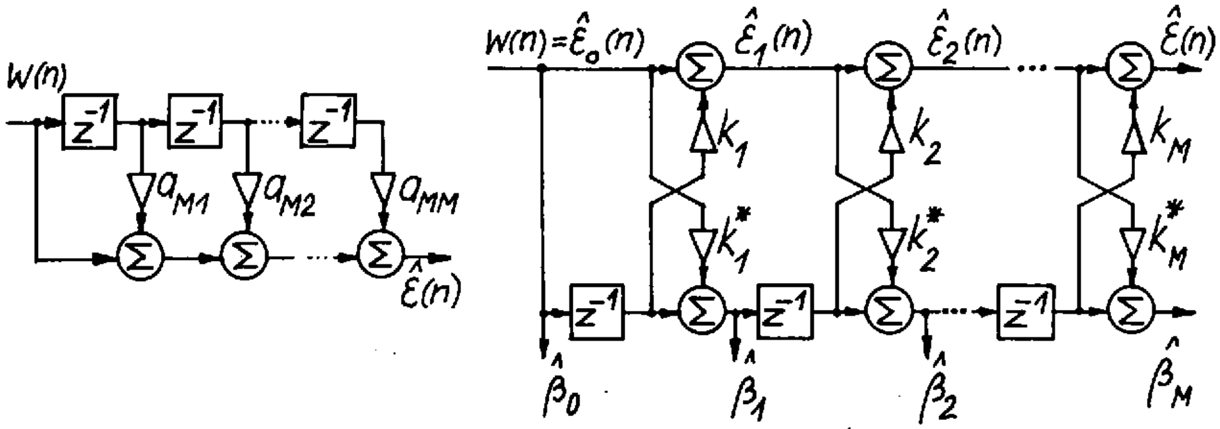

Fig.5. Transversal and lattice structures of PEF; $\hat{\mathcal{E}}_m(n)$ denotes m-th order forward prediction error, $\hat{\beta}_m(n)$ - backward.

CONCLUSION

It was the authors intention to develop the manner of mastering the model & thus the predictor as well as the fast start-up equalizer of reverberations from the position of accessibility of incomplete information about the identified signal, being contained exclusively in the echo envelope. Further investigations which have been undertaken and are actually being continued concentrate on computer programming of aforecited algorithms aimed to recognition and combatment of physical reverberations registered in Baltic.

REFERENCES

[1] Giordano A.A., Hsu F.M.: Least Square Estimation with Applications to Digital Signal Processing. J. Wiley 1985.

[2] Makhoul J.: Linear prediction. A tutorial review. Proc. IEEE, vol. 63, Apr.1975, pp.561-580.

[3] Makhoul J.: Stable and efficient lattice methods for linear prediction. IEEE Trans., vol. ASSP-25, Oct.1977, pp.423-428.

[4] Makhoul J.: A class of all-zero lattice digital filters: properties and applications. IEEE Trans.,vol.ASSP-26, Aug.1978 pp.304-314.

[5] Hasan T.: Complex demodulation, in: Brillinger D.R., Krishnaiah P.R.: Handbook of Statistics, vol.3, Elsevier 1983, pp.125-156.
[6] Haykin S.: Introduction to Adaptive filters. McMillan 1984.
[7] Haykin S. (ed.): Nonlinear Methods of Spectral Analysis. Springer 1983.
[8] Haykin S. Radar signal processing. IEEE ASSP Magazine, Apr. 1985 pp.2-18.
[9] Hönig M.L., Messerchmitt D.G.:Adaptive Filters: Structures, Algorithms and Applications. Kluwer 1984.
[10] Rabiner L.R., Gold B.: Theory and Applications of Digital Signal Processing. Prentice Hall 1975.
[11] Signal Processing. A NATO advanced study. Academic Press 1973.
[12] Voelcker H.B.: Toward a unified theory of modulation. Proc. IEEE, vol. 54, March, pp.340-353, 1966.

Proceedings of the Institute of Acoustics

COUNTERACTION OF MULTIPATH INTERFERENCE BY A COMBINATION OF BEAMSTEERING AND ADAPTIVE EQUALIZATION

Geir Helge Sandsmark (1) and Arne Solstad (2)

(1) University of Trondheim, Norwegian Institute of Technology, N-7034 TRONDHEIM, NORWAY, (2) Elektronikklaboratoriet ved NTH, N-7034 TRONDHEIM, NORWAY.

INTRODUCTION

High speed hydroacoustic data transmission are strongly interfered by multipath propagation due to reflections from the sea surface, the bottom or obstacles from offshore installations. In order to achieve bandwidth effective transmission, the communication system has to adapt itself to the current hydroacoustic channel, thus rejecting the multipath interference or compensate for it. Adaptive beamforming is an example of the rejection technique while equalization is a compensation technique. By being different in nature these techniques offers partly complementary qualities thereby fitting well in a combined system. This paper presents simulation results showing the performance of a combined system and how the two described techniques supplement each other in combating the multipath propagation interference.

THE IMPACT OF ADAPTIVE BEAMFORMING AND ADAPTIVE EQUALIZATION ON THE CHANNEL IMPULSE RESPONSE

Beamforming/beamsteering

As described in the previous section, reflections from surface, bottom and in-sea obstacles may cause the transmitted signal to reach the receiver via different paths. These rays will usually approach the receiver from different angles. It is therefore possible to attenuate some of these unwanted signals by applying a narrow transducer beam directed towards the direct path.

When applying a simple tracking algorithm [1, 6] together with traditional beamforming [2] unwanted signals (including multipath signals and noise sources) outside the main lobe are attenuated according to the side-lobe level at the actual angle of incidence. Further suppression are possible by using Widrow's side-lobe canceller [3] or an optimum beamforming method [2, 4, 5].

An interesting aspect of the beamforming technique is revealed by observing a relation between incidence angle and propagation delay. This is illustrated in Fig. 1.

The longest possible path from transmitter to receiver via one single reflector within the joint area is the route via one of the area borders. Consequently the longest delay relative to the direct path depends heavily upon receiver and transmitter beamwidths. By simplifying the channel impulse response to consist only of the direct path together with single reflector paths within the joint area, this also gives a limit of impulse response duration.

From the figure we calculate the delay difference between the direct path and the maximum delayed path as

$$\Delta\tau_{max} = \frac{l_1 + l_2 - r}{c} = \frac{r}{c}\,\frac{\sin\frac{\varphi_1}{2} + \sin\frac{\varphi_2}{2} - \sin(\frac{\varphi_1+\varphi_2}{2})}{\sin(\frac{\varphi_1+\varphi_2}{2})} \tag{1}$$

COUNTERACTION OF MULTIPATH INTERFERENCE BY A COMBINATION OF BEAMSTEERING AND ADAPTIVE EQUALIZATION

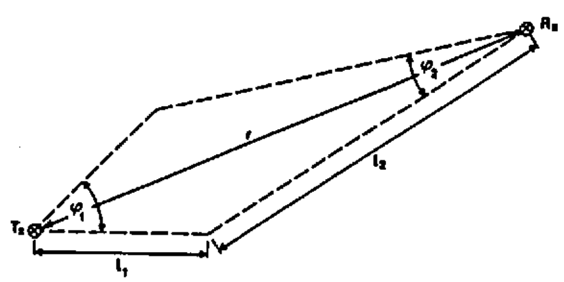

Figure 1. Geometry of area covered by transmitter and receiver mainlobes.

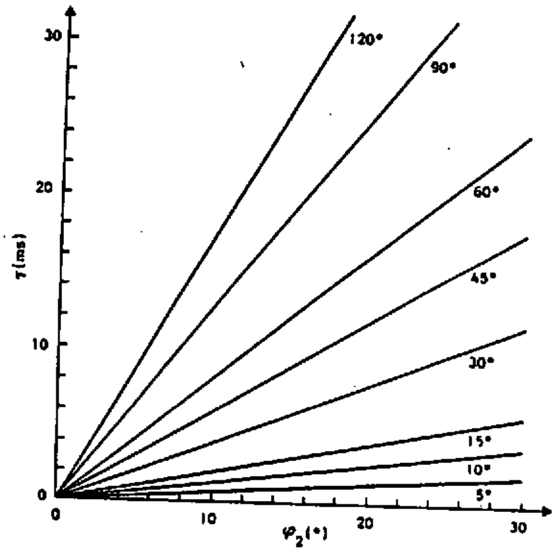

Figure 2. Delay difference as a function of transducer beamwidth.

where c is the sound speed in sea water.

Fig. 2 depicts the maximum delay difference as a function of beamwidths at 500 m distance between the transducers.

From this we deduce that the impulse response duration may be forced as small as wanted by making narrow transducers.

Now installation and alignment of the transducers may become difficult. The receiver transducer may be controlled automatically by some beam steering algorithm thus allowing fairly narrow beams. However, the tracking requirements increase with decreasing beamwidth and practical considerations also limits the possibility to manufacture transducers with mainlobe width less than about 5°. Of course the transmitter transducer also allows for automatic alignment but this will require some kind of signalling from the receiver. In addition the transmission delays will limit the tracking capability of such a system. When using no kind of steering of the transmitting transducer, the width of the main lobe will limit the area of operation. A beamwidth of 60° is considered as a practical choice. Now returning to Fig. 2 this gives a maximum impulse response duration of about 4 ms. That is 40 symbol intervals when transmitting symbols at rate 10 kHz (20 kbits/s with 4 PSK modulation). During operations near bottom or in between structures, reflectors may very well appear within the area covered by the mainlobes of both transducers. Thus some intersymbol interference is likely to be present in the received signal. This motivates the use of an adaptive equalizer together with the transducer system.

<u>Adaptive equalization</u>
While the narrow beam transducer prevents intersymbol interference by attenuation of auxiliary paths, the equalizer attempts to compensate for the resulting channel transfer function.

COUNTERACTION OF MULTIPATH INTERFERENCE BY A COMBINATION OF BEAMSTEERING AND ADAPTIVE EQUALIZATION

Assume the following model of the received signal

$$y(t) = \underline{h}_N^H \, \underline{d}_N(t) + n(t) \tag{2}$$

where $y(t)$ is received signal sample at time t, $\underline{h}_N$ is the $N\times1$ Channel impulse response vector and $\underline{d}_N(t)$ is the vector of the N last transmitted data symbols, $n(t)$ is an additive white noise term. Superscript H means Hermitian transpose.

$$\underline{h}_N = [h_0, h_1, \dots h_{N-1}]^T \tag{3}$$

$$\underline{d}_N(t)[d(t), d(t-1), \dots d(t-N+1)]^T \tag{4}$$

Now let

$$\underline{y}_L(t) = [y(t), y(t-1), \dots y(t-L+1)]^T \tag{5}$$

Then

$$\underline{y}_L(t) = \underline{H}_{M,L}^H \, \underline{d}_M(t) \tag{6}$$

where

$$H_{M,L} = \begin{bmatrix} \underline{h}_N & 0 \dots\dots & 0 \\ 0 & \underline{h}_N & \cdot \\ \cdot & 0 & 0 \\ \cdot & \cdot & \underline{h}_N \\ \cdot & \cdot & 0 \\ \cdot & \cdot & \cdot \\ 0 & 0 & 0 \end{bmatrix} \tag{7}$$

is the MxL matrix of Toeplitz structure constructed as described in Eq. (7).

With these signal definitions we turn to the well known normal equation [4] to calculate the optimum equalizer impulse response vector $\underline{W}_K$.

$$\underline{W}_K = [E(\underline{y}_K(t) \, \underline{y}_K^H(t))]^{-1} \, E(\underline{y}_K(t) \, d^*(t-T)) \tag{8}$$

$$\underline{W}_K = (\underline{H}_{M,K}^H \, \underline{H}_{M,K} + \sigma^2 I)^{-1} \, \underline{H}_{M,L}^H \begin{bmatrix} 0 \\ \vdots \\ 1 \\ \vdots \\ 0 \end{bmatrix} \tag{9}$$

where σ^2 is the noise variance, and $\underline{I}$ is the unity matrix.

The remaining interference is given by

$$\varepsilon = 1 - \underline{W}_K^H \; E(y_K(t)\; d^*(t)) \tag{10}$$

$$\varepsilon = 1 - \underline{W}_K^H \; \underline{P}_K \tag{11}$$

where

$$\underline{P}_K = \underline{H}_{M,L}^H \begin{bmatrix} 0 \\ \cdot \\ 0 \\ 1 \\ 0 \\ \cdot \\ 0 \end{bmatrix} \tag{12}$$

When increasing the equalizer order K, ε asymptotocally approaches a value slightly greater than σ^2.

SIMULATION PRELIMINARIES

Channel model

The channel model for high frequency underwater data communication is based on a ray-tracing model, and includes the most important phenomena in underwater acoustic transmission. The modelled phenomena are sound refraction due to vertical sound velocity variation, reflections from the sea floor and from the surface, diffuse reflection due to surface waves and finally the surface motion. Various types of transducer diagrams can be modelled. Single element transducers as well as line arrays are available. The bottom is considered plane and horizontal, given by its sound speed and density. Thus, the reflection coefficient is complex, and depends on the angle of incidence. The channel model is designed to investigate point to point transmission conditions and utilizes a dedicated direction algorithm to find the possible ray paths from transmitter to receiver. The sound speed variation is described by a piecewise linear velocity gradient.

Surface reflection. The direction algorithm computes the possible ray paths from transmitter to receiver when the transmission channel is bounded by the plane bottom and a plane ocean surface. A rough surface, given by a surface function $S(x,t)$, changes the surface reflected sound characteristics. The surface function is split into two parts, the large scale wave function, and the corrugation function. The wave function is modelled as a sum of sinusoids with variable frequencies and amplitudes. This time dependent function makes specularly reflected ray paths possible via a number of surface segments, each path carrying limited energy.

The corrugation function is stochastic, and represents small capillary waves on the surface. In our model, the corrugation function is not time dependent. The mean wave amplitude of this function should be less than one sound wavelength. These capillary waves cause the occurance of diffuse surface reflections. The resulting pressure of the surface reflected sound at the receiver is found by a surface integration of incident sound pressure compensated in amplitude and phase due to variations in propagation range, surface angle, incident angle, reflection angle, transducer directivities, etc. The following algorithm describes how the integration is performed. The ray path is known through the specular reflection point of the plane surface case. Now, the surface is divided into a number of segments which are short enough to be considered plane. Ray paths are traced via some of these segments. The number of paths depends on the wavelengths of the surface wave. The first segments computed are those nearest the specular point. Surface segments further away are then successively included, until the pressure contribution is negligible.

Channel data

During our work, we have put some effort in investigating how the channel parameters influence the transmission conditions. The channel simulations done in this context represent typical transmission channels for ROV - surface communication. The horizontal range is varied to achieve a set of different channels.

Channel parameters:

Sea depth	: 50 m	Salinity	: 35 o/oo
Bottom sound velocity	: 2500 m/s	Bottom density	: 3000 kg/m^3
Wave function	: A = 0 m	Capillary wave	: σ = 1 mm
Carrier frequency	: 150 kHz	Transmitted effect	: 10 W
Transmitter depth	: 47 m	Transmitted beamwidth	: 60 deg.
Receiver depth	: 5 m	Receiver beamwidth	: 10 deg.
Bandwidth	: 1 kHz and 10 kHz		
Horizontal range	: 100 m/150 m/200 m		

Velocity gradient:

Winter gradient taken by M/K Simrad near Horten, Norway, 24.11.1986, 14:00, and approximated to a piecewise linear function. The gradient is shown in Fig. 3.

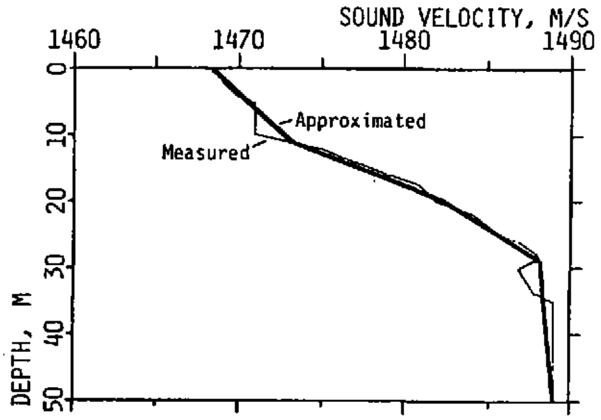

Figure 3. Sound velocity profile.

The receiver transducer with beamwidth 10 deg. points along the ray path from the trasmitter while the transmitter transducer is centered about the horizontal plane. The two transducer diagrams are quite simple. The main lobe level is constant as is the side lobe level with 20 dB attenuation. Because of this simplified model, the conditions stay constant for receiver beamwidths from 5 to 15 degrees, since the number of different ray paths inside the main lobes remains the same.

COUNTERACTION OF MULTIPATH INTERFERENCE BY A COMBINATION OF BEAMSTEERING AND ADAPTIVE EQUALIZATION

Resulting impulse response

An example of a simulated impulse response is showed in Fig. 5 a-b. This curve shows the module of the complex impulse response. The horizontal range of the case is 150 m. The bandwidths are 1 kHz (a) and 10 kHz (b). The shape of the curves is characterized by the different ray path arrivals. In the 150 m case, the delay of the directly transmitted signal is 105.5 ms. The bottom reflection arrives at 106.1 ms, the surface reflection at 107.2 ms, and the bottom/surface (BS) reflected ray at 108.6 ms. Because of the plane surface and the very small capillary wave, the surface reflections appear to be quite distinct. The next group of paths arrives at about 145 ms and contains the SB, SBS, BSB and BSBS rays. The SBSB, SBSBS, BSBSB and BSBSBS arrive at approx. 195-200 ms, and the last important group of rays, those that have crossed the sea depth seven times, give its contribution at 250-260 ms. Further multiple reflections are neglected by the model program because of low energy. The distinct peaks are followed by exponentially decaying tails which are typical for the diffuse reflections. The shorter the horizontal range, the larger is the time spacing between the ray groups, but the multiple reflections are more heavily attenuated relative to the direct sound.

SIMULATION RESULTS

We shall now examine the results from a simulation example. Block diagram of the simulations are given in Fig. 4.

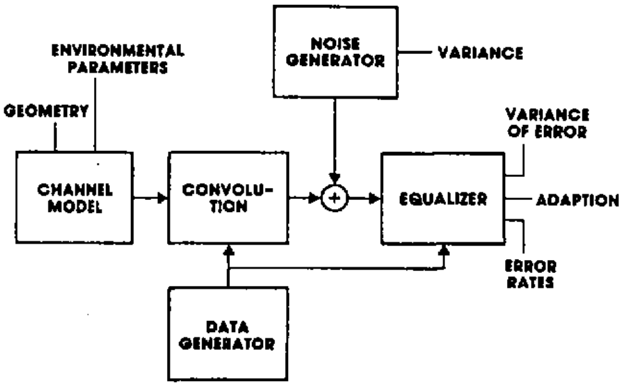

Figure 4. Block diagram of simulation system.

The horisontal distance is varied between 100 m and 200 m. This variation will only affect the impulse response and not the signal to noise ratio as the channel simulation produces noise free signals to which noise is added afterwards. Similarly the receiver beamwidth is varied between 5^{o} and 15^{o}. Also this variation is done without affecting the signal to noise ratio.

The transmitter beamwidth and center direction are chosen in a manner which sites both the direct path and the bottom reflection within the transmitter transducer main lobe. This is done to produce a "difficult" channel.

Fig. 5 shows the resulting impulse response at 150 m horisontal distance. The receiver beamwidth does not affect the channel very much. This is due to the special geometry. That is, there are no significant signal contributions approaching the receiver in the intervalls between $\pm 2.5^{o}$ to $\pm 7.5^{o}$ relative the beam axis. The strong bottom reflection thus reaches the receiver at an

COUNTERACTION OF MULTIPATH INTERFERENCE BY A COMBINATION OF BEAMSTEERING AND ADAPTIVE EQUALIZATION

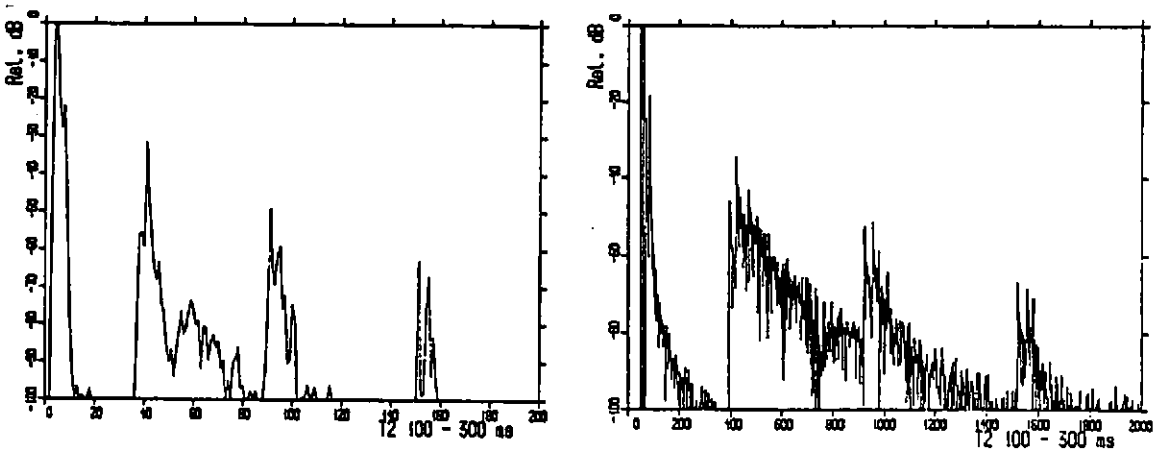

a) Bandwidth 1 kHz. b) Bandwidth 10 kHz

Figure 5. Resulting impulse response at 150 m horizontal distance and receiver beamwidth 15°.

incident angle less than 2.5° away from the direct signal path.

Now turning to equalizer performance. Fig. 6 shows the theoretical calculated mean square error at the output of an adaptive equalizer for orders between 50 and 300 and at different signal to noise ratios.

This is a result of applying Equations (8) - (12) to the simulated channel impulse response. We observe that the curve converges to a value slightly greater than the actual noise variance. The convergence appears for smaller order values when decreasing the signal to noise ratio. We also note that for S/N = 30 dB or poorer, an equalizer of order 80 is appropriate to reach the optimum performance.

Fig. 7 shows the learning characteristics of the stochastic gradient lattice equalizer [7, 8]. As noticed, the asymptotic mean square error is about 3 dB above the theoretical value. This is due to the noise caused by fluctuations of the equalizer coefficients.

Finally we present detection performance of the receiver with and without the adaptive equalizer. These results are presented in Table 1.

We notice that the error rates obtained from noise-free transmission through the channel are unacceptable for communication. On the contrary, by adding the adaptive equalizer to the system, the bit error rates turns considerably lower and allows for reliable transmission. This confirms that even with a narrow beam (5°) receiver transducer multipath propagation may introduce severe intersymbol interference. Further it is shown that by including adaptive equalization reliable communication is still achievable.

COUNTERACTION OF MULTIPATH INTERFERENCE BY A COMBINATION OF BEAMSTEERING AND ADAPTIVE EQUALIZATION

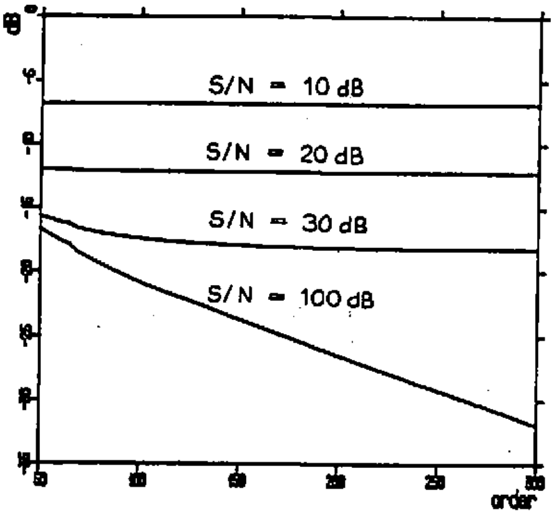

Figure 6. Minimum mean square error versus order.

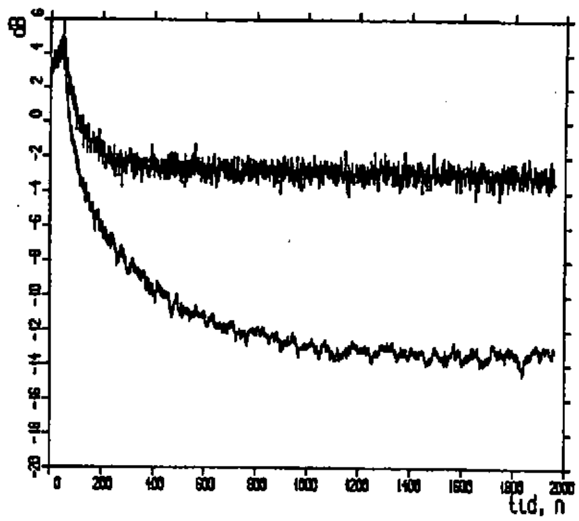

Figure 7. Learning characteristics of the stochastic gradient lattice equalizer.

Table 1. Error rate measured for different channels

a) Noise-free transmission without equalizer

Horizontal distance	Receiver beamwidth	Bit error rate
150 m	15^{0}	0,25
150 m	10^{0}	0,25
200 m	10^{0}	0,12

b) Simulations applying equalizer

Horisontal distance	Receiver beamwidth	S/N	Bit error rate
150 m	15^{0}	20 dB	$1,6\ 10^{-4}$
150 m	10^{0}	20 dB	$1,6\ 10^{-4}$
200 m	10^{0}	10 dB	0,0046
200 m	10^{0}	20 dB	$1,6\ 10^{-4}$
200 m	10^{0}	30 dB	0

CONCLUSION

This paper has pointed out potential features of a digital coherent receiver consisting of an adaptively steered antenna feeding an adaptive equalizer. Because a narrow beam transducer array causes shortening of the impulse response duration, an adaptive equalizer of moderate length will yield good receiver performance. It is also shown that even a receiver beamwidth of 5^{0} may allow severe multipath interference. Thus the combined system offers potential advantages for a high bitrate link between a ROV and a surface vessel. Especially during operations near the sea floor or in between offshore installations are situations likely to appear where simpler systems capitulate while the described system still renders a good connection.

COUNTERACTION OF MULTIPATH INTERFERENCE BY A COMBINATION OF BEAMSTEERING AND ADAPTIVE EQUALIZATION

ACKNOWLEDGEMENTS

Thanks to Mr. K. Rimstad for programming of the Equalizer Algorithm.
Special thanks to A.B. Bodsberg and G.U. Kjærland for typing the manuscript.

REFERENCES

[1] J.S. Collins, J.L. Galloway & M.R. Balderson: "Auto aligning system for narrow band acoustic telemetry". Conf. rec. Oceans '85, San Diego, 1985.

[2] R.A. Monzingo & T.W. Miller: "Introduction to Adaptive Arrays". J. Wiley & Sons 1980, ISBN 0-471-05744-4.

[3] B. Widrow & S.D. Stearns: "Adaptive Signal Processing". Prentice-Hall Inc. N.J. 1985. ISBN 0-13-004029.

[4] S. Haykin (editor): "Array Signal Processing". Prentice-Hall Inc. N.J. 1985. ISBN 0-13-046482-1.

[5] S. Haykin: "Adaptive Filter Theory". Prentice-Hall Inc. N.J. 1986. ISBN 0-13-004052-5.

[6] S.J. Roberts: "An Echo Cancelling Technique Applied to an Underwater Acoustic Data Link". Ph.d. thesis Herriott-Watt University, Edinburgh 1983.

[7] J.G. Proakis: "Digital Communications". McGraw-Hill 1983. ISBN 0-07-066490-0.

[8] M.L. Honig & D.G. Messerschmitt: "Adaptive Filters, Structures, Algorithms and Applications". Kluwer Academic Publishers 1984. ISBN 0-89838-163-0.

Proceedings of the Institute of Acoustics

UNDERWATER ACOUSTIC COMMUNICATIONS: A REVIEW AND BIBLIOGRAPHY

R. Coates and P. A. Willison

School of Information Systems, University of East Anglia, Norwich NR4 7TJ

INTRODUCTION

The literature surrounding the subject of underwater acoustic communications is, in some respects, surprisingly scant. This is particularly the case if one concentrates only upon that material directly concerned with actual underwater communication systems. For example, covering that particular area and excluding general review papers whilst searching back over the past two decades, the authors have retrieved only some sixty titles.

In this paper we have deliberately chosen to take a broader view of underwater communications, to include consideration of the acoustic channel. In so doing, we have drawn upon material which, if not exactly remote from the topic of communications, is none the less of substantially wider scientific interest and application. The paper thus divides into four broad areas of interest, which are "Review and Fundamental Papers", "The Channel", "Engineering Aspects of Underwater Communications" and "Specific Communication Systems".

It must be said that, insofar as the first and second of these areas are concerned, there has been a distinct need to prune the available material, in order to fit within the space allocated to this paper. Hopefully the pruning and the organisation of the material as a whole, although idiosyncratic, will yet leave a useful collection of references for those who wish to pursue further the subject of underwater acoustic communication.

REVIEW AND FUNDAMENTAL PAPERS

In compiling this section, it has been necessary to eliminate a significant number of titles which only provide a low-level review for a general audience. That stated, one such paper by Anderson [1] is included, since it sets the scene in underwater communications as of two decades ago, and neatly reviews the major difficulties which, then as now, revolve around the problems of reverberation and multipath transmission and high attenuation at high acoustic frequencies. Quazi and Conrad [2] also contribute an interesting historical insight and make the suggestion that parametric transmission, because of its ability to establish pencil-beam transmission at relatively low frequencies, with physically small transducers, might have particular advantage in avoiding surface and sea-floor reflections and thus minimising or eliminating the corruptive effects of multipath transmission.

Parametric sonar might be less attractive than Quazi and Conrad suggest, since high directivity at a frequency approaching one of the parametric primaries is, in any case, readily achieved using conventional transmission. One of the remaining advantages of the parametric method is that transmissions using the lower, secondary frequency are less strongly attenuated, in water, than conventional transmissions at the primary frequency. For many applications this advantage would be offset by the poor power efficiency of parametric conversion. Another potential advantage is the possibility of making use of the extreme frequency agility of the secondary frequency. At least in sofar as bandwidth is concerned, the absolute width of sweep of the secondary cannot in any case exceed the primary bandwidth. Finally, the added complexity of a parametric projector would increase cost and could adversely affect robustness.

Acoustics is not, of course, the only method of obtaining underwater communication. The paper by Tregonning [3] outlines state-of-the art and problem areas, as identified during a one-day symposium at the Society for Underwater Technology. The symposium covered acoustical, cable, fibre-optic, electomagnetic and laser methods. On a rather more selective basis, an excellent review, specifically aimed at acoustic telemetry, is provided by Baggeroer [4].

Turning finally to more fundamental material, covering in some detail the mathematical basis of the subject, we have papers by Middleton [5] and by Urick [6].

THE CHANNEL

In discussing the nature of the acoustic channel, since it must necessarily dictate the engineering of the communication system, we consider first a sequence of papers concerned with what might best be described as channel models [7] - [24]. By this we intend to refer primarily to overall end-to-end channel transfer functions of varying complexity, mathematical "models" of channel response and models relating to specific phenomena, such as surface and sea-floor reflection. Of particular mention as a ready source of copious information for the pragmatist who wishes to establish computer models with minimum effort, is the Generic Sonar Model [20],[21].

Moving on from the definition of the channel model, the communication engineer is instinctively inclined to investigate channel capacity, in an information theoretic sense. Three references to papers by Hummels [25], Kwon and Birdsall [26] and Rowlands and Quinn [27] cover this topic. It is interesting to question the significance of a classical information theoretic approach to such a problem. As with more conventional above-water communications, such an approach can provide only upper bounds to performance, perhaps significantly far removed from practical operating levels.

A large body of work is represented in the next section of the bibliography, which covers measured channel characteristics [28] - [45]. Here we see the accumulation of data in both real-sea and test-tank experiments which may provide input for the successful use and extension of the various channel models. A sequence of papers by Gulin and co-workers is concerned with establishing temporal amplitude, phase and frequency as well as spatial correlations for signals reflected from randomly rough surfaces [30] - [36]. Other papers, particularly those by Jobst and Dominijanni [37] and by Veenkant [43] discuss channel stability.

In a separate section we consider the subject of noise as a major corrupting influence [46] - [51]. Urick [50] provides, in his book "Ambient Noise in the Sea", a broad account of this topic with an extensive bibliography. Dunbar [47] considers the under-resourced area of acoustic noise in the vicinity of oil extraction platforms, a subject also touched upon much earlier by Lagoe [48]. The book "Mechanics of Underwater Noise" by Ross [49] provides an excellent background to such studies, which are currently in great need of re-inforcement.

Although, in a later section, we review a selection of papers concerned with the subject of "anti-multipath strategies", it seems appropriate to introduce at this stage a set of papers concerned with multipath identification, partly because the topic should be of fundamental interest and partly because, in future system designs, perhaps more particularly for long-range communication, knowledge of the nature of the multipath structure of the channel might assist in establishing self-training "machine intelligent" processing systems. Papers by Fjell [52] and by Hassab [53],[54] explain how to acquire such information via the cepstrum analysis technique. Although we remain sceptical of this, they further suggest that the cepstrum approach is intrinsically superior to evaluation of the autocorrelation function in identifying delay-domain attributes of a received signal. Two further papers describe actual multipath investigations in the Atlantic [56] and Pacific [57] Oceans.

UNDERWATER ACOUSTIC COMMUNICATIONS: A REVIEW AND BIBLIOGRAPHY

ENGINEERING ASPECTS OF UNDERWATER COMMUNICATIONS

Here we consider first the estimation of error probability [58] - [67]. Papers by Aboteen et al. [58],[59], by Andrews and Turner [60] - [62] and by Maras et. al. [63] - [66] address various aspects of these problems. Some element of field experiment is contained within the papers by Andrews and Turner. Next we turn to the topic of devising error protection codes for underwater communication systems [68] - [73] and follow this with papers on anti-multipath strategies [74] - [78].

The section concludes with two papers concerned with aspects of timing and synchronisation [79],[80].

SPECIFIC COMMUNICATION SYSTEMS

This area has been considered under two headings, although further subdivision would be possible. The larger class of systems is concerned with aspects of through-water communication [81] - [109]. No particular attempt has been made to isolate high efficiency or high rate systems since such descriptors seem often to be incorrectly or at least ill-advisedly used in underwater applications.

The second, smaller, class is concerned with penetrator telemetry, where the signal must first pass through a significant layer of (relatively) highly attenuating ocean floor sediment. Such systems are employed for a variety of geo-technical tests [110] - [112].

BIBLIOGRAPHY

REVIEW AND FUNDAMENTAL PAPERS

[1] V.C. Anderson, "Acoustic Communication is Better than None", *IEEE Spectrum*, October 1970, pp.63-68

[2] A.H. Quazi and W.L. Conrad, "Underwater Acoustic Communications", *IEEE Commun. Magazine*, Vol. 20, No.2, March 1982, pp. 24-30

[3] K. Tregonning, "Data Communications Underwater", *Underwater Technology*, Vol. 10, No. 2, Summer 1984, pp. 19-22

[4] A.B. Baggeroer, "Acoustic Telemetry - An Overview", *IEEE J. Oceanic Eng.*, Vol. OE-9, No.4, Oct. 1984, pp.229-235

[5] D. Middleton, "The Underwater Channel as a Generalised Communication Channel", in *Underwater Acoustics and Signal Processing* (ed. Bjorno), Publ. Reidel (Netherlands) 1981, ISBN 90 277 1255 7, pp. 589-612

[6] R.J. Urick, "Multipath Propagation and Its Effects on Sonar Design and Performance in the Real Ocean", in *Aspects of Signal Processing* (ed. Tacconi), Part 1, pp. 3-18, D. Reidel Publishing Co., 1977

THE CHANNEL

Channel Models

[7] S.L. Adams and J. Doubek, "Dispersive Properties of the Underwater Acoustic Channel", *IEEE Intl. Conf. Acoustics, Speech and Signal Processing*, Phiadelphia, Pa., April 1976, pp. 664-7

[8] Ye. I. Chvertkin, "The Hydroacoustic Data Transmission Channel for Ocean Data Buoys", *Oceanology (USA)*, Vol. 13, No. 2, 1973, pp.309-311

[9] J.E. Ehrenberg, "Reverberation: Signal Related Noise in Acoustic Systems", *Proc. IEEE Intl. Conf. Communications*, 1973, pp. 38-5 to 38-8

[10] A.I. Eller, H.J. Venne and D.W. Hoffman, "Evaluation of Ocean Acoustic Reverberation Models", *Proc. IEEE Oceans '82 Conf.*, pp. 206-210

[11] A.A. Gerlach, "Acoustic Transfer Function of the Ocean for a Motional Source", *IEEE Trans. Acoustics, Speech and Signal Processing*, Vol. ASSP-26, No. 6, December 1978, pp. 493-501

[12] D. Howse and A. Zielinski, "Multipath Modelling for Acoustic Communication", *Proc. IEEE Oceans '82 Conf.*, pp.217-222

[13] R. Laval, "Sound Propagation Effects on Signal Processing", *Proc. NATO Advanced Study Institute on Signal Processing*, (ed. Griffith, et. al.) Academic Press, London, 1972, pp. 223-41

[14] J.F. McDonald and F.B. Tuteur, "Moment Characterisation of a Doubly Spread Surface-Scatter Channel at High Rayleigh Parameters", *Proc. IEEE*, Vol. 62, No.11, Nov. 1974, pp. 1606-8

[15] J.F. McDonald, "Fresnel-Corrected Second-Order Interfrequency Correlations for a Surface-Scatter Channel, *IEEE Trans. Commun.*, Vol. COM-22, No.2, Feb. 1974, pp.138-145

[16] R.C. Spindel and P.M. Schultheiss, "Acoustic Surface-Reflection Channel Characterisation Through Impulse Response Measurements", *J. Acoust. Soc. Am.*, Vol. 51, No. 6, Pt. 1, June 1972, pp. 1812-24

[17] R.L. Swarts and W.P. Harthill, "Correlation of Signals Scattered from Rough Surfaces: Heuristic Approach" *Proc. IEEE Intl. Conf. Communications*, 1973

[18] A.N. Venetsanopolous and F.B. Tuteur, "Stochastic Filter Modelling for the Sea-surface Scatter Channel", *J. Acoust. Soc. Am.*, Vol. 49, No. 4, Part 1, 1971, pp. 1100-1107

[19] A.N. Venetsanopolous, "Modelling of the Sea-Surface Scattering Channel and Undersea Communications", in *Communication Systems and Random Process Theory* (ed. Skwirzynski), Publ. Sitjhoff and Noordhoff, Netherlands, ISBN 90 286 0568 1, 1978, pp. 511-531

[20] H. Weinberg, "Generic Sonar Model", NUSC Technical Document 5971C, 1981

[21] H. Weinberg, "Generic Sonar Model", *IEEE Oceans '82 Conference*, pp. 201-205

[22] A.B. Wood, "Scale Model Study of Propagation in Shallow Seas: A Visual Method of Representation of Low-Intensity Sound Fields", in *Underwater Acoustics* (ed. Albers), Plenum Press, New York (1961), pp. 159-192

[23] L.J. Ziomek, "Generalised Kirchoff Approach to the Ocean Surface Scatter Communication Channel. Part I. Transfer Function of the Ocean Surface", *J. Acoust. Soc. Am.*, Vol. 71, No.1, Jan 1982, pp. 116-126

[24] L.J. Ziomek, "Generalised Kirchoff Approach to the Ocean Surface Scatter Communication Channel. Part II. Second Order Functions", *J. Acoust. Soc. Am.*, Vol. 71, No. 6, June 1982, pp. 1487-1495

Channel Capacity

[25] D.R. Hummels, "The Capacity of a Model for the Underwater Acoustic Channel", *IEEE Trans. Sonics and Ultrasonics*, Vol. SU-19, 1972, pp. 350-353

[26] H.M. Kwon and T.G. Birdsall, "Channel Capacity in Bits per Joule", *IEEE J. Oceanic Eng.*, Vol. OE-11, No. 1, Jan 1986, pp. 97-9

[27] R.O. Rowlands and F.G. Quinn, "Transmission Rate Limits in Underwater Acoustic Telemetry", in *Underwater Acoustics, Vol II.* (ed. Albers), Plenum Press, New York (1967), pp. 393-408

Measured Channel Characteristics

[28] S.J. Campanella and A.G. Favret, "Time Autocorrelation of Sonic Pulses Propagating in a Random Medium", *J. Acoust. Soc. Am.*, Vol. 46, pp. 1234-1245, 1969

[29] H-H. Essen, F. Schirmer and B. Schmalfeldt, "Influence of Tides on Acoustic Continuous-Wave Propagation", *Acustica*, Vol. 48, No. 5, Aug. 1981, pp. 285-292

[30] E.P. Gulin, "Amplitude and Phase Fluctuations of a Sound Wave Reflected from a Statistically Uneven Surface", *Sov. Phys.-Acoust.*, Vol. 8, No. 2, Oct.-Dec. 1962, pp. 135-140

[31] E.P. Gulin, "Amplitude and Phase Fluctuations of a Sound Wave Reflected from a Sinusoidal Surface", *Sov. Phys.-Acoust.*, Vol. 8, No. 3, Jan.-Mar. 1963, pp.223-227

[32] E.P. Gulin and K.I. Malyshev, "Statistical Characteristics of Sound Signals Reflected from the Undulating Sea Surface", *Sov. Phys.-Acoust.*, Vol. 8, No. 3, Jan.-March 1963, pp.228-234

[33] E.P. Gulin, "The Correlation of Amplitude and Phase Fluctuations in Sound Waves Reflected from a Statistically Rough Surface", *Sov. Phys.-Acoust.*, Vol. 8, No. 4, April-June 1963, pp. 335-339

[34] E.P. Gulin and K.I. Malyshev, "Experiments in the Spatial Correlation of the Amplitude and Phase Fluctuations of Acoustic Signals Reflected from a Rough Ocean Surface", *Sov. Phys.-Acoust.*, Vol. 10, No. 4, April-June 1965, pp. 365-368

[35] E.P. Gulin and K.I. Malyshev, "Spatial Correlation of Amplitude Fluctuations of A Continuous Tone Signal with Reflection from Ocean Surface Waves", *Sov. Phys.-Acoust.*, Vol. 11, No. 4, April-June 1966, pp. 428-430

[36] E.P. Gulin and K.I. Malyshev, "Some Results of an Investigation of the Frequency Correlation of Amplitude Fluctuations in Sound Signals", *Sov. Phys. -Acoust.*, Vol. 12, No. 1, July-Sept. 1966, pp. 87- 88

[37] W. Jobst and L. Dominijanni, "Measurements on the Temporal, Spatial and Frequency Stability of an Underwater Acoustic Channel", *J. Acoust. Soc. Am.*, Vol. 65, No. 1, Jan 1979, pp. 62-9

[38] J.R. Olson and R.H. Nichols, "Correlation Measurements of Surface Reflected Underwater Acoustic Signals at Several Sea States", *J. Acoust. Soc. Am.*, Vol.71, No. 6, June 1982, pp. 1453-1457

[39] R.G. Stone and D. Mintzer, "Range Dependence of Acoustic Fluctuations in a Randomly Inhomogenous Medium", *J. Acoust. Soc. Am.*, Vol. 34, pp. 647-653, 1962

[40] R. Thiele, "Measurement of the Weighting Function of the Time-Variant Shallow Water Channel" *Proc. NATO Advanced Study Institute of Signal Processing* (ed. Tacconi), Publ. Reidel, Netherlands, 1977, ISBN 90 277 0799 5, pp. 109-122

[41] R.S. Thomas, J.C. Moldon and J.M. Ross, "Shallow Water Acoustics Related to Signal Processing", *Proc. NATO Advanced Study Institute on Signal Processing*, (ed. Griffith, et. al.) Academic Press, London, 1972, pp. 281-298

[42] O.S. Tonakanov, "Sound Fluctuations During Propagation in a Shallow Layer of Water", *Sov.Phys.-Acoust.*, Vol. 7, No. 2, Oct-Dec. 1961, pp.185-189

[43] R.L. Veenkant, "Investigation of the Propagation Stability of a Doubly Spread Underwater Acoustic Channel", *IEEE Trans. Acoustics, Speech and Signal Processing*, Vol. ASSP-25, No.2, April 1977, pp. 109-116

[44] L.N. Zakharov, "The Effect of Seiche Oscillations of the Surface of a Reservoir on the Phase Fluctuations of an Acoustic Signal", *Sov. Phys.-Acoust.*, Vol. 8, No. 4, April-June 1963, pp. 340-343

[45] J.G. Zornig and J.F. McDonald, "Experimental Measurement of the Second-Order Interfrequency Correlation Function of the Random Surface Scatter Channel", *IEEE Trans. Commun.*, Vol. COM-23, No. 3, March 1975, pp. 341-7

Noise

[46] D.M.F. Chapman, "Surface Generated Noise in Shallow Water: A Model", *Proc. Inst. Acoustics*, Vol. 9, December 1987

[47] R.M. Dunbar, "Electric, Magnetic and Acoustic Noise Generated Underwater During Offshore Piling Operations", *Proc. Inst. Acoustics*, Vol.9, December 1987

[48] J.A. Lagoe, The Subsea Acoustic Communications Environment", *7 th. Ann. Conf. Marine Technology Society*, Aug. 1971, Washington, D.C., pp. 259-264

[49] D. Ross, "Mechanics of Underwater Noise", Pergamon Press, New York, (ISBN0-08-021182-8) (1976)

[50] R. Urick, "Ambient Noise in the Sea", Peninsula Publishing (ISBN 0-932146-13-9), (1986)

[51] P.C. Wille, "Ambient Noise: Characteristics of the Noise Field", in *"Adaptive Methods in Underwater Acoustics"*, H.G. Urban (ed.), Reidel, Holland (ISBN 90-277-1982-9)

Multipath Identification

[52] Per O. Fjell, "Use of the Cepstrum Method for Arrival Times Extraction of Overlapping Signals due to Multipath Conditions in Shallow Water", *J. Acoust. Soc. Am.*, Vol 59, No. 1, January 1976, pp. 209-211

[53] J.C. Hassab, "Time Delay Processing Near the Ocean Surface", *J. Sound and Vib.*, Vol. 35, No. 4, 1974, pp. 489-501

[54] J.C. Hassab and R. Boucher, "Analysis of Signal Extraction, Echo Detection and Removal by Complex Cepstrum in the Presence of Distortion", *J. Sound and Vib.*, Vol. 40, No.3, 1975, pp. 321-335

[55] P. Hirsch, "The Metacepstrum", *J. Acoust. Soc. Am.*, 69 (3), March 1981

[56] G.R. Legters, N.L. Weinberg and J.G. Clarke, "Long-Range Atlantic Acoustic Multipath Identification", *J. Acoust. Soc. Am.*, Vol.73, No. 5, 1983, pp. 1571-1580

[57] J. Northrop and R.C. Shockley, "Long-Range Pacific Multipath Identification", *J. Acoust. Soc. Am.*, Vol. 75, No. 6, 1984, pp. 1760-1765

ENGINEERING ASPECTS OF UNDERWATER COMMUNICATIONS

Error Probability

[58] R.A. Abotteen, N.M. Shehadeh and J.C. Vanelli, "Error Probability of a Binary NRZ Signal over a Parallel Channel", *IEEE Trans Sonics and Ultrasonics*, Vol. SU-21, No. 4, Oct. 1974, pp. 300-301

[59] R.A. Abotteen, "Probability of Error of a Binary Infinite Impulse Train Signal Over a Random Parallel Channel", *IEEE Trans. Sonics and Ultrasonics*, Vol. SU-25, No. 2, March 1978, pp. 104-107

[60] R.S. Andrews and L.F. Turner, "Amplitude Fluctuation of Underwater Signals and its Effect on the Bit-Error Probability of Underwater Data Transmission Systems", *Proc. IEE*, Vol. 124, No. 2, Feb. 1977, pp. 115-119

[61] R.S. Andrews and L.F. Turner, "On the Performance of Underwater Data Transmission Systems Using Amplitude Shift Keying Techniques", *IEEE Trans. Sonics and Ultrasonics*, Vol. SU-23, No. 1, Jan. 1976, pp. 64-71

[62] R.S. Andrews and L.F. Turner, "Investigation of the Amplitude Fluctuations of High-Frequency Short-Duration Sound Pulses Propagated Under Shallow-Water Conditions", *J. Acoust. Soc. Am.*, Vol.58, No.2, 1975, pp. 331-335

[63] A.M. Maras, H. Davidson and A.G.J. Holt, "Error Rates for M-ary Noncoherent FSK in Impulsive Reverberation Noise", *Electron. Lett.*, Vol 19, No. 11, May 1983, pp. 405-6

[64] A.M. Maras, H. Davidson and A.G.J. Holt, "Diversity for Binary Noncoherent Frequency Shift Keying in Impulsive Reverberation Noise", *Electron. Lett.*, Vol 20 No. 19, Sept. 1984, pp. 775-777

[65] A.M. Maras, H. Davidson and A.G.J. Holt, "Diversity Improvement for M-ary Noncoherent Frequency Shift Keying in Impulsive Reverberation Noise", *Electron. Lett.*, Vol 21, No. 20, Sept. 1985, pp. 944-5

[66] A.M. Maras, H. Davidson and A.G.J. Holt, "Threshold Performance of M-ary Noncoherent Frequency Shift Keying in Non-Gaussian Noise", *Electron. Lett.*, Vol 22, No. 16, 1986, pp. 842-843

[67] N.M. Shehadeh, "Bit Error Probability for a Multipath Channel", *IEEE SoutheastCon '83 Conf. Proceedings*, Orlando, Fla., April 1983, pp. 537-41

Error Protection Codes

[68] J.L.Backes, B.M. Bell and J.B. Miller, "Implementation of Error Detection and Correction Codes for Acoustic Data Telemetry", *Proc. Oceans '83 Conf.*, San Francisco, Calif., August 1983, pp.167-75

[69] T. Hasegawa, "On a Coder of Fibonacci Code for Underwater Digital Data Transmission, *Rec. IEEE Conf. Engineering in the Ocean Environment*, San Diego, Calif., Sept. 1971, pp. 381-3

[70] T. Hasegawa, "A Coding Scheme for Underwater Digital Data Transmission", *Digest IEEE Conf. Engineering in the Ocean Environment*, Panama City, Fla., Sept. 1970, pp. 60-3

[71] D.B. Heckman, "Secure Command Coding Using Amplitude Modulation", *7 th. Ann. Conf. Marine Technology Society*, Aug. 1971, Washington, D.C., pp. 265-269

[72] J. Pieper, R. Reed, J. Proakis and J. Wolf, "The Use of Constant Weight Block Codes for the Underwater Channel", *EASCON-77 Record*, Arlington, Va., Sept. 1977, pp. 36-9

[73] B. Woodward, "A Variable Code Underwater Acoustic Transducer", *Acoustics Letters*, Vol. 6, No. 7, 1983, pp. 94-99

Anti-Multipath Strategies

[74] J.L. Galloway, J.S. Collins and M.R. Balderson, "Auto Aligning System for Narrow Beam Acoustic Telemetry", *Proc. IEEE Oceans '85 Conf.*, San Diego, Calif., Nov. 1985, pp. 490-3

[75] C. Gazanhes, J.L. Garnier and J.P. Sessarego, "Signal Processing for Multimodal Transmission in Shallow Water Propagation: Application to Underwater Acoustic Communication", *Signal Process.* (Netherlands), Vol.6, No.3 June 1984, pp. 167-85

[76] G. Loubert, "Estimation of the Transmission Sequence in a Marine Medium. Presentation of Different Propagation Paths", *Rev. Cethedec* (France) Vol.19, No.71 1982 pp. 55-68

[77] R.E. Williams and H.F. Battestin, "Coherent Recombination of Acoustic Multipath Signals Propagated in the Deep Ocean", *J. Acoust. Soc. Am.*, Vol. 50, No. 6 (Part 1), 1971, pp. 1433-1442

[78] S.J. Roberts, "An Echo Cancelling Technique Applied to an Underwater Acoustic Data Link", Ph.D. Thesis, Heriot-Watt University, Edinburgh, Scotland, 1984

Timing and Synchronisation

[79] D.M. Coffey and D.L. Paquette, "Accuracy of Acoustic Multipath Timing and Ranging Predictions Over Extended Ranges", *Proc. IEEE Oceans '85 Conf.*, San Diego, Calif., Nov. 1985, pp. 480-9

[80] S.D. Morgera, "Digital Filtering and Prediction for Communication Systems Time Synchronisation", *IEEE J. Oceanic Eng.*, Vol. OE-7, No. 3, July 1982, pp. 110-19

SPECIFIC COMMUNICATION SYSTEMS

Through-water Communication Systems

[81] J.L. Backes, B.M. Bell and L.O. Olson, "Long-baseline Deep Ocean Acoustic Tracking and Telemetry System", *Oceans '81*, Boston, Mass., pp. 1-8

[82] T.G. Birdsall, "Acoustic Telemetry for Ocean Acoustic Tomography", *IEEE J. Oceanic Eng.*, Vol. OE-9, No. 4, Oct. 1984, pp. 237-241

[83] D.C. Brock, S.C. Bateman and B. Woodward, "Underwater Acoustic Transmission of Low-Rate Digital Data", *Ultrasonics*, Vol. 24, No. 4, July 1986, pp. 183-8

[84] D.W. Burrows, "Cableless Underwater Television Link Design and Test Results", Internal Rept., Ball Brothers Research Corp., Boulder, Colorado.

[85] J. Capotvic, A.B. Baggeroer, K. Von der Heydt and D. Koelsch, "Design and Performance of a Digital Acoustic telemetry System for the Short Range Underwater Channel", *IEEE J. Oceanic Eng.*, Vol. OE-9, No. 4, Oct. 1984, pp. 242-52

[86] J.V. Chase, "A Tracking and Telemetry System for Severe Multipath Acoustic Channels", *Proc IEEEOceans '81 Conf.*, Boston, Mass., pp. 35-39

[87] J.S. Collins and J.L. Galloway, "Acoustic Telemetry of Video Information", *Proc. IEEE Oceans*

'83 Conf., San Francisco, Calif., August 1983, pp. 163-6

[88] D. Garrood, "Applications of the MFSK Acoustic Communications System," *Proc. IEEE Oceans '81 Conf.*, Boston, Mass., pp. 67-71

[89] D. Garood and N.D. Miller, "Acoustic Telemetry for Underwater Control", *Proc. IEEE Oceans '82 Conf.*, Wash., pp. 111-114

[90] P.O. Kearney and C.A. Laufer, "Sonarlink - A Deep Ocean, High Rate, Adaptive Telemetry System", *Proc IEEE Oceans '84 Conf.*, Washington, D.CV., Sept. 1984, pp. 49-53

[91] W.L. Konrad, "Applications of the Parametric Source to Underwater Acoustic Communications", *EASCON-76 Record*, Washington, D.C., Sept. 1976, 124A/1-9

[92] B. Leduc and A. Glavieux, "Long Range Underwater Acoustic Image Transmitting System", Institut Francais de Rechereche pour l'Exploitation de la Mer, BP 337, 29273 Brest Cedux.

[93] G.R. Mackelburg, S.J. Watson and A. Gordon, "Benthic 4800 Bits/s Acoustic Telemetry", *Proc Oceans '81,Conf.*, Boston, Mass., p. 72

[94] J. Mackelburg, "BUMP/AUSS Deep Water Acoustic Link Tests", NOSC Intl. Rept. No. SER 5211/194-81

[95] M. Mandelberg, "An Oceanographic Acoustic beacon and Data Telemetry System Powered by a SNAP-21 Radioisotope Thermoelectric Generator, *Rec. IEEE Conf. Engineering in the Ocean Environment*, San Diego, Calif., Sept. 1971, pp. 220-3

[96] C.S. Miller and C.E. Bohman, "An Experiment in High-Rate Underwater Telemetry", *IERE Conf. on Eng. in the Ocean Environment"*, 1972

[97] R.B. Mitson, T.J. Storeton-West and N.D. Pearson, "Trials of an Acoustic Transponding Fish Tag Compass", *Biotelem. and Patient Monitoring*, Vol.9, No. 2, 1982, pp. 69-79

[98] R.B. Mitson, T.J. Storeton-West and M.G. Walker, "Fish Heart-Rate Telemetry in the Open Sea Using Sector Scanning Sonar", *Biotelem. and Patient Monitoring*, Vol. 5, No. 3 1978, pp. 149-53

[99] S.D. Morgera, K.A. Reuben and C. Cole, "A Microprocessor-based Acoustic Telemetry System for Tide Measurement", *IEEE J. Oceanic Eng.*, Vol. OE-11, No.1, Jan. 1986, pp.100-8

[100] J.H. Okerlund, "A Phase Shift Keyed Acoustic Data Link", *Proc. IEEE Intl. Conf. Communications*, 1973, pp. 38-9 to 38-11

[101] K.E. Prada, K. Von der Heydt and T.F. O'Brien, "A Versatile Multi-Channel Data Acquisition System for Seismic and Acoustic Applications", *Proc. Oceans '81 Conf.*, Boston, Mass., pp. 43-47

[102] S. Riter and P.A. Boatright, "Design Considerations for a Pulse Position Modulation Underwater Acoustic Communications System", *Digest IEEE Conf. Engineering in the Ocean Environment*, Panama City, Fla., Sept. 1970, pp. 21-24

[103] S. Riter, "Pulse Position Modulation Communications via the Underwater Acoustic Communication Channel", *IEEE SWIEECO Rec. 22 nd. Southwestern Conf. & Exhib.*, Dallas, Texas, April 1970, pp. 453-7

[104] C.L. Tyndale, G.H. Efinger and S.O Raymond, "Multichannel Underwater Acoustic Telemetering System", U.S. Patent 3444510, 10 th. Oct. 1969

[105] D. Wax, "MFSK - The Basis for Robust Acoustic Communications", *Proc IEEE Oceans '81 Conf.*, Boston, Mass., pp. 61-66

[106] R.M. Dunbar, S.J. Roberts and S.C. Wells, "Communications, Bandwidth Reduction and System Studies for a Tetherless Unmanned Submersible", *Proc. IEEE Oceans '81 Conf.*, Boston, Mass., pp. 127-131

[107] A. Zielinski and M. Caldera, "Digital Acoustic Communication in Multipath Underwater Channels", *Proc. IEEE Oceans '85 Conf.*, San Diego, Calif., Nov. 1985, pp. 1296-1301

[108] A. Zielinski, W. Jacobs and D. Howse, "The Multichannel Acoustic Telemetry System", *Proc. IEEE Oceans '81 Conf.*, Boston, Mass., pp. 40-42

[109] A. Zielinsky, "Swept Carrier Acoustic Underwater Communication", *Proc. IEEE Oceans '78 Conf.*

Penetrator Telemetry

[110] R. Coates, "Acoustic Data Telemetry from Beneath the Ocean Floor", *Proc. IEEE Oceans '87 Conf.*, Nova Scotia

[111] C.G. Flewellen, "PATSY: The Pulsed Acoustic Telemetry System", *Proc. Inst. Acoust.*, Vol. 7, December 1987

[112] D.M. Talbert, "Wireless System Transmits Sea-Bed Data", *Ocean Industry*, January 1985, p. 55

Proceedings of the Institute of Acoustics

A RELIABLE UNDERWATER ACOUSTIC DATA LINK EMPLOYING AN ADAPTIVE RECEIVING ARRAY

H. Davidson, P. Mullholland, A.G.J. Holt

Department of Electrical and Electronic Engineering,
University of Newcastle upon Tyne. NE1 7RU

ABSTRACT

One of the main problems encountered when trying to produce a reliable underwater acoustic data link is that of multipath reflections from the sea surface and seabed. The most common method of overcoming this multipath problem is to use transmitting and receiving transducers with very narrow beamwidths. However, this solution makes alignment of the beampatterns critical, and any mis-alignment or motion of the transmitter or receiver may destroy the acoustic link completely.

In this paper, a reliable underwater data link which employs an adaptive receiving array is described. The purpose of the array is to provide automatic mainlobe tracking of the transmitter and to suppress directional mulitpaths and interferences. This adaptive array therefore solves the problems of beampatterns mis-alignment whilst also providing a certain degree of beampattern nulling to suppress directional multipaths and interferences.

The adaptive receiving array requires some prior knowledge of the desired incoming signal in order to distinguish it from the multipath reflections. This is provided by using a PN coded DPSK modulation scheme, where the PN coding is known at both the transmitter and receiver.

1. INTRODUCTION

High data rate acoustic telemetry for underwater communications has been pursued ever since it was recognised that the ocean could support signal transmission. In the past, most of the applications for underwater communications have arisen from military needs. However, as a result of oil and gas exploration work there are now an increasing number of offshore commercial applications (e.g. well-head monitoring and control, untethered submersibles etc). In all of these applications the major requirement is for a reliable, high data rate acoustic link.

The ocean is an extremely difficult medium in which to achieve the high data rates required for many applications. The ability of the ocean to support reliable high data rate transmissions is limited by the available transmission bandwidth and the detrimental effects of multipath propagation caused by boundary reflections and volume scattering. Also the maximum range of propagation in the ocean is limited by the increased absorption of acoustic energy at higher frequencies.

The complex properties of the acoustic channel therefore require a careful choice of modulation scheme and the use of multipath reduction techniques to achieve a reliable high data rate acoustic link. The modulation scheme must be chosen to make the best possible use of the available bandwidth. After considering the most common digital modulation techniques (i.e. OOK, FSK and PSK), a PSK type modulation scheme was chosen for its ability to provide low error probability for a given signal-to-noise ratio (SNR) and allow high data rate to be achieved in the available bandwidth [1]. Unfortunately, this PSK type modulation scheme, in common with the other basic binary modulation techniques, is unable to overcome the effects of multipath by itself. The most common method of overcoming this multipath problem is to use directional transducers with narrow beamwidths at both the transmitter and receiver. However, this solution makes alignment of the beampatterns critical, and any mis-alignment or motion of the transmitter or receiver may destroy the acoustic link completely. In order to reduce the effects of multipath an adaptive receiving array was used to provide automatic mainlobe tracking of the transmitter and to suppress multipaths and any other directional interferences. The adaptive receiving array therefore solves the problem of beampattern mis-alignment and is also able to operate in environments where the transmitter or receiver may be in motion.

2. THE UNDERWATER ACOUSTIC DATA LINK

The block diagram of the proposed underwater acoustic data link is shown in Fig. 1.

The transmitter employs a PN coded DPSK modulation scheme and operates at a centre frequency of 50kHz. The transmitting array provides a useable bandwidth of 20kHz and has a conical beampattern of 16° beamwidth.

The adaptive receiving array is controlled by a least-mean-square (LMS) algorithm which determines the beampattern and frequency response of the array [2]. This adaptive array requires some prior knowledge of the desired incoming signal in the form of a reference signal. The reference signal must be correlated (spacially and temporally) with the desired incoming signal and uncorrelated with any multipaths or interferences. To provide such a reference signal, a PN coded DPSK modulation scheme was used with the PN code known at both the transmitter and receiver. At the receiver this PN code is used to distinguish the desired incoming signal from any multipath reflections or interferences. This combination of the PN coded DPSK modulation scheme and the LMS adaptive array provides a high level of multipath and interference protection.

2.1 <u>THE MODULATOR - DEMODULATOR</u>

Refering to the basic block diagram of the transmitter shown in Fig. 1a, the incoming data stream (rate Rd) is exclusive -ORed with a higher rate maximal length linear PN code (rate Rc, where Rc/Rd is an integer) whose properties[1,3-5] are:

i The value of the PN code's autocorrelation function is high at zero shift and very low elsewhere (to aid synchronisation)

ii The PN code has good statistical properties and equal numbers of 0's and 1's (to suppress the generation of an unwanted carrier frequency component) and

iii The length of the PN code is long enough to ensure that the code is not repeated during the transmission of a message (to prevent synchronisation problems)

The PN coded data stream is then used to DPSK modulate (PSK modulation requires additional receiver circuitry to resolve its phase ambiquity [3]) the chosen 50kHz carrier frequency, so that a data '1' produces a phase change and a data '0' causes the phase to remain the same as for the previous data value. The resultant PN coded DPSK signal has a spectrum whose null to null bandwidth (containing 90% of the total signal power and all the necessary phase information) is Rc/Rd times larger than the bandwidth of the incoming data stream (2Rd) [4]. The ratio of PN code to incoming data rate Rc/Rd, known as the spreading ratio (SR), therefore indicates that the resultant PN coded DPSK signal has a bandwidth of 2Rd x SR. As this bandwidth is necessary for the successful transmission of the PN coded DPSK signal through the underwater medium, the desire for a high data rate to be realised in a fixed (20kHz) transmission bandwidth indicates that the value of SR must be small and Rd = (10kbit/s)/SR. Thus, values of SR = 4 and SR = 8 (switchable) are chosen for this proposed data link, so that data rates of 2.5 and 1.25kbit/s respectively can be achieved.

At the output of the adaptive array shown in Fig. 1b, the received signal (PN coded DPSK + noise + interference) is coherently demodulated by extracting a reference carrier signal (directly from the received signal) with a suppressed carrier tracking loop, and using the reference in an optimum DPSK demodulator [3]. (The use of an auxillary channel for synchronisation or reference purposes is not only wasteful of transmission bandwidth, but is of little benefit in the underwater channel, as the channel is temporally and spatially variant as well as being frequency dependent). The resultant baseband signal containing contributions from the PN coded stream, interference (multipath and/or CW) and noise, is then multiplied by a synchronised version of the PN coded signal is then despread to the original data bandwidth (2Rd). All signal contributions not synchronised with the PN code (i.e. CW interference, multipath and noise) are spread to a larger bandwidth (>2Rc) with a resultant reduction in their spectral densities and correlation with the data stream in the despread data bandwidth. This reduction in the unwanted signal level causes an increase in the SNR observed in the data bandwidth (known as the process gain Gp, where Gp = 10log(SR) dB [4]) and indicates that by spreading and despreading the incoming data spectrum, the detrimental effects of the multipath may be reduced. The level of this improvement in performance is however small, as the chosen values of SR (4 or 8) restrict the process gain to either 6 or 9 dB. Finally, the decision on the value of each data bit is performed by taking a majority decision over the SR 1/Rc time slots of each despread data bit, after bit synchronisation (i.e. the location of the start/end of each data bit) has been performed with a data transition tracking loop [3,5]. As the majority decision performs as an error correction, the resultant error probability is further decreased.

In order for the despreading operation to be performed properly at the receiver, it is essential that the receivers' PN code is synchronised with the identical version present in the received signal. The task of obtaining and maintaining the required is synchronisation complex [3-5], but can be summarised as follows:

i Initial Synchronisation (Acquisition)

After a cold start (e.g. power-up) when there is no prior knowledge of the timing difference between the received and the receiver's PN code, the first task of the synchroniser is to rapidly obtain synchronisation with ±1 bit. This can be achieved by rapidly correlating the received PN code (at this point data is not usually sent) with all the receiver's PN code phases until a correlation peak (PN property (1)) is detected. In practice, this operation can take a considerable time, and it is common practice to transmit a known section of the PN code (preamble) to reduce the required search range

ii Tracking

Once the PN codes have been aligned to within ±1 bit, it is necessary to fine tune and maintain the alignment to within ±0.1 bit. This is achieved by using a closed loop configuration to adjust the phase of the receiver's PN code by small amounts in order to maximise the correlation (at zero shift) between the two codes.

2.2 THE ADAPTIVE RECEIVING ARRAY

A block diagram of the adaptive receiving array is shown in Fig. 1(b). This diagram can be divided into two parts: the adaptive array and the reference signal generation loop.

The adaptive array uses a rectangular transducer consisting of 96 elements arranged as 16 horizontal stores of 6 elements, with an interelement spacing of $\lambda/2$. In the system that was tested only 7 staves of this transducer were used, with either a $\lambda/2$ or λ spacing between staves. This gives an azimuth beamwidth of 17^{o} and elevation beamwidths of either 14^{o} ($\lambda/2$ spacing) or 7^{o} (λ spacing). Since the multipath propagation is mainly caused by reflections from the sea surface and sea bed, the adaptive array was used to perform beamforming in elevation only. The input signals from the 7 array stores are adjusted in phase and amplitude by a set of finite impulse response (FIR) filters and then summed to produce the adaptive array output y. The array output y is then subtracted from the reference signal d to produce an error signal e for the LMS algorithm. The LMS algorithm is used to control the weights of the FIR filters and therefore determines the beampattern and frequency response of the adaptive array. The LMS alogrithm is a correlation loop which adjusts the FIR filter weights in order to minimise the mean-square-error between the reference signal d and the array output y. Therefore, the LMS algorithm adjusts the array beampattern and frequency response such that the array output y is an estimate of the reference signal d. The reference input can therefore be chosen to make the adaptive array track a desired input signal. For the LMS adaptive array the reference signal must be highly correlated with the desired signal at the array output and uncorrelated with any interference components at the array output [6]. If the reference signal satisfies this condition then the adaptive array's beampattern will track the desired signal and null any directional interferences (i.e. multipaths). The generation of reference signal d for the adaptive array will now be considered.

The reference signal generation loop shown in Fig. 1(b) is used to generate a reference signal d for the adaptive array from the adaptive arrays output y. Consider that a desired signal s and a directional interference i (i.e. multipath) are present at the receiving array. Therefore the array output y consists of a desired signal component and an interference component. The desired signal is demodulated by the DPSK demodulator and then despread (bandwidth compressed) by the synchronised PN code generator to the data bandwidth. The interference is also present after DPSK demodulation, but since it is not synchronised with the PN code generator its spectrum is spread to at least the PN code bandwidth. Therefore, the data signal is available at the receiver output for data bit detection and the interference power is reduced, since only a small part of the interference spectrum is present at the data bandwidth. The data signal is then passed through a limiter which controls the amplitude of the reference signal. Finally, the limited data is PN coded and DSPK modulated to produce a constant amplitude of the reference signal s at the reference signal input d of the adaptive array. The remaining interference at the receiver output also passes through the limiter and its spectrum is spread again by the PN code generator. This interference is then DPSK modulated and appears at the reference signal input d of the adaptive array. However, this interference i' is now decorrellated with the original interference i at the output of the adaptive array. Therefore, the desired signal s at the array output passes through the reference signal generation loop virtually unaltered, except for a constant amplitude and possibly a small delay. Whereas the interference i at the array output is decorrelated by the loop as denoted by i' at the reference signal input.

The reference signal input to the adaptive array s + i' is therefore highly correlated with the desired incoming signal s at the array output and uncorrelated with the interference i at the array output. This satisfies the necessary requirements for a reference signal for the LMS adaptive array. Therefore the LMS algorithm adjusts the FIR filter weights form a beampattern mainlobe in the direction of the desired signal s and a null in the direction of the interference i (i.e. multipath). After the LMS algorithm has fully converged the array output will contain only the desired signal component s which passes through the loop to appear at the reference signal input. The adaptive array then has an ideal reference signal and the mean-square-error approaches zero.

After the adaptive array has converged then the multipath protection for the desired signal consists of the array gain phases the multipath nulling plus the protection offorded by the process gain of the PN code. In the previous example it was assumed that perfect synchronisation had already been required. In practice, the adaptive array beamforming and the synchronisation are performed simultaneously.

2.3 RESULTS

An all digital implementation of the PN coded DPSK modulator - demodulator described in Section 2.1 was realised and tested in the presence of Gaussian noise, without the generated signals being transmitted through the underwater medium or the adaptive array being used [5]. Typical performance results (probability of error against SNR) are shown in Fig. 2 for DPSK and PN coded DPSK (SR=4 and 8), and indicate that the modulator - demodulator is able to achieve the required reliability (low error probability). For example, Fig. 2 shows that the PN coded DPSK modulator - demodulator is able to attain an error probability of 10^{-5} (suitable for submersible control commands) when SNR (at the input to the demodulator) is 2.06 dB and -2.74 dB for SR= 4 and 8 respectively.

The adaptive array was implemented digitally using the bit-slice technology to achieve the high sampling frequencies required for operation at the carrier frequency [7]. To assess the performance of the adaptive array it was first tested by itself, without the reference signal generation loop. A few of the results of these tests are presented here. A 127-bit long PN code sequence was PSK modulated and then transmitted over a path length of 2 metres to the adaptive receiving array. The separation distance was kept short because of the small water tank that was used for these tests. An ideal reference signal was provided for the adaptive array by means of a "cheat-wire" from the transmitter. This reference signal was a time delayed version of the transmitted PN coded PSK modulated signal with the time delay corresponding to the direct path delay through the water. Therefore the reference signal for the adaptive array was an ideal direct path signal. The transmitted and received waveforms for this test are shown in Fig. 3. The PN code is shown in Fig. 3(a) and the transmitted PN coded PSK modulated signal is shown in Fig. 3(b). The adaptive array output waveform after convergence is shown in Fig. 3(c). This waveform is a delayed version of the transmitted signal and although it has some distortion due to bandlimiting, the phase changes are clearly visible. The weights of the FIR filters were originally set-up to give a mainlobe beamwidth of over 100°. After the adaptive array had converged, the filter weights were frozen and a beampattern was taken. This beampattern is shown in Fig. 4. It can be seen that a mainlobe of approximately 14° beamwidth has been formed at the 0° direct path signal. This therefore shows that the adaptive array has tracked the direct path signal.

3. CONCLUSIONS

In this paper, a brief description of a proposed reliable high data rate underwater acoustic data link has been given. The main sections of the link consisting of a PN coded DPSK modulator - demodulator and an adaptive receiving array have been shown to provide the required high data rate and multipath reduction properties respectively. In addition, it has been shown that the PN coded DPSK modulation scheme chosen to provide a reference for the adaptive array, is able to produce the desired low error probability at attainable SNR's.

REFERENCES

[1] F.G. Stremmler, "Introduction to Communication Systems", Addison-Wesley, 1982

[2] B. Widrow, P.E. Mantey, J.J. Griffiths and B.B. Goode, "Adaptive Antenna Systems", Proceedings IEEE, No. 55, 1967, pp2143-2159

[3] W.C, Lindsey and M.K. Simon, "Telecommunication Systems Engineering", Prentice-Hall, 1973

[4] R.C. Dixon, "Spread Spectrum Systems", Wiley-Interscience, 1976

[5] H.D. Davidson, "A Reliable Data Channel for Underwater Communications using Phase Shift Keying", PhD Thesis, University of Newcastle, to be published.

[6] R.A. Monzingo and T.W. Miller, "Introduction to Adaptive Arrays", Wiley-Interscience, 1980

[7] P.J. Mulholland, "Adaptive Filters and their Application to an Adaptive Receiving Array for an Underwater Acoustic Data Link", PhD Thesis, University of Newcastle, to be published.

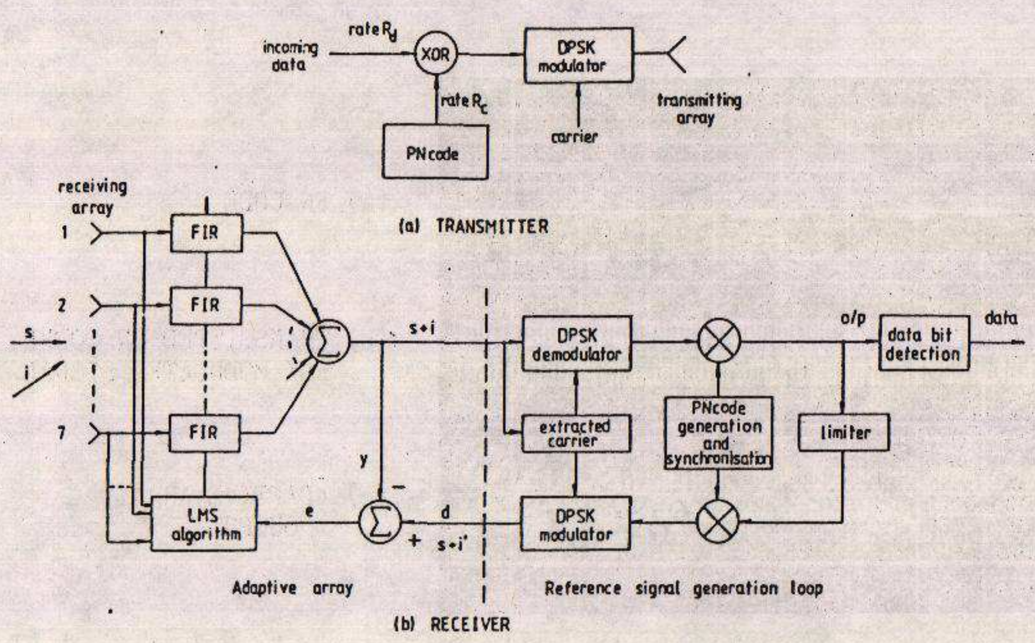

FIG.1 THE PROPOSED UNDERWATER ACOUSTIC DATA LINK

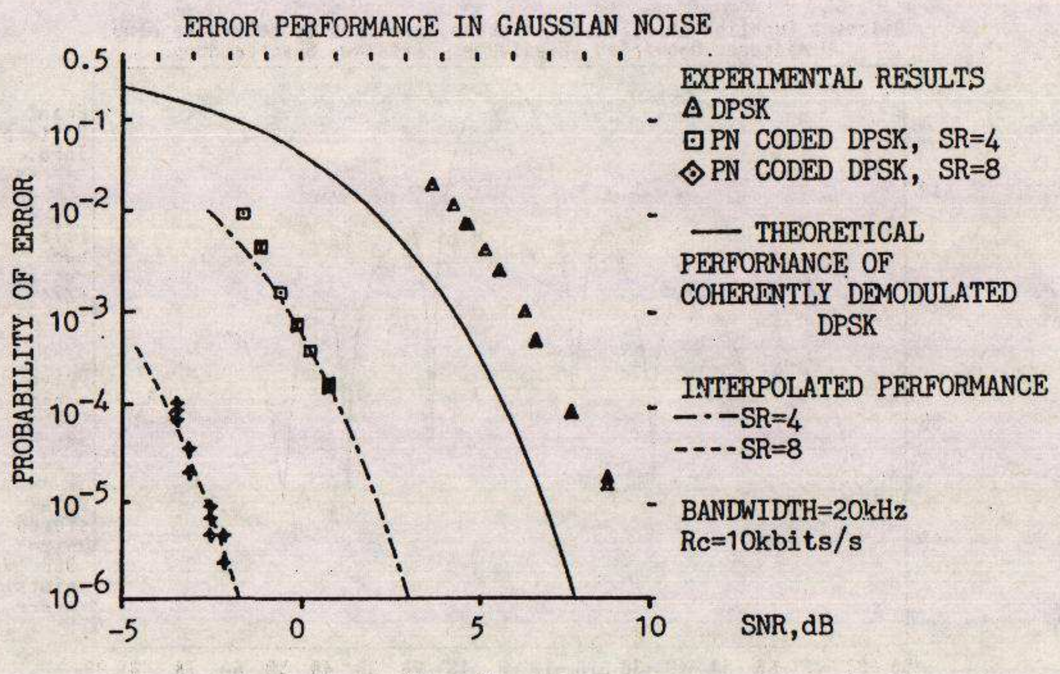

Fig. 2

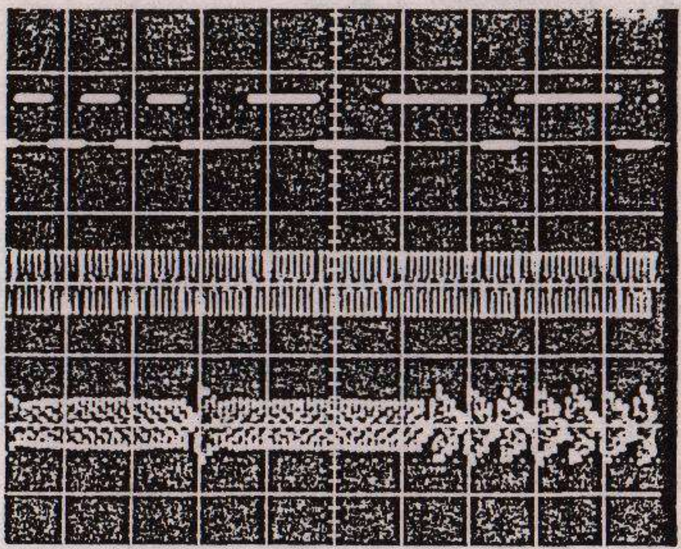

(a) PN CODE

(b) TRANSMITTED PN CODED PSK MODULATED SIGNAL

(c) ADAPTIVE ARRAY OUTPUT

Fig. 3

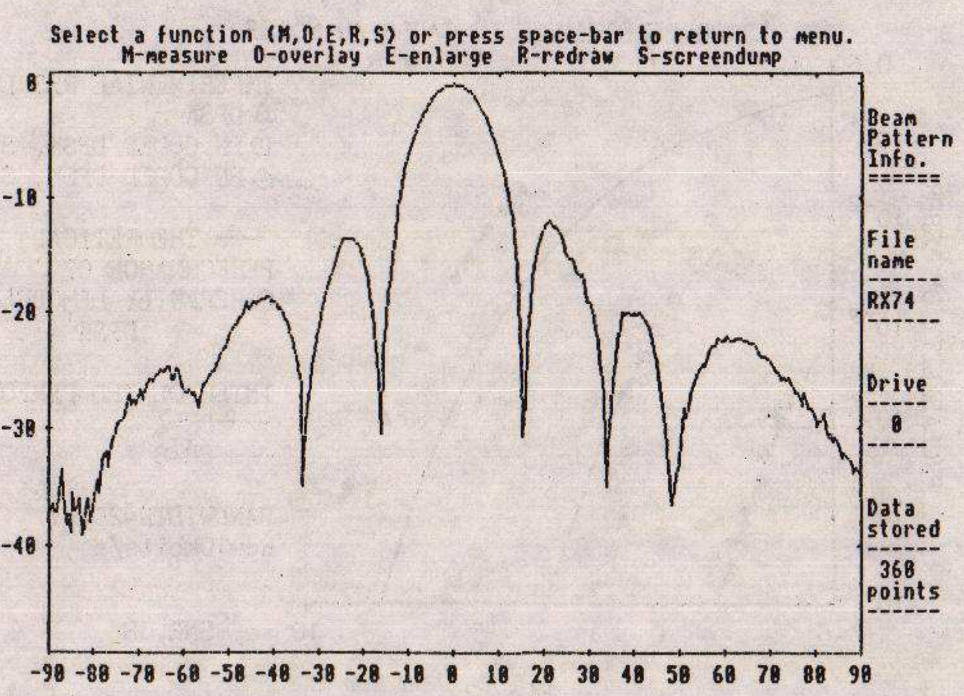

Fig. 4

Proceedings of the Institute of Acoustics

PATSY: THE PULSED ACOUSTIC TELEMETRY SYSTEM

C.G. Flewellen

Institute of Oceanographic Sciences, Deacon Laboratory,
Wormley, Godalming, Surrey GU8 5UB

INTRODUCTION

PATSY was developed under a joint contract with the Department of the Environment and the Joint Research Centre, to provide a means of transmitting information from a Deep Ocean Model Penetrator (DOMP) buried in sediment.

A penetrator is a 2 tonne projectile that is allowed to fall from a ship, reaching a terminal velocity of around 50 m/sec before impacting with the sediment. Penetrations of between 20 and 40 metres have been achieved.

Penetrators have been equipped with continuous wave acoustic transmitters (operating at 12 kHz). The doppler shift in the signal, received at the ship, has been used to measure the penetrator's velocity and by differentiation and integration, the depth of penetration and the deceleration, respectively.

It was desired to measure directly the deceleration of the centre-of-mass and log data from a range of sensors during the descent through the water-column, during deceleration and after the penetrator had come to rest. The sensors were to include tilt-meters, accelerometers, a temperature sensor and differential pore-pressure gauges.

A computer controlled logging system was developed able to sample sensors at a variety of rates during the descent of the penetrator and then to encode and transmit these data.

A number of advantages to be gained over the doppler system include:-

(i) The information would not be transmitted through the noisy wake of the penetrator.
(ii) Deceleration could be sampled faster than the information bandwidth of a doppler system.
(iii) A great deal more information could be transmitted.
(iv) A lower frequency could be used to reduce the effect of attenuation through the sediment.

DESIGN CONSIDERATIONS

Signal to noise ratio and operating frequency

The signal level received at the ship from the penetrator transmitter, in 30 to 40 metres of sediment and 6000 metres of water, should be higher than the noise level in poor weather conditions by at least 10 dB. In deep water beyond about 1 kHz the dominant noise is due to breaking waves and the oscillation of vapour bubbles and falls off at about 5 to 6 dB/octave [1]. As attenuation in water is rising at about 6 dB/octave the signal to noise ratio can remain substantially constant in the range 1 to 20 kHz. However, the attenuation in the sediment is an exponential function of both frequency and penetration depth and this dictates the use of a low frequency.

Using a figure of 0.1 dB $m^{-1}kHz^{-1}$ for the attenuation in deep ocean sediments (Clay and Medwin [2]) the attenuation through 40 metres of sediment would be:-

at 1 kHz 4.0 dB
at 20 kHz 80.0 dB.

(Measurements made in the Great Meteor East Abyssal Plain at 12 kHz suggest a figure of about 0.05 dB $m^{-1}kHz^{-1}$ [3]. This low figure may be due to the fact that the sediment drawn in behind the penetrator is not as compact as undisturbed sediment).

Ship's self noise can become dominant in the low kHz but this is at least an avoidable source as the ship can be allowed to drift with main engines off during listening.

A frequency of 3.5 kHz was chosen (slightly lower than optimum) because the Institute uses this frequency for sub-bottom profiling and thus receiving equipment would be available.

Sonar calculations were made assuming this frequency and the use of a commercially available ceramic ring transducer with about 200 Hz bandwidth. PATSY was designed both to telemeter data at a crystal controlled rate as well as to transpond to interrogation by the ship's 3.5 kHz transceiver.

Sonar Calculations

Assuming:-

Operating frequency	= 3.5 kHz
Water depth	= 6000 m
Penetration depth	= 35 m
Attenuation in sediment	= 0.1 dB/m-kHz
	= 12 dB one way
Power of ship's system	= 2 Kw
with directivity index	= 10 dB
Power of telemetry system	= 100 W
with directivity index	= 5 dB
and with 5 msec pulse, bandwidth	= 200 Hz
Sea-state 6 noise in 200 Hz bandwidth	= -42 dB re 1 Pa

(1) Sound pressure level at transducer

Transceiver source level	= 33 dB re 1 watt
+ 50.8 dB re 1 Pa/watt @ 1 metre	= 83.8 re 1 Pa
+ 10 dB directivity index	= 94 dB re 1 Pa
Losses:	
Spreading loss over 6000 m	= 75.6 dB
Water attenuation (@ 0.25 dB/km)	= 1.5 dB
Scattering loss	= 3.0 dB
Loss due to acoustic impedance mismatch at the bottom	= 1.0 dB
Attenuation through sediment	= 12 dB
Total	= 93 dB
Thus sound pressure level at transducer	= 1 dB re 1 Pa

(2) Sound pressure level at the ship	
Transducer source level	= 20 dB re 1 watt
+ 50.8 dB re 1 Pa/watt @ 1 metre	= 70.8
+ 5 dB directivity index	= 76 dB
With the same losses the level at the surface will be	= -17 dB re 1 Pa

This is about the same level as the profiler's bottom echo assuming 30% reflectance.

Thus the signal to noise ratio at the ship would be about 25 dB.

(3) Sing-round level at transponder	
The total losses will be greater by 6 dB because of the double path plus the remaining losses repeated, i.e.	= 93 dB
Extra distance	+6
Other water losses	+5.5
Sediment attenuation	+12
Total	= 116.5 dB re 1 Pa
With a transponder source level of 76 dB re Pa the sound pressure level back at the transponder will be	= -40.5 dB re 1 Pa

This is about 40 dB below the expected level from the ship. This assumes 100% reflection at the surface.

(4) Noise level at transducer	
The level near the surface will be about -42 dB re Pa and there will be a few dBs drop in the water-column due to attenuation, scattering and refraction. It is expected that the noise will receive a similar attenuation in the sediment, as the signal. Allowing 15 dB for these losses	
Noise level at transducer	= -57 dB re Pa
Ship's noise could, however, add considerably to this.	
(5) Transducer receiving sensitivity	-95 db re 1V/Pa

Data Encoding

The encoding techniques available for acoustic telemetry of data include modulation of the phase, frequency or amplitude of a carrier and modulation of the time interval between pulses.

Amplitude and phase modulation of a carrier are impractical in deep water for at least three reasons:-

(1) Signal to noise ratios better than 20 dB are rarely achieved so there would be very limited dynamic range.
(2) Acoustic signals do not travel by simple "line-of-sight" paths but by multiple paths differing by only fractions of a wave-length due to small angle scattering and turbulence. The combination of signals produces randomly varying amplitude and phase distortions at the receiving hydrophone.
(3) Reverberation from layers within the sediment and from the water surface interfere with the direct signal, although the effect can in theory be removed if the pattern of echoes is constant or only changing slowly.

Frequency modulation suffers like phase modulation unless frequency shifting is used though this uses available bandwidth and energy less efficiently than other techniques.

Time modulation, using the time delay between two short pulses to carry the information, can be very efficient and can have a large dynamic range. Its disadvantage is that it is slow, though signals can be multiplexed to increase the effective data rate.

Digital coding using frequency shift keying could have unlimited resolution by merely extending the number of bits in a sequence but is very expensive in energy. Pulse interval telemetry (P.I.T.) uses only one pulse per data word (plus one reference pulse) and the resolution is limited only by the maximum time that can be allowed to elapse between the pulses. P.I.T. is, however, a form of analogue modulation and will suffer from timing noise. This will arise from amplitude noise riding on the signal and variations in path-length as the receiving "fish" heaves up and down with the swell.

The effect of additive noise is to produce a timing jitter on the edge of the received pulse of about:

$\Delta t = \left(\frac{VN}{VS}\right)$ tr where tr is the pulse rise time
VN is the rms noise voltage
VS is the pulse amplitude

The assumption is made that the signal to noise ratio is at least +6 dB.

This jitter will be present on both the reference and signal channels but will be uncorrelated, so the jitter on the time difference is:-

$$\sqrt{2}.\left(\frac{VN}{VS}\right).tr$$

If the maximum time delay available is tm then the resolution of the channel is

1 part in $\frac{1}{\sqrt{2}} \cdot \left(\frac{VS}{VN}\right).\frac{tm}{tr}$

given $tr \approx \frac{.4}{B}$ $\quad B = 200$ Hz

$tm = 2$ seconds, say

and $\frac{VS}{VN} = 2$, i.e. 6 dB S/N

then the resolution is 1 in 1414, i.e. between 10 and 11 bits. The bit rate is thus around 5 bits/sec for a single channel. However increasing the number of channels from 1 to N is straightforward, the only decision required concerns whether the pulse intervals for different channels will be allowed to overlap, in which case for (N+1) pulses transmitted 10N bits equivalent are communicated. In previous underwater applications of P.I.T. overlapping intervals have been allowed and not found to cause undue confusion using a form of direct line scan recorder display. However, this feature clearly relies on the recognition of which pulse belongs to which channel at every new frame of pulses.

If the shipborne receiving transducer is heaving at a rate V m/s between the arrival of reference and signal channel pulse, the timing error introduced in addition to the random noise component above is given by (V/C) td where C is the sound speed (~1500 m/s) and td the signal delay. Generally V will be less than 1.5 m/s, in which case the error amounts to less than .1% of the signal.

THE FINAL DESIGN

To cope with the complexity of sequencing the logging of a variety of sensors at different rates and then encoding and transmitting these data; the design was based around a microprocessor running FORTH. Signals were sampled via an eight way multiplexor and a 12 bit digital-to-analogue converter under direct control of the microprocessor and stored in about 40 kilobytes of memory. Duplicate accelerometers were sampled at 500 Hz during the critical phase of deceleration through sediment. Figure 1 shows the appearance P.I.T. received and displayed on a line-scan recorder with a repetition period of 2 seconds. The two accelerometer signals were encoded with different offsets from the reference pulse to separate the displays and to allow for the small negative excursion as the penetrator bounces up about 1 cm before coming to rest.

Each return represents a 5 millisecond pulse of 100 watts at 3.5 kHz. This data was recorded in shallow water in the Mediterranean off Cap d'Antibes. During this experiment some 760 Kbits of data were transmitted at an average baud-rate of 13.6.

Fig. 1 P.I.T. of deceleration through sediment.
Sampled at 500 Hz. Duration of deceleration = 570 mSec.

REFERENCES

[1] G.M. Wenz, 'Acoustic ambient noise in the ocean: spectra and sources', J.A.S.A., Vol. 34 (1962).

[2] C.S. Clay and H. Medwin, 'Acoustical oceanography', Wiley, New York (1977).

[3] T.J. Freeman, A.K.R. Bromley, N. Cooper and C.N. Murray, 'BRE/JRC penetrator experiments: analysis of results and comparison with predictions', A contribution to the report of the 1985 ESOPE cruise, which is being published by the Joint Research Centre, Ispra, Italy.

[4] C.G. Flewellen, 'Development of a pulsed acoustic telemetry system for penetrators', London, Department of the Environment (1987).

ACKNOWLEDGEMENTS

This work was performed as part of the Department of the Environment's radioactive waste management research programme, and in the framework of the European Atomic Energy Community's indirect research programme on 'Management of Radioactive Waste'.

Special thanks to:-

Building Research Establishment (D.O.E.) (T.J. Freeman, A.K.R. Bromley).
Joint Research Centre, Ispra (C.N. Murray).

Proceedings of the Institute of Acoustics

FINMAP - A DIVER-CARRIED, UNDERWATER, NAVIGATION, MAPPING AND DATA AQUISITION SYSTEM

P.J. Hanna and R.D. Peden

School of Sciences, Deakin University, Victoria 3217 Australia

INTRODUCTION

FINMAP (Fig. 1) is an acronym for Fisheries Navigation and Mapping by Acoustical Positioning and consists of an underwater computer, a data logger and a personal navigation system that allows a scuba diver to navigate and map his or her way on the sea floor, simultaneously recording marine observations. The FINMAP computer controls a diver-carried active sonar, transmitting to triad of underwater acoustic transponders. The sonar system provides personal navigation and mapping during day and night, and does away with the need for underwater grids for the collection of marine data. The underwater keyboard provides the diver with means of entering data observations directly into computer memory. The display gives a direct read-out of position and depth which can be automatically stored in memory together with any observed data.

Keyboard switching is determined by infrared reflection from a diver's finger touching on a solid state key. The display unit is a memory mapped array of seven segment light emitting diodes (LEDS). Both the keyboard and display are totally encapsulated in a plastic potting medium and are thus able to withstand submersion to over 100 metres and the corrosive effects of seawater. Computer interfaces are being developed that allow the connection of marine instrumentation and the automatic collection of data such as temperature and salinity.

FINMAP will be used in marine research, underwater archaeological mapping, underwater surveillance and monitoring and underwater industrial applications.

COMPUTER

The computer (Fig. 2) is carried in a sealed waterproof tube on a diver's back together with the interfaced sonar navigation system. The microcomputer is the Rockwell R65F12, [1] an 8-bit NMOS chip, compatable with the well known 6502 microporcessor of the Apple computer. On a single chip, measuring 41 mm x 17 mm, is fabricated an enhanced 6502 microprocessor, an internal clock oscillator, 192 bytes of random access memory (RAM), 3K bytes of read only memory (ROM). 40 bidirectional input/ output (I/O) lines, two 16-bit programmable counter/timers, a serial port and ten interrupts. Externally there are 16K bytes of memory and 16K bytes

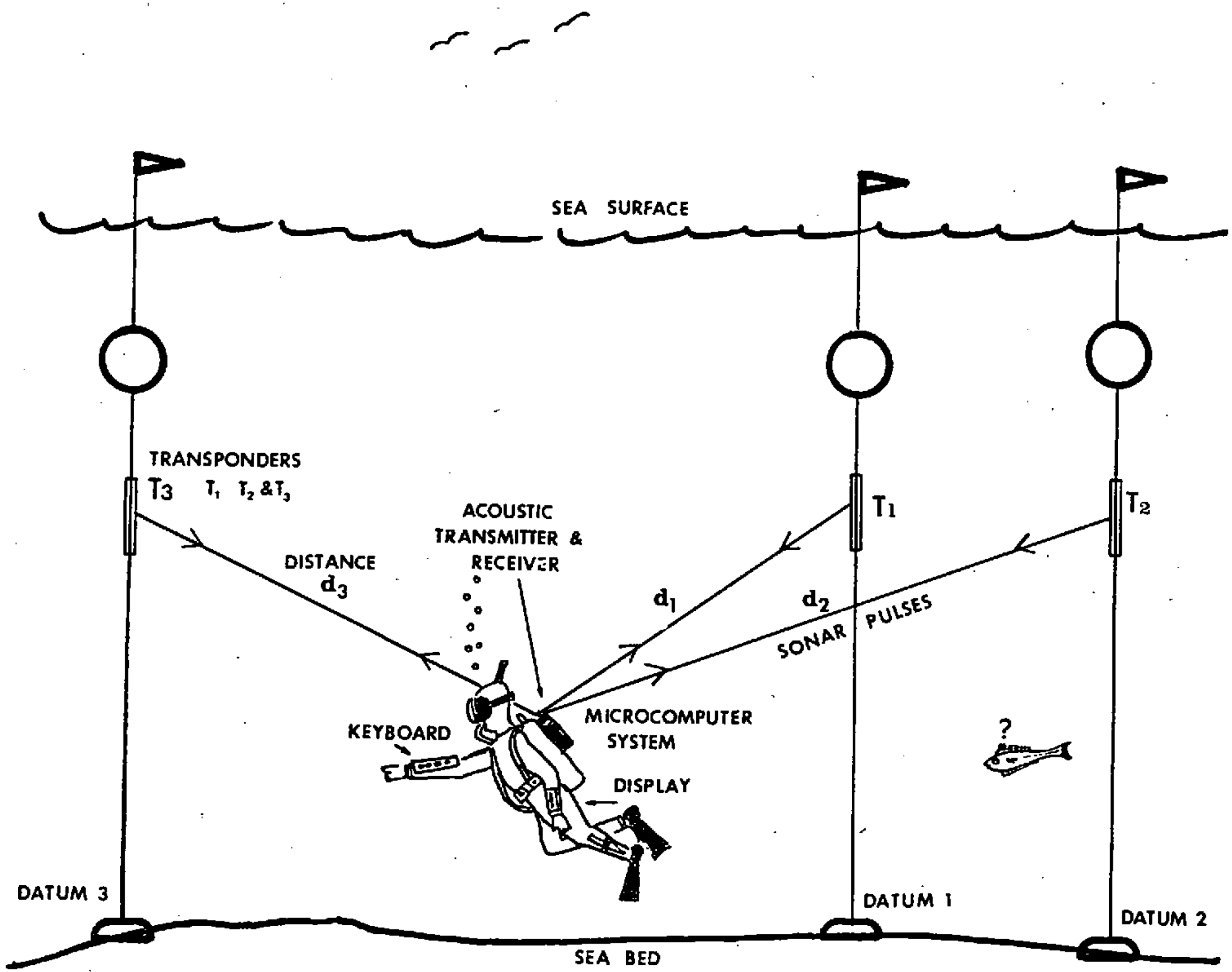

FIG 1. BASIC FINMAP SYSTEM

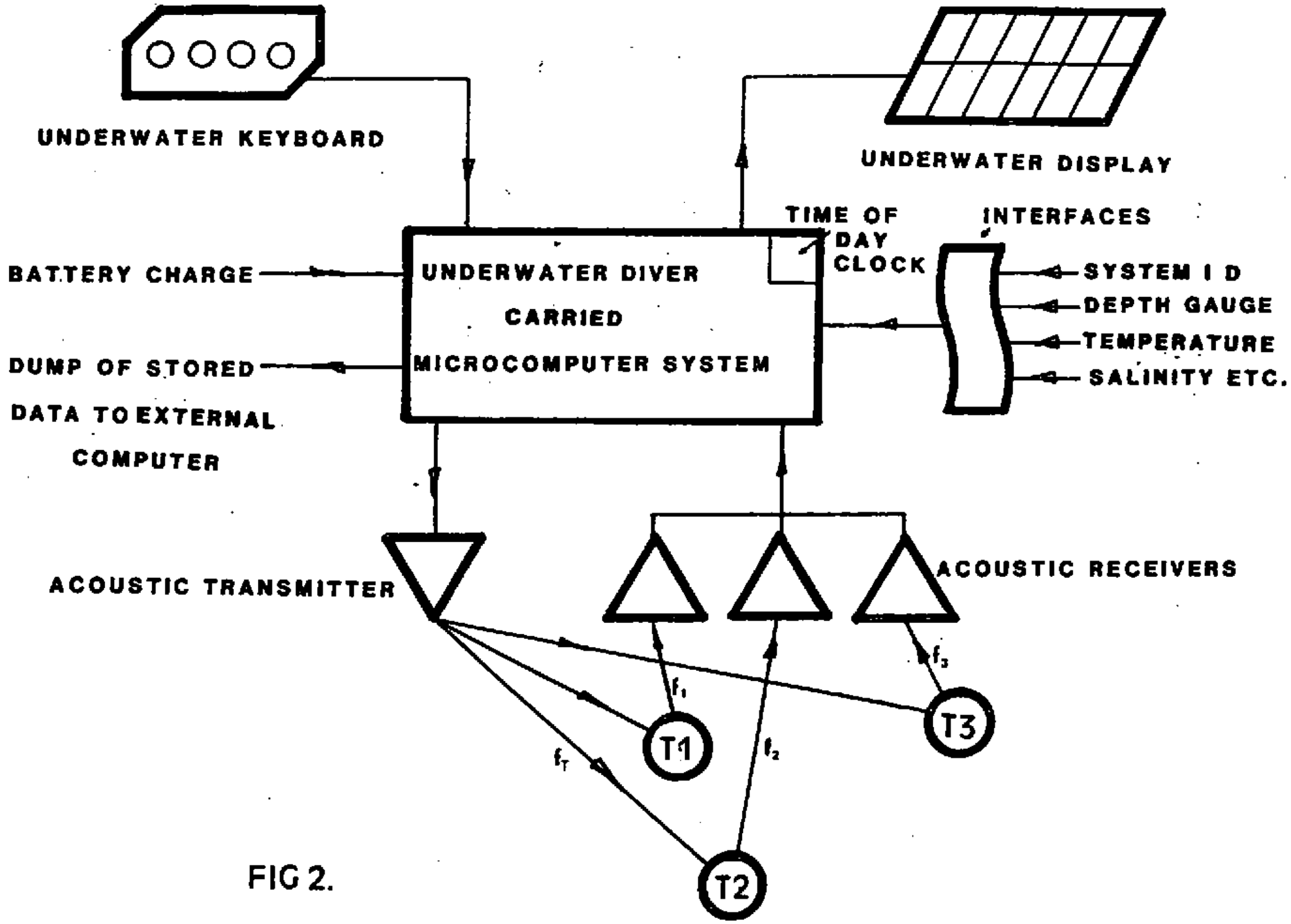

FIG 2.

FINMAP – UNDERWATER PERSONAL NAVIGATION, MAPPING AND DATA AQUISTION SYSTEM of banked switched memory, 10 analogue to digital converter (DAC) output lines, an RS232 serial port, a parallel printer port and a disk controller interface.

During diving the computer is controlled by a wrist-mounted five-key keyboard and an 18 character LED display. Data entered through the keyboard or input via the ADC lines or from the navigation system can be stored in memory for later graphing and analysis. The sonar navigation system is controlled through an I/O port, and the programmable timers measure the acoustic time intervals. Onboard ship or back in the laboratory the computer connects directly to a terminal or host computer (e.g. IBMPC or Macintosh). Separate disk drives may be connected, or those of the host computer used. Thus the full power of any host computer software may be used to process the collected data or to map the results of a survey. It is possible to program FINMAP remotely using a modem and a telephone or radio link. Thus expensive computer equipment need not be exposed to the hazards of a sea environment.

SOFTWARE

A basic element in the development of FINMAP has been the use of the Forth computer language [2] in the development of software. This was the main reason for the choice of the Rockwell R65F12 microcomputer as it has the nucleus of the Forth language stored in ROM. The program controlling FINMAP, the navigation algorithms, the disk interface, the printer port, the memory mapped LED wrist display, are programmed in Forth.

Forth provides a unique method of rapid software development. For the non-programmer programmer (e.g. an engineer), Forth provides efficient and error (bug) free environment for programming controllers, instrumentation and data loggers.

KEYBOARD

The keyboard (Fig. 3) is totally encapsulated in plastic; an effective way of isolating the electronics from seawater. The FINMAP keyboard uses a reflected infrared beam to detect a key closure. A narrow beam of infrared radiation is modulated in intensity by a frequency of 1000 Hz. The beam shines at an angle through a depressed clear portion of the encapsulating plastic. A diver's finger, when placed into the key area has this modulated

FINMAP KEYBOARD

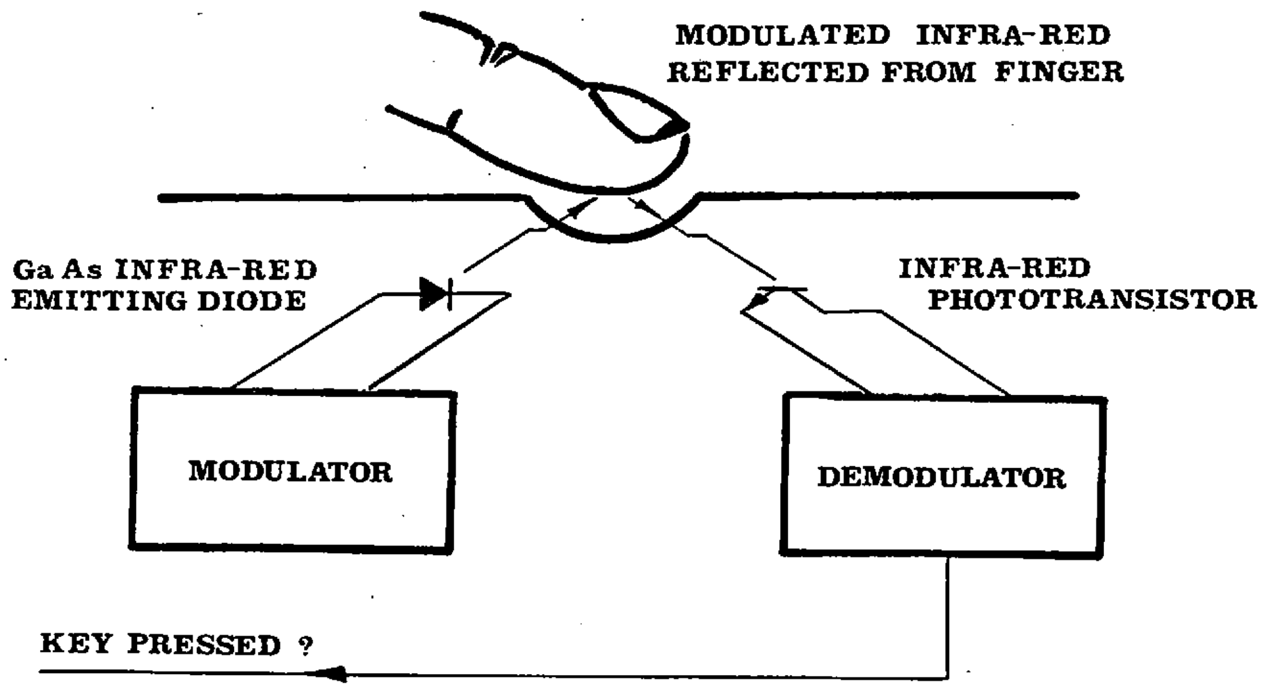

FIG 3.

PRINCIPLE OF THE FINMAP UNDERWATER INFRA-RED KEYBOARD

light reflected back down towards an electronic infrared receiver. The received infrared is tested for modulation (otherwise the direct rays of the sun might close the switch) and if present, a key closure is recorded.

The keyboard consists of five keys. However with mode switching the keys can be multi-purpose. Consideration of how divers react underwater, particularly the difficulty in performing intricate underwater tasks, lead to the choice of a simple five key arrangement over a more elaborate keyboard.

DISPLAY

With the help of divers at the Marine Science Laboratories at Queenscliff [3], the requirements of underwater displays were investigated with regard to colour, intensity and size. In brief the subjective findings were that the best viewing colour was red, that the intensity should be low relative to normal above water viewing and that a good size for comfortable viewing on the wrist was a character height of 8 mm.

Like the keyboard the display is totally encapsulated. An aim was to serially control the display to minimise the number of connecting wires to the computer. The FINMAP display (Fig. 4) is memory mapped with an 8-bit register associated with each of the 18 displayed characters. The display is switched at 100 Hz with an 'on' duty cycle of 10%. The displayed characters are sent in 'packets' of serial data transmitted at 500K baud. All the circuitry is constructed in complementary metal oxide semiconductor (CMOS) to minimise power consumption.

NAVIGATION SYSTEM

The position of the diver is determined relative to the location of a datum transponder, one of a triad of underwater acoustic transponders tethered some hundreds of metres apart on the sea floor. The shape and size of the triad is determined under mode 1., one of the eight modes of operation of FINMAP. The Forth control word TRIAD is invoked to measure the sides of the triangle and to locate the X-Y co-ordinates. The transponders upon receiving an acoustic pulse from the diver, return corresponding pulses at three different frequencies. The FINMAP computer determines the acoustic travel time from each transponder. As sound travels at almost exactly 1500 m/sec underwater, the three distances between diver and transponders can be accurately determined. The Forth word DIVER then calculates the diver position relative to the previously determined X-Y co-ordinates. If necessary FINMAP can make allowances for both temperature and salinity, in selecting the acoustic velocity. If, because of acoustic shielding one or more transponder signals are not received, an error condition is signalled and an algorithm is invoked (the Forth word ? WHERE) to best estimate the current position.

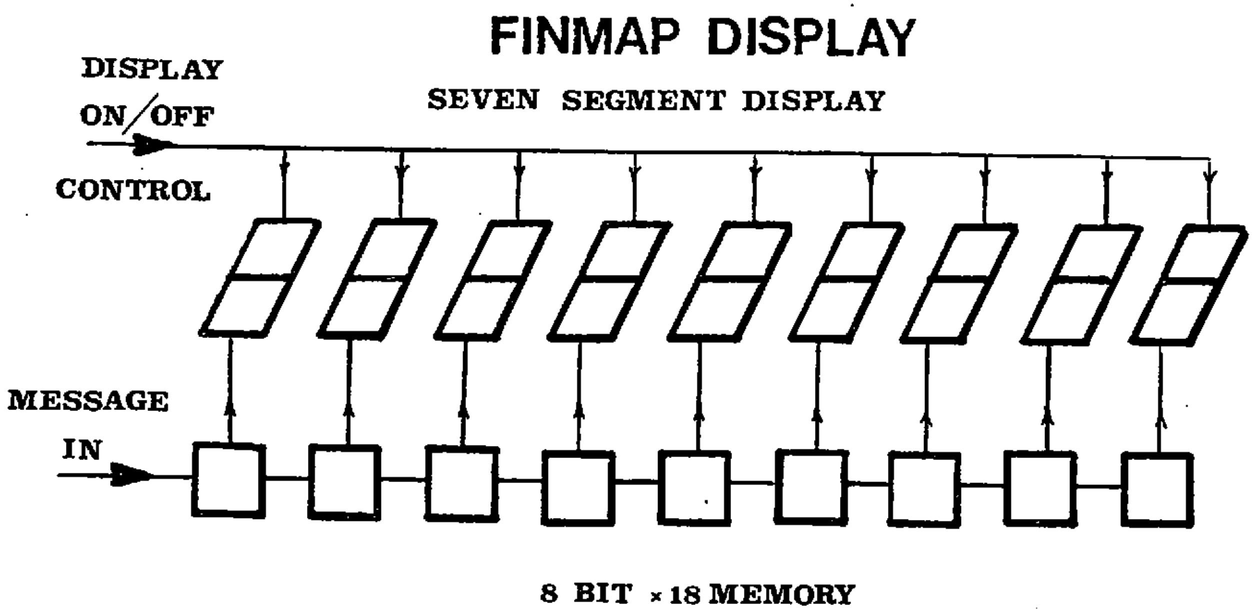

FIG 4.

BASIC CIRCUIT OF THE FINMAP UNDERWATER, MEMORY MAPPED, DISPLAY UNIT

The co-ordinate diver location is displayed as two four digit decimal numbers corresponding to units of 10 cm. Alternatively diver position can be displayed in polar co-ordinates of radius and angle in degrees. If a depth transducer is interfaced to the computer the depth below sea level can also be displayed. It is noted that in principle a three transponder navigation system can also calculate a depth reading. However in normal shallow water diving conditions the accuracy of the depth measured is low and hence in practice a depth transducer needs to be interfaced.

APPLICATIONS

The most important use of FINMAP is as a portable personal underwater navigation system. Marine biologists are often required to collect quantitative data on environmental conditions and to sample the many attributes of individuals, populations, communities and ecosystems. The high degree of variability of the observations requires that proper statistical techniques be used, with sampling being carried out in a random manner. Commonly this is done by marking out an underwater grid with observations then made at randomly selected grid squares. The process is time consuming and costly.

FINMAP can generate a random selection of co-ordinates appropriate to the area being investigated. The display can be set to simultaneously show selected random co-ordinate positions together with actual position. The diver swims until the co-ordinates coincide and the sample is taken. If the transponder locations are fixed the diver can reposition at some later time and hence make repeated observations.

Any sampling procedures can be offered such as sampling by quadrats. An elongated rectangle is a typical shape. Quadrats are usually physically marked out on the sea floor. FINMAP however will effectively produce an electronic quadrat. A diver simply swims so as to keep one co-ordinate at a time constant. Thus a diver is able to swim around the quadrat and of course within it. Plotless sampling is easily made available via the generation of random co-ordinate pairs. Line intercept techniques are possible by generating co-ordinate positions along line transects or if using the polar co-ordinate mode, producing lines of constant angle. Any sampled data can be input via the keyboard (this is presently done by slate) and is stored in computer memory together with co-ordinate positions.

It follows from the navigation function that mapping is also available. With a depth transducer interfaced three dimensional mapping is possible. Maps can be automatically created by simply swimming around the perimeter of the physical feature being mapped or FINMAP can be set to take co-ordinate readings under the control of the diver. The recorded observations can be later graphed on display or plotter and of course manipulated and reoriented by one of the many software graphics packages. Marine archaeologists should find this facility of great benefit.

One of the first applications of FINMAP will be to observe the movement of the Crown-of-Thorns starfish on Australia's Great Barrier Reef. Tiny magnetic-induction-field operated transponders from System ID [4], precoded with a unique identifying number, are to be implanted in selected starfish. The FINMAP computer will interface to a search coil that will excite the transponder, detect the returned code number thus identifying the starfish, and record this identity number together with underwater location. Repeated observations over a period of time will help determine the pattern of starfish movement along a reef.

In conclusion it is noted that FINMAP is a general purpose underwater computer. Hence in principle it can be applied to any underwater application requiring computer power. Thus FINMAP can act as a stand along underwater personal computer, it can operate as a data logger, it can connect to any variety of instrumentation, digital or analogue, and it can operate as an underwater controller. It offers both navigation and mapping and back on land it can directly connect to host computer to use sophisticated software analysis packages.

HYPERBOLIC SYNCHRONOUS NAVIGATION

For commercial applications it was considered necessary that more than one diver be able to simultaneously navigate and utilise the FINMAP transponder system. Hyperbolic synchronous navigation, or Hysyn for short, is one of a number of optional position fixing techniques being considered for FINMAP that allows simultaneous diver position fixing. Hysyn employs a combination of hyperbolic and real time position fixing. Using Hysyn a diver carries a clock that is periodically locked in phase with a system master clock associated with a master transponder. Hyperbolic position fixing is used to locate the position of a diver relative to the master acoustic transponder acting during this activity only as an acoustic projector. The master projector excites the other FINMAP transponders which respond with acoustic replies after known time delays. The hyperbolically determined position is compared with a real time position calculation and the diver clock adjusted so that both positions equate. This effectively locks the diver clock in synchronism with the master system clock. Calculation of a diver's position by the FINMAP microprocessor can now proceed directly using real times without recourse to time differences and hyperbolic calculations. Periodically the diver clock is re-synchronised using a hyperbolic calculation. The establishment of a common clock for all divers, in synchronism with a master clock, also allows data transmission between divers and divers and any surface vessel during agreed upon time slots.

ACKNOWLEDGEMENTS

P.C. Smith, Technical Officer; Steven Kok, postgraduate student; Ian Kaminskyj, postgraduate student.

FINMAP - A DIVER-CARRIED, UNDERWATER, NAVIGATION, MAPPING AND DATA AQUISITION SYSTEM

The FINMAP project is supported by a research grant from DATA ELECTRONICS PTY. LTD., 46 Wadhurst Drive, Boronia, Victoria, 3155, Australia.
A commercial version of the FINMAP system is under development by DATA ELECTRONICS PTY. LTD.

REFERENCES

[1] Rockwell, R6511 and R6512 Forth Microcomputers (October 1984) Document No. 29651N49. Rockwell International, Newport Beach, California.

[2] Brodie, Leo (1981) Starting Forth. Forth Inc. Prentice Hall.

[3] Marine Science Laboratory, Weeroona Avenue, Queenscliff, Victoria, 3225, Australia.

[4] System I.D. Identification Devices Inc., 9101 Harlon Street, Suite 300, Westminster, Co. 80030.

Proceedings of the Institute of Acoustics

DIVER NAVIGATION AND SEA-BED SURVEYING EQUIPMENT

R.L. Mansfield, B.K. Gazey and B.V. Smith.

Dept. of Electronic and Electrical Engineering,
University of Birmingham, England.

INTRODUCTION

There has been a continuing interest shown in the literature [1,3,5] in diver navigation systems. This present paper describes a real time, self contained, battery operated, personal diver navigation system. In addition to functioning as a ship guidance system for use in difficult waters it also offers modes for shallow water sea bed surveying with consequent applications in mapping archaeological sites, oil rig sites, harbours, sea shores and estuaries. In operation a hand held interrogator unit enables a free swimming diver to obtain precise positional information relative to two transponder base stations deployed on the sea floor. Although the use of only two base stations has consequent operational restrictions it has never the less proved suitable for specific applications. Depth and positional information relative to these fixed base stations are stored at regular intervals in the diver held interrogator unit under micro-computer control for later retrieval. Range is measured conventionaly in terms of the round trip flight time of a short duration sound pulse between the interrogator and the activated transponder. Depth is measured using the pulse echo principle. This allows specified sites on the sea bed to be surveyed enabling depth contour lines to be mapped. If required both battery operated base stations can be left in position, in an automatic shut down mode, for later navigational use. Results obtained with a prototype system in a flooded quarry are presented and confirm the feasibility of the method.

PRINCIPLES OF OPERATION

The main problems envisaged with an acoustic navigation system of this type is in its operation near the water surface and in areas of shallow water. The signal processing involved will have the task of discriminating between sonar pulses and the combined effect of ambient noise, reverberation and, in particular, multi-path effects. A long baseline system (LBL) can be utilised for accurate navigation in areas of shallow water, positional information being determined by multiple range measurements. The accuracy of this LBL system relies upon the estimation of sound speed in water and the accuracy of emplacement of two transponders in line of sight with each other. The advent of intelligent transponders enables transponder baseline distances to be independently established.

In operation one of the base stations, for convenience termed the slave, is deployed on the sea-bed at a desired location. The diver held interrogator unit is switched to mode one which gives the range between the interrogator unit and the slave base station. The diver then deploys the second base station, for convenience termed the master base station, using the interrogators visual display to give an estimate of its range from the slave base station. To obtain precise baseline information the interrogator unit is switched to mode two and plugged into the master base station via an umbilical link (figure 1A). The master base station transmits a frequency, F_0, which the slave base station replies to at its own individual frequency, F_1. The range data thus obtained is transferred to the interrogator unit via an optical data link. The depth of water above the base stations is recorded at the time of transponder deployment and used to compute surface ranges from slant range data. The interrogator unit is then disconnected from the base station and switched to the survey mode, illustrated in figure 1B. The surface swimming diver follows a pre-determined path with the aid of positional information received, and the interrogator unit automatically records and stores at regular intervals transponder range and water depth measurements. These can also be visually displayed. With this information available to the interrogator, the x,y co-ordinates of the diver with respect to the transponders can be computed. If required both base stations can be left in position on the sea-bed and switched to a low-power, shut-down mode ready for reactivation by the interrogator unit.

Applying the sonar equation

The electrical power that must be supplied to produce a specified signal-to-noise ratio can be deduced from the one-way active sonar equation.

The following operational criteria were chosen:-

maximum range = 700 m

nominal operating frequency = 50 kHz

An operating frequency of 50 kHz was chosen due to the availability of transducer elements and from considerations of attenuation and noise. The three signal frequencies have to be contained within the 3 dB bandwidth of the transducer element. A separation of 3 kHz between each frequency results in F_0 being 50 kHz, F_1, 47 kHz and F_2, 53 kHz. The required source level, SL, expressed in dB is then defined:-

$$SL = SNR + TL + (NL - DI) \qquad (1)$$

Where: SNR= signal-to-noise ratio

TL = transmission loss

NL = noise level

DI = directivity index of receiver

Calculation of receiving directivity index.

A cylindrical transducer working at 50 kHz with an outside diameter of 25 mm and a length of 50 mm (see equipment design) will radiate uniformly in the horizontal plane and have a 35 degree, 3 dB, beamwidth in the vertical plane, determined by the finite length of the cylinder. Assuming that the length of the cylinder is much greater than one wavelength (λ) then the directivity index may be approximated by:-

$$DI = 10 \log (2\,l/\lambda) \qquad (2)$$

Where l is the cylinder length. Substituting values gives an approximate DI of 5.2 dB. As a single element will be used for transmission and reception the above directivity index will apply to both.

Noise level.

Very little data is available for shallow water conditions and coastal areas. In such locations the noise is likely to be impulsive and highly variable. Consider an estimated worst case noise spectrum level of:

$$-108 \text{ dB rel. } 1\ Wm^{-2}Hz^{-1}$$

The above noise spectrum level is taken from data for noise spectra in coastal locations with a wind speed of 40 knots [4].

The interrogators transducer transmits at F_0 and receives at F_1 and F_2. Let each channel have a bandwidth of 2.5 kHz.
Therefore the noise in a 2.5 kHz band becomes: NL = -74 dB rel. 1 Wm^{-2}

Transmission loss.
The transmission loss is a function of geometrical spreading (assumed to be spherical for worst case conditions but in practice probably less) and absorption. Spherical spreading results in the energy being spread over an area proportional to r^2, where r is the range. For a one-way trip from array to target the transmission loss is given by:

$$TL = 20 \log(r) + \alpha r \qquad (3)$$

Where α is the absorption coefficient in dBm^{-1}.
At a frequency of 50 kHz the absorption coefficient is approximately 0.01dBm^{-1}
Therefore TL = 64 dB

Signal-to-noise ratio.
During one survey operation the system can store a maximum of 4000 transponder range measurements. At maximum range the signal-to-noise ratio was chosen such that the system would tolerate one undetected pulse per survey, giving a probability of detection of 99.97 %. It was decided that 1×10^{-6} would be an acceptable probability of false alarm and from the receiver-operating-characteristics this predicts that a signal-to-noise ratio of 16 dB is necessary.

Substituting the above into the sonar equation gives a required source level of 0.77 dB rel. 1 Wm^{-2} at 1 m range. The source level, which is a measure of the intensity of radiated sound, may be defined for a directional array as:-

$$SL = 10 \log (1/4\pi) + 10 \log (W) + 10 \log (DI) \qquad (4)$$

Where W is the acoustic power. Therefore the transmitted acoustic power for a signal-to-noise ratio of 16 dB is approximately 4.5 watts.

Positional accuracy

The range of the diver to each transponder is found by measuring the time interval between transmission and reception of an acoustic pulse, from which range is calculated assuming a knowledge of the sound speed in water. An approximate local sound speed in water is calculated by temperature measurement to better than 1°C. As the water temperature is likely to change during the exercise it will be monitored at regular intervals and used to calculate the speed of sound according to an equation given in reference 4. Figure 2 shows contour lines of equal error for a range resolution of 0.3 m and a sound speed uncertainty as a result of temperature measurement with a 1°C maximum error [2]. Although this plot does give an indication of positional errors in practice the front end amplifier will be driven into saturation resulting in a much reduced range resolution error (see equipment design).

EQUIPMENT DESIGN

The detection circuitry has the task of discriminating between sonar pulses and ambient noise. The ambient noise level is likely to have a steady state content and an impulsive content, which will be considered individually. In order to avoid multi-path signals only the first threshold crossing in a given ranging cycle is considered. At maximum range the signal-to-noise voltage ratio has been estimated at approximately 16 dB, this being significantly improved at closer ranges. It can be seen from figure 3 that the signal-to-noise ratio (SNR) for a given threshold level determines the range resolution as a consequence of the timing error. Thus, a high signal-to-noise ratio results in an improved range resolution.

For a fixed threshold level a low ambient steady state noise level will allow a high amplifier gain to be used thereby improving the range resolution without compromising the systems discrimination. As the steady state noise level is a variable parameter, then the receive amplifier is fitted with an automatic gain control (AGC) which can be varied accordingly. A measure of the ambient noise can be obtained by its progressive amplification up to a pre-set noise threshold level (figure 4). The signal threshold level can now be set relative to the noise threshold level to accommodate the worst case signal-to-noise ratio. It will be assumed that both the transponders and the interrogator unit will detect the same level of ambient steady state noise and therefore apply the same amplifier gain.

The ambient noise is likely to have a significant impulsive content during shallow water exercises. Thus by choosing a long pulse length detection period the much shorter impulsive noise signals will be rejected. This will have the effect of reducing further the probability of false alarm.

Amplifier gain

The received signal in the water at the interrogator and the transponder has an intensity, I, given by:

$$I = SL - TL \qquad (5)$$

Which gives: $I = -63.2$ dB rel. 1 $Wm^{-2} = 0.48 \times 10^{-6}\ Wm^{-2}$

$$\text{Also, } I = P^2 \rho^{-1} c^{-1} \qquad (6)$$

Where: P = Acoustic pressure (Pa)
ρ = Density of water (10^3 kgm^{-2})
c = Nominal velocity of sound (1500 ms^{-1})
Therefore the pressure, P, = 0.848 Pa

A typical value for the receive sensitivity, M, of a capped tube = 150 μVPa^{-1}. Therefore the r.m.s. received open-circuit voltage, $V_{o/c\,(rms)}$, for a pressure of 0.484 Pa becomes 127 μV, i.e., the peak value, $V_{o/c\,(peak)}$, = 180 μV. Hence for a 5 V supply rail a receive amplifier gain of approximately 89 dB is required.

Electronic Design

Figure 5 shows, in block form, the complete interrogator unit. Transponder range information is obtained by measuring the time interval between transmission and reception of an acoustic pulse, found by counting 50 kHz cycles using a 16-bit software counter. The transmitted signal is fed into a vmos f.e.t. and then transformed using a step-up voltage transformer, this being matched to the transducer element. The transmitted 50 kHz pulse is received by both transponders who in turn reply on a frequency individual to that transponder. If the interrogator has not received both transponder reply signals before the counter overflows then the operation is aborted. This cycle is repeated every 5 seconds. The received signal is fed into an automatic gain control (AGC) amplifier before being heterodyned up to 455 kHz. The two unwanted frequency components, i.e. F_0 and F_1 or F_2 are filtered out using a narrow band 455 kHz ceramic filter. After rectification the signal is put through a threshold detector which in turn triggers the micro-computer. A decision can then be made as to which of the two transponders is transmitting, i.e. frequency F_1 or F_2. In order to discriminate against impulsive noise that may have tripped the threshold detector, the pulse will be sampled several times before a decision is made as to whether the signal is a valid return or noise. If valid, the micro-computer stores the appropriate count number. This sequence is repeated for each of the transponders. All accumulated data is stored in a 32k byte cmos ram chip, six bytes being allocated to each system operation.

Upon receipt and storage of both transponder reply signals the counter is reset and used to measure the flight time of the depth sounder pulse. The maximum working depth for the echo sounder is not expected to be greater than 30 m. The operating frequency of the depth sounder can be increased resulting in an improved range resolution. An operating frequency of 455 kHz enables the receiver circuit to use 455 kHz ceramic filters without the need for heterodyning. A 15 degree, 3 dB, beamwidth was used to give adequate ground coverage. Figure 6 shows, in block diagram form, the complete depth sounder unit. The depth sounder is packaged with the interrogator unit and is controlled by the interrogators micro-computer but for clarity has been shown in isolation.

Figure 7 shows, in block diagram form, the base station unit. Both transponders receive pulsed signals at 50 kHz and reply on one of two possible frequency channels i.e. 47 kHz or 53kHz. The master base station is also able to transmit at 50 kHz (F_0) and receive at 47 kHz (F_1) for communication with the slave base station in order to obtain the baseline range (see figure 1).

Transducer Design

A thin walled tube was selected for both the transmitting and the receiving elements. The two main modes of resonance in this case are the radial and the length mode. The equation for these modes can be solved for different length/radius ratios. Using this equation and avoiding the critical region where the length resonance approaches the radial resonance, tube dimensions for an operating frequency of 50 kHz were selected. This resulted in a tube of dimensions 25 mm in diameter and 50 mm in length. The tubes were capped and encapsulated in epoxy resin which gave the transducer a final resonant frequency of 49 kHz and a bandwidth of 8 kHz.

RESULTS OF FIELD TRIALS

A prototype of the equipment described was used for a preliminary survey of an area of a flooded quarry at Dosthill, Tamworth. The survey was carried out by towing the interrogator unit behind an inflatable boat. The base stations were deployed on floating platforms securely anchored at fixed positions. During the survey the boat was rowed along the track shown in figure 8c and data collected at 360 points. It can be observed in figure 8c that there was one sharp deviation from an otherwise smooth track, marked by the letter X, this was attributed to a false alarm.

The data collected by the interrogator unit was later downloaded onto a Honeywell main-frame computer and analysed to produce a three dimensional and depth contour plot of the area. These are presented in figures 8a and 8b. Although this quarry has not been previously mapped in detail the survey would seem to have produced a plot which is consistent with what is known about the area.

CONCLUSION

This paper describes a portable system for personal diver navigation and sea-bed surveying in prescribed areas of water. The hand-held, mobile, interrogator unit collects, stores and displays depth readings and precise positional information, obtained from two fixed transponder base stations, for later computation. Data is presented from a trial with a prototype of the equipment at a flooded quarry. Processing of the data has allowed evaluation of the equipments performance in underwater surveying and confirmation of its design. This divers aid has important applications in underwater archaeology, marine biology and geology, as well as uses in guiding and searching operations.

ACKNOWLEDGEMENT

This work was supported throughout by Compact Energy Ltd., Kidderminster, Worcestershire.

REFERENCES

[1] P.H. Milne, 'Underwater Acoustic Positioning Systems', Spon (1983).

[2] C.J. Partridge, 'Electronic Aids to Navigation', Elec. Eng. Ocean Tech., Inst. Elec. Radio Engrs., Symp. Sept. (1970).

[3] G. Shorrock and B. Woodward, 'A Multiple Function Sonar Rangefinder for Divers', Ultrasonics, Jan. (1984).

[4] R.J. Urick, 'Principles of Underwater Sound', McGraw-Hill (1983).

[5] B. Woodward and L.A.A. Warnes, 'Signal Processing Considerations in the Design of a Sonar System for divers', Proc. Inst. Acoustics (1980).

DIVER NAVIGATION AND SEA-BED SURVEYING EQUIPMENT

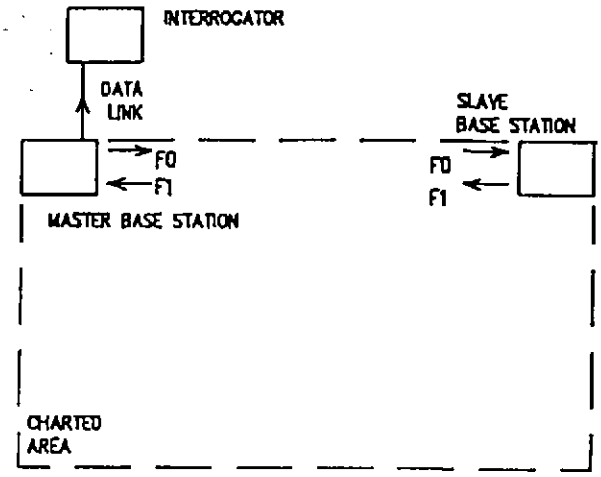

TRANSPONDER RANGE MODE

FIGURE 1A

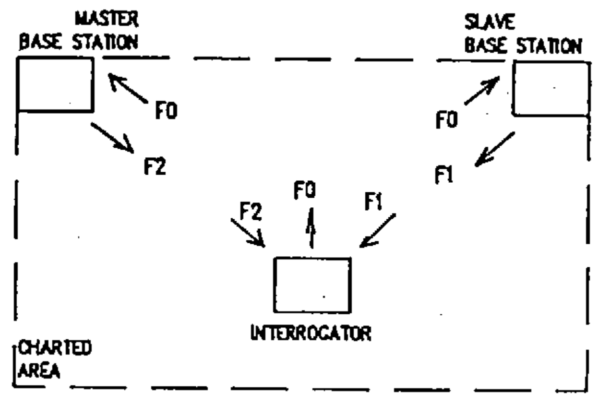

SURVEY MODE

FIGURE 1B

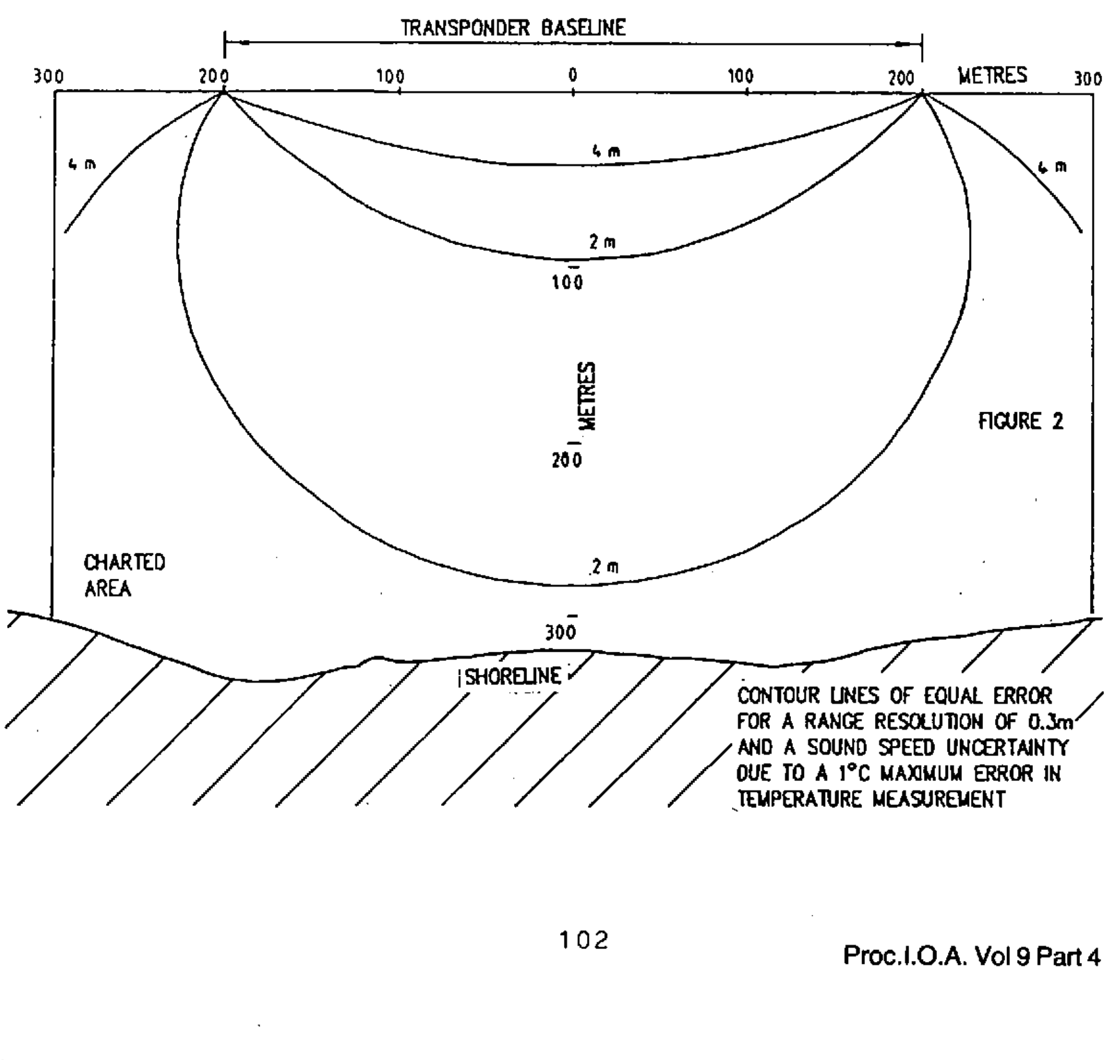

FIGURE 2

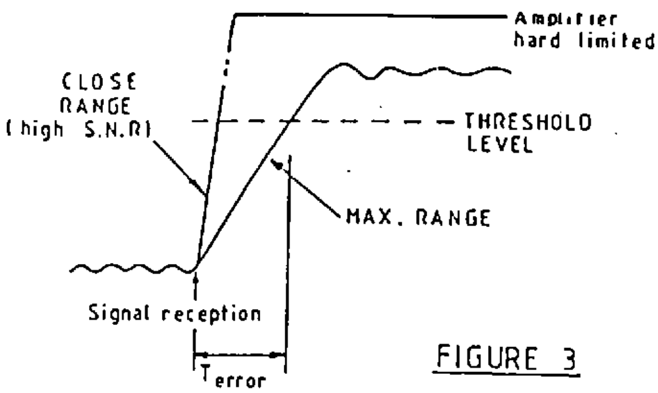

FIGURE 3

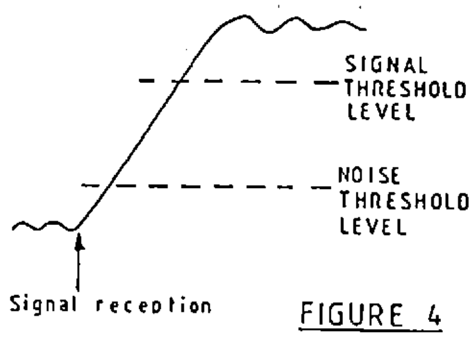

FIGURE 4

BLOCK DIAGRAM OF INTERROGATOR UNIT

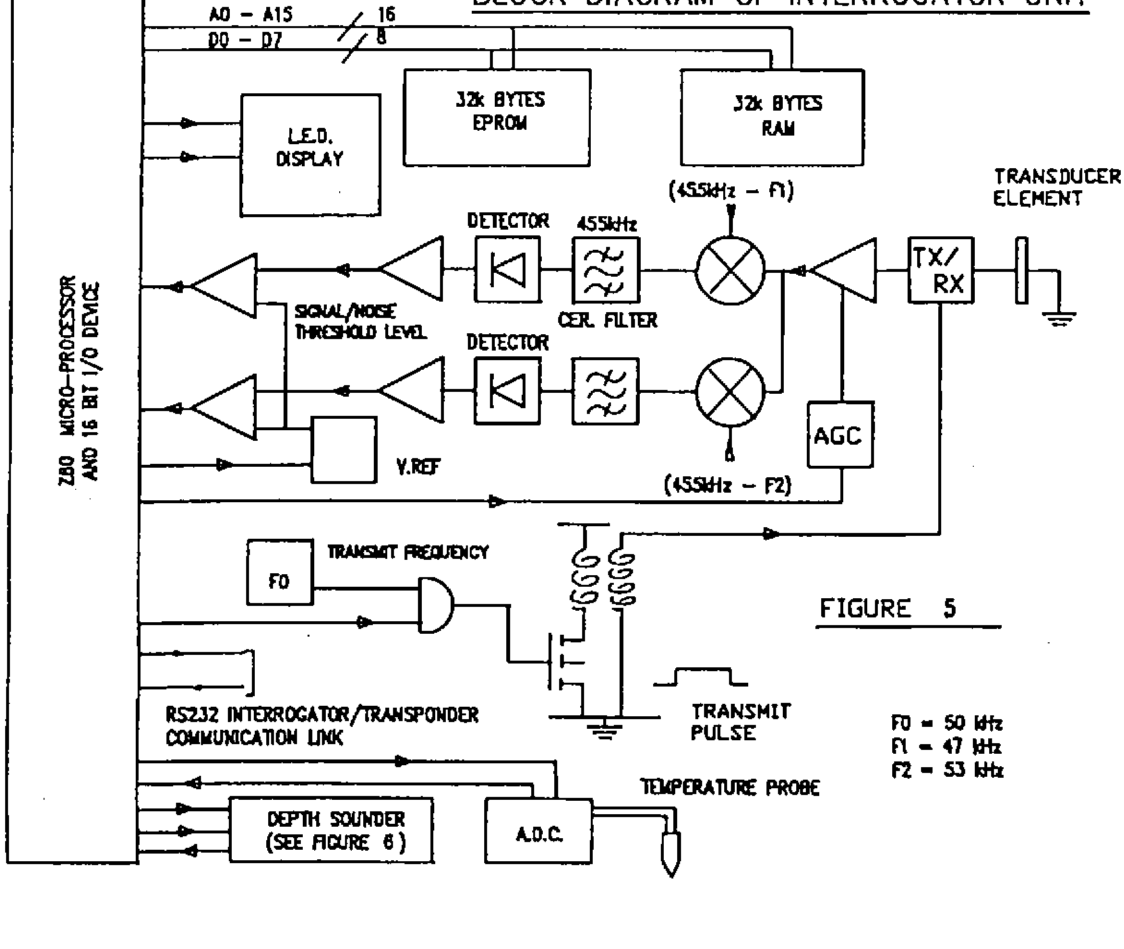

FIGURE 5

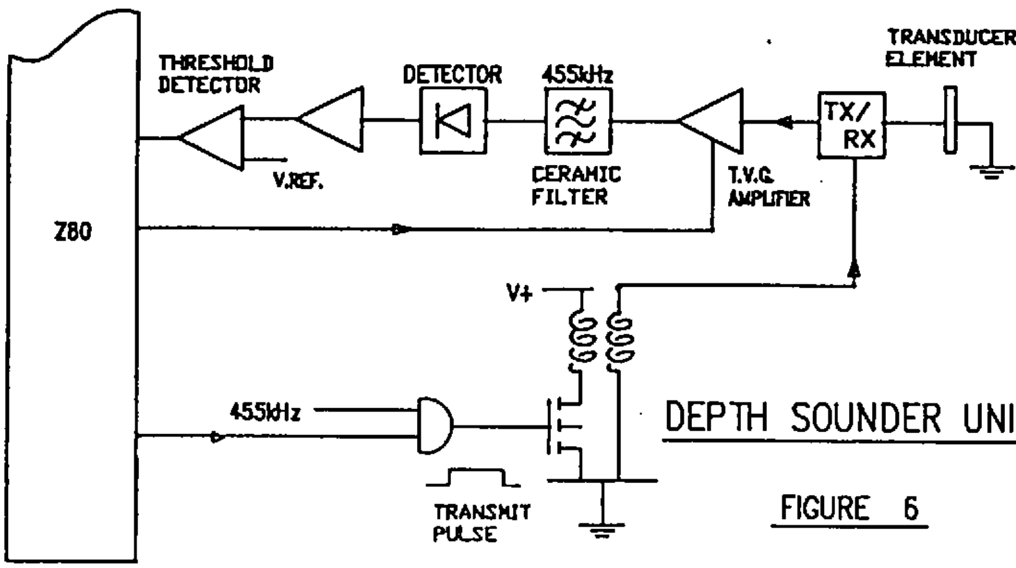

DEPTH SOUNDER UNIT

FIGURE 6

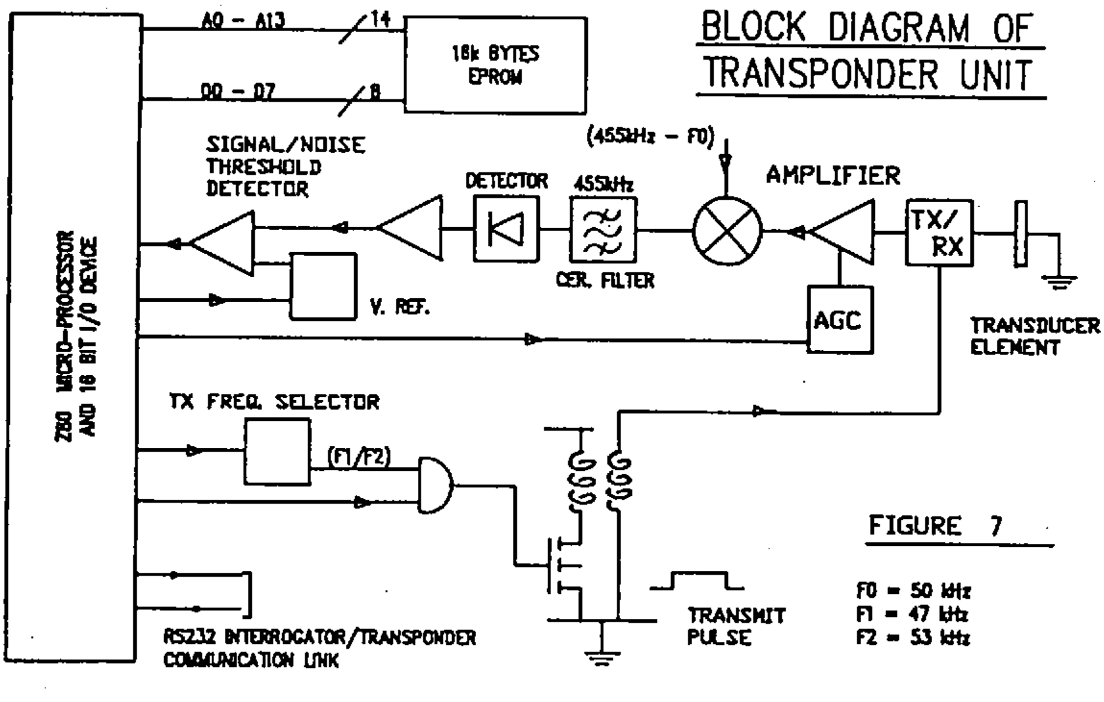

BLOCK DIAGRAM OF TRANSPONDER UNIT

FIGURE 7

F0 = 50 kHz
F1 = 47 kHz
F2 = 53 kHz

DIVER NAVIGATION AND SEA-BED SURVEYING EQUIPMENT

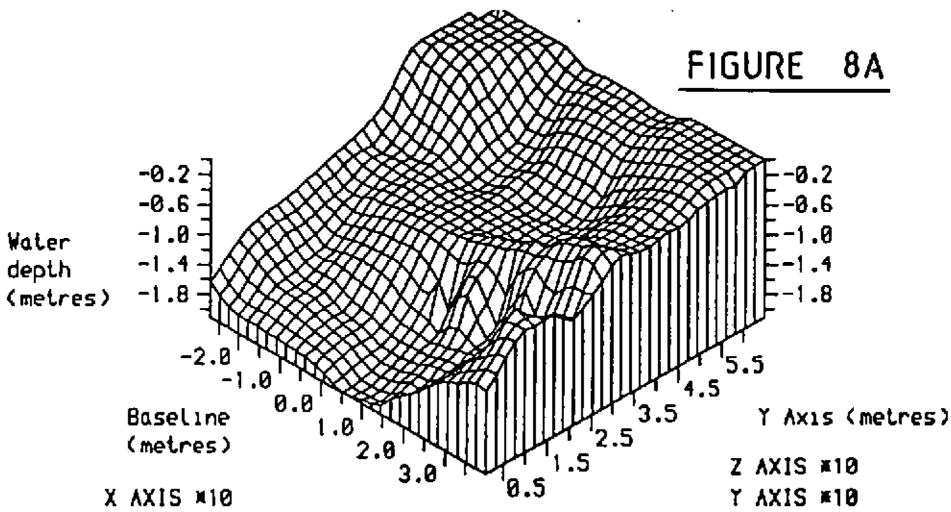

FIGURE 8A

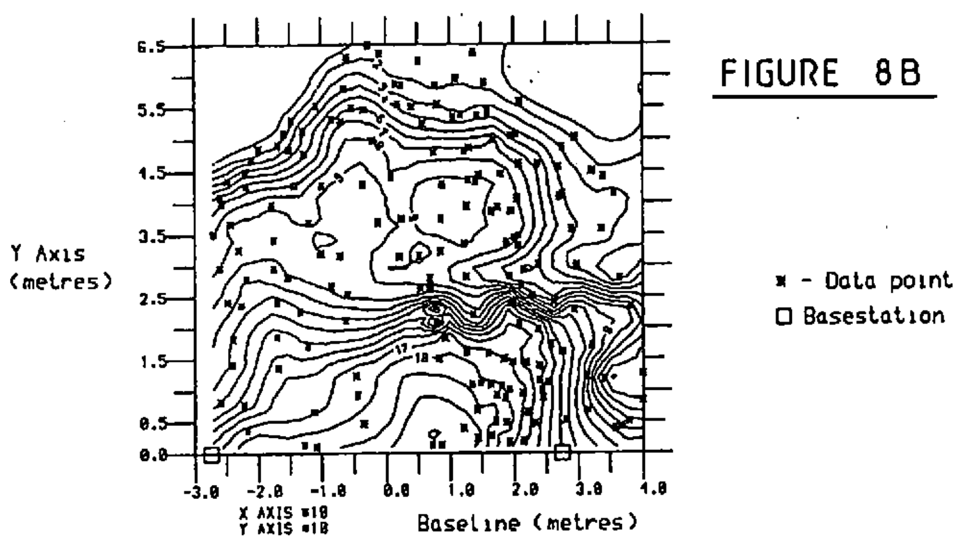

FIGURE 8B

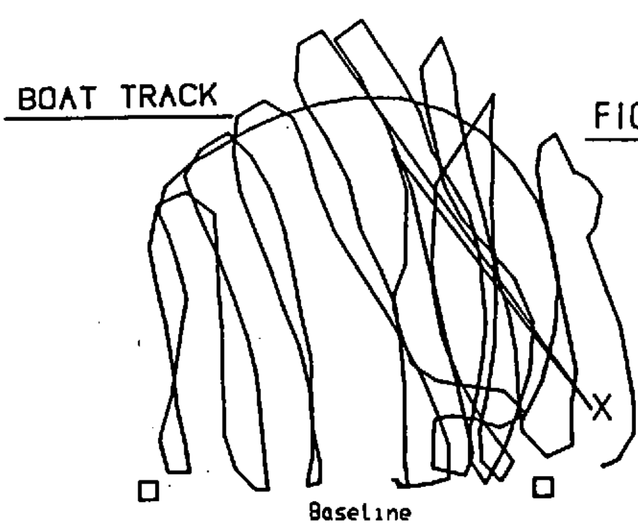

FIGURE 8C

Proceedings of the Institute of Acoustics

UPOS, A HYDROACOUSTIC POSITIONING SYSTEM FOR HIGH PRECISION AND LARGE DYNAMICS

Geir Vavik

Continental Shelf and Petroleum Technology Research Institute A/S (IKU)
P.O.Box 1883 Jarlesletta, N-7001 TRONDHEIM, Norway

ABSTRACT

This paper describes UPOS, a hydroacoustical system for three-dimensional, real-time position fixing of submerged objects. Originally it was designed for positioning and precise tracking of moving models in a research tank, the maximum range approaching 100 meters. Some of the most important design criteria were positioning of free running objects, sub-mm resolution, mm-range precision, high sampling rates (10 Hz), configuring flexibility, modular construction and to a maximum degree self calibrating.

To allow these rigid spesifications to be met, UPOS utilizes long proven, conventional techniques along with new technology. The hardware is built around a VME multiprocessor system although the concept is essentially independent of processor or bus structure. The complex handling of a maximum of 96 detections per sampling is secured by using modern FIFO components. PALs with up to 1800 gates are used where ever the constrainment of circuit complexity and space limitations dictate it.

The unique modular construction and design simplicity of UPOS invites to any configuration of number of hydrophones and frequency or time multiplexing within the frequency range of several octaves. A majority of these features are software controlled.

The mathematical processing of acoustical data is comprised by three main parts; calibration of the system, synchronizing the system timebase and real time positioning.

The UPOS system has greatly benefitted from the participating engineers and researchers' experience with satellite navigation software, real-time processing and hydroacoustical systems.

INTRODUCTION

In the spring of 1986, IKU, Department of Exploration Technology, was asked by MARINTEK, a second SINTEF institute, to undertake a very significant part of a new instrumentation project at their ocean laboratory site in Trondheim. The intentions of the project may be summerized as that of providing an integrated tool for testing submerged models in the Ocean Laboratory basin offering much the same properties as the then already existing fascilities for surface models. Main objectives had already been pointed out to be positioning of models and communication between model and data acquisition equipment.

The various backgrounds at IKU that facilitated participation in the project were various work within hydroacoustics, sub-sea position fixing and electromagnetic propagation. At a later stage, recent experience with the development of the Navstar [1] based DIFFSTAR [1] navigation system contributed largely to a healthy course of the project.

UPOS, A HYDROACOUSTIC POSITIONING SYSTEM FOR HIGH PRECISION AND LARGE DYNAMICS

The story about UPOS begins back in 1981 when a hydroacoustic positioning system for MARINTEK was developed over a very short period of time in order to carry out a model experiment involving some slowly moving offshore structures. This system employed no processor system, had a very simple interface to the host computer and provided no software controlled parameters. However, practical experience with this system showed good resolution and accuracy in the sub-cm range. A hydroacoustical positioning system had therefore to be strongly considered when feasibility studies incorporating the various instrumentation requirements were carried out during spring and summer of 1986 [2].

The concepts for a positioning system reviewed were different configurations of hydroacoustic equipment, but also the use of radio frequencies (VHF) and the use of laser technology was covered. Briefly summarized, specifications were; accuracy to a few mm, six degrees of freedom, ability to upgrade to 10 Hz sampling rate, auto calibration and ease of operation. Considerations of dynamics were not exact, but the aspects of models turning 180 degrees in 2 seconds had to be taken into account.

The evaluation concluded that a hydroacoustic, puls-based hyperbolic three dimensional positioning system could be realized within the time and finances available. Designing and developing UPOS consequently commenced august-september 1986.

MEASUREMENT SYSTEM SPECIFICATIONS

In order to anticipate the various possible model experiments at MARINTEK laboratories, the UPOS system had to meet some basic requirements.

Positioning should be global meaning that the entire basin measuring 80 by 50 by 10 metres could be covered without rearranging equipment or having to interrupt experiments. This calls for adequate signal to noise ratios over transmission ranges in excess of 90 metres. It also makes multipath conditions a worst case. On the other hand, this specification has led to developing more of a general purpose instrument than would have been the case if only local coverages had been chosen.

Accuracy down to a couple of millimetres would be required for some purposes. Systems had to operate without electrical connection to a free running model.

In addition to the three transmitters required on the model to enable computation of heave, roll and pitch, a fourth transmitter was requested for cases with chained models.

Limited by multipath noise, using three transmitters in time multiplexing the total sampling rate could not be expected higher than 3 Hz. Sampling rates in the order of 10 Hz can then only be realized using frequency multiplexing of the pingers. Since UPOS was to meet future requirements for higher sampling rates and increased overall accuracy, a modular system evolved, incorporating four frequency multiplexed channels.

UPOS had to be a self calibrating system that could be operated by most members of the staff. This implicated that all hydrophones other than those serving as precalibrated references should be calibrated each time the system was initiated. Clocks in the model transmitter and the receiving equipment had to be automatically synchronized and kept in a constant phase relationsship throughout a typical test period of several days without the aid of a direct connection between them.

SYSTEM DESCRIPTION

System Outline

As shown in Fig. 1 UPOS consists of fixed hydrophones at different sites around the basin. The object to be tracked carries a four channel transmitter with from one to four active transmitting hydrophones depending on the type of measurement to be performed. The fixed hydrophones are equipped with bidirectional preamplifiers allowing transmitting and receiving through the same hydrophone. This is accomplished using only standard coaxial connections to the preamplifiers for simplicity and easy maintanance, see Fig. 2.

TVG amplifiers, detectors and calibration transmitter are housed in one cabinet allowing the most critical analog circuits to be physically located independently of the rest of the equipment. The cabinet allows for 24 hydrophones in 4 channels. This requires 96 TVG amplifiers and 96 detectors. TVG amplifiers are divided into 12 Single Euroboards, each with 8 amplifiers handling 2 hydrophones, each with 4 separate channels. Detectors are divided into 24 single extended Euroboards. One board handles 4 different hydrophones on the same frequency channel. A calibration transmitter power amplifier can be switched to any of the hydrophones. Selections, TVG, listening windows, detections and transmitter exitation are passed between this cabinet and the processor cabinet by various cables that may approach a length of 30 m. A three wire synchronous bus is used to control the listening windows of the detector system. RS422 interface is extensively used.

The processor cabinet consists of two parts; the VME bus and the Motorola I/O bus. Interfaced to the I/O bus are the trig board and the receiver boards. On the VME bus are the I/O cpu board, the cpu boards for mathematical processing and the inter cpu driver board. Each receiver board can handle 8 individual incoming detections. The I/O cpu communicates with the math cpu's via the VME bus. The I/O processor also handles communication with the external host computer through a gpib interface card.

The prototype

The prototype of the system which already has been undergoing some important initial testing is fitted with sufficient components to support 4 transmitters in a time multiplexed configuration using up to 8 fixed hydrophones. The first position tracking trials were done with only 4 fixed hydrophones used each time. Expanding the prototype is made easy by the modular design and can mostly be realized by adding plug in boards since all necessary hardware and wiring are in place. Working frequency of the prototype is 140 kHz.

Design solutions

Various methods of synchronizing the clocks of receiving and transmitting system were reviewed. The principle chosen uses stable clocks (max. 10 ppm) and phase locking of the timebase in the receiving system based on feed back from the mathematical processing.

UPOS, A HYDROACOUSTIC POSITIONING SYSTEM FOR HIGH PRECISION AND LARGE DYNAMICS

Calibration software utilizes the ability of pinging with any of the fixed hydrophones. For this purpose both pinger frequency and power are software controlled. This allows reversable distance measurements between any two hydrophones and permits echo sounding measurements to water surface and bottom of basin (Calibrate).

Detectors have approximately a 15-20 dB adaptive range in addition to tvg-regulation. This enables detections with still unknown transmit trig time and is fundamental for detecting when listening windows cannot be predicted, as is the case during synchronization of timebases (Initmob).

To allow future improvements of sampling rates it is required that the pingers can operate simultaneously on separate working frequencies. Each fixed hydrophone should be able to listen to all 4 pingers but detect them individually. Therefore the mobile transmitter is an extensive design using five PAL circuits, yet all is realized on a single eurocard including power output stages. It secures full synchronous operation of all four pingers while permitting independent choices of frequencies, pinging sequences, ping-rates and burst lengths. Thus, the receiving equipment can be expanded to 4 different frequency channels from low frequencies and up to 600 kHz. Selectivity is provided for by analog filtering in order to exclude typical noise accossiated with the use of digital filter types in weak signal applications. This allows for simultaneous pinging and independent detection of up to 4 pingers.

Preamplifiers incorporate a T/R switch to enable pinging and receiving with the same hydrophone and cable.

Switching control of listening windows are sent on a serial synchronous bus from receiver cards to the detectors, one of the receiver boards being the master. This results in simple cabling between the cabinets for the 96 possible individual window settings.

Analog design

Spherical hydrophones of 1/2 inch diameter and resonance frequency at 140 kHz were chosen mainly because of their ruggedness and tollerance to rough handling as would be the case of a protype system. Signal to noise ratios may be optimal when both pinger and receive hydrophones are operated at resonance. The most serious drawback is that all hydrophones should be closely calibrated and selected to avoid unwanted signal variations caused by operating near resonance frequency.

The dynamic range of the TVG regulated amplifiers and preamplifiers are tailored to a range of maximum 100 m and is in excess of 40 db but can be made larger. In addition there is a 15 db dynamic range from the adaptive principle of the detectors. This is achieved by sampling pulse amplitudes within listening windows. The result is a selfstarting detector which very easily locks to the directly travelling pulse.

Digital design

Each detector board hosts 4 analog channels and considerable digital circuitry i.e. one large PAL for decoding the serial window setting informa tions. The board has been successfully realized with four layers in order to avoid onboard noise and crosstalk. The Trig card uses conventional counters and the processor clock to provide a system trig at the same rate as the model transmitter and synchronous with the processor system and system time. A special register allows the trig counter rate to be altered with 62.5 ns resolution permitting software to phase lock the receive system with the transmitters. Other circuitry are TVG generator, function generator for calibration transmitter exitation and control logic. The Receiver board uses a 24 bit counter to measure distances and the results are stamped and stored in FIFO memory where it is read by the I/O processor. Each receiver board handles 8 detections and times 8 window settings to the respective detectors. Both boards uses the available interrupts on the I/O bus. A few of the various boards are shown in Fig. 3.

ACCURACY CONSIDERATIONS

With a system resolution of 9/100 mm and application of zero crossing detection, the accuracy of the distance readings is mainly determined by signal to noise ratio. Calculations have shown that mm precision can be achieved with less than 100 v p-p applied to a spherical hydrophone with the given ambient background noise level. Optimizing for very short pulses prevent multipath distortion in some critical conditions. Fig. 4 illustrates some relationships between hydrophone geometry and redundancy. Erroneous detections degrade overall accuracy but the extensive redundancy from a large number of detections limits this influence. The chance of window predictions being upset by errancy is extremely small since they are a result of xyz precision.

POSITIONING SOFTWARE

This software is installed on a separate cpu board for mathematical processing. The design of the software allows parallel processing on several cpu boards in order to effort real-time processing even for higher sampling rates.

The programming language is Standard C. However, functions for matrix operations and calculations are recoded to Assembly in order to minimize the processing time.

Calibrate/newref

This program supports the self calibration mode. Distance counts between all hydrophones connected to the receiver are used after being prefiltered. A minimum of four hydrophones serve as accurately positioned references. In the Least Squares Adjustment routine the following parameters are estimated:

- acoustic speed in water
- x, y and z (Cartesian coordinates) for receiver hydrophones with unknown position
- variance for acoustic speed and x, y and z
- variance for distance measurements

No approximate positions are required for receiver hydrophones with unknown position.

UPOS, A HYDROACOUSTIC POSITIONING SYSTEM FOR HIGH PRECISION AND LARGE DYNAMICS

Initmob

This is the start procedure for the positioning of the transmitter hydrophone(s). The program solves two essential tasks:

- finding the start position for the transmitter hydrophone(s)
- synchronizing between time base of pingers and receiver time base

No approximate positions are required for transmitter hydrophones. However, the approximate sampling rate have to be known (boot parameter).

Poscalc

When initmob has been run, this main positioning software undertakes the real-time position estimation and support. The algorithm is a 8-state Kalman filter for each transmitter hydrophone. The states refers to the system time when the signal is transmitted:

- x, y and z): models position states
- vx, vy and vz): models velocity states
- b and vb): range bias and clock drift

The two last states are common for all transmitter hydrophones since they are controlled by the same clock.

The System noise appears in two different ways:

- time exponential aging of the covariance matrixes
- noise calculation based upon the residuals of the measurements

Using these thecniques allows both apriori optimal tuning of the filters, based upon the models and the clocks dynamics, and real-time tuning.

The program forces the range bias to zero by controlling the receiver. This gives more confident estimation of the listening windows for the receiver channels.

The software in the UPOS system is made flexible and supports many model configurations and gives the possibility to estimate a rigid models' all 6 degrees of freedom when at least 3 transmitters are located on it. The Kalman filter gives complete covariance matrixes and allows the user to effort intelligent processing on his own computer.

INITIAL SYSTEM TESTS

Results from the first laboratory tests confirms the expected performance of UPOS. Figs. 5 and 6 show results from a dynamic test; circular motion using one pinger with a radius of 1.0 m. The test was carried out with only 4 reference hydrophones and a sampling rate of 2 Hz.

	Fig. 5:	Fig. 6:
Perisph. vel.:	0.4 m/s	1.4 m/s
Centr. acc.:	0.2 m/s^2	2.0 m/s^2

UPOS, A HYDROACOUSTIC POSITIONING SYSTEM FOR HIGH PRECISION AND LARGE DYNAMICS

The graphic presentation is disturbed by straight line drawing from one position fix to another.

CONCLUDING REMARKS

It remains to complete the test program which include tracking a ROV with improved accuracy and determining six degrees of freedom. Restricted project economy has temporarily postponed these concluding trials, however, results so far have clearly demonstrated that UPOS will fullfill most of its goals.

The author would like to acknowledge professor Jens M. Hovem and dr. Aage Kristensen for sharing with the project their experience and knowledge of hydroacoustics. Acknowledgements also to Terje Frøysa, ELAB for his efforts of configuring the processor system and to Hans K. Kjeserud and Tore Flobakk, MARINTEK for contributing to thorough specifications of UPOS. Special thanks to dr. Torgeir Torkildsen who is responsible for the mathematical programming and contributions to this paper.

REFERENCES

[1] Hermod Fjæreide, 'DIFFSTAR: A concept for Differential GPS in Northern Norway', pp. 284-295, Navigation, Vol. 33, No. 4.

[2] Nils K. Rossing, 'Forprosjekt: Instrumentering av Undervannslegemer', Rapport No. MT51.9650.00/01/86.

UPOS, A HYDROACOUSTIC POSITIONING SYSTEM FOR HIGH PRECISION AND LARGE DYNAMICS

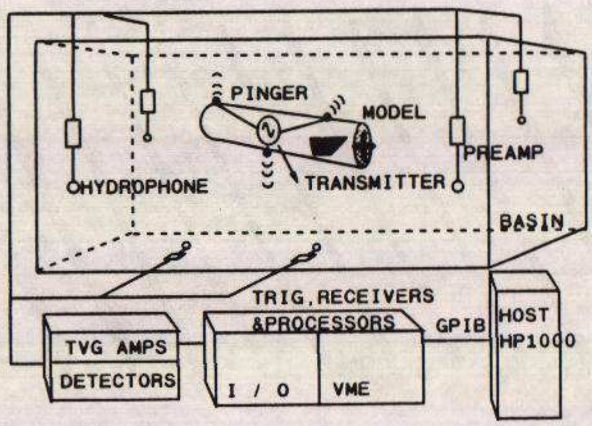

Fig. 1

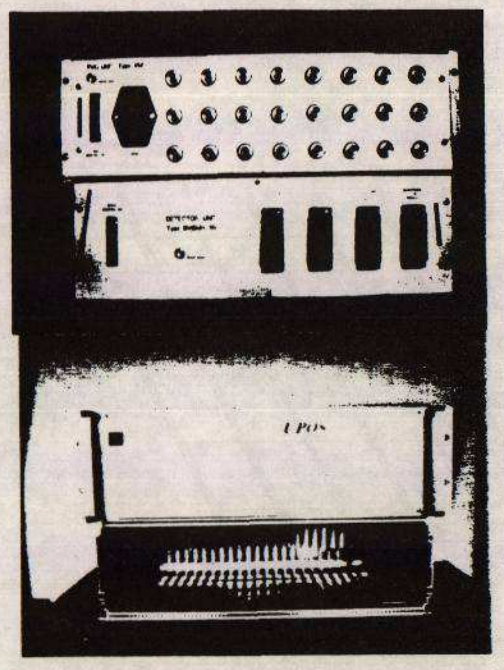

Fig. 2

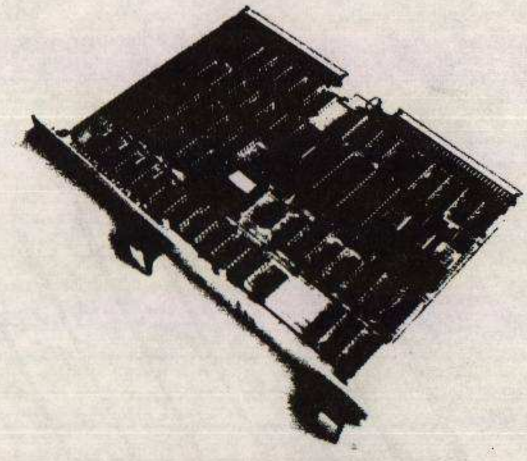

Receiver board

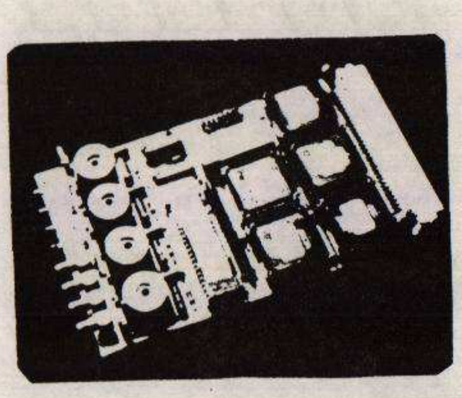

Pinger board
Fig. 3

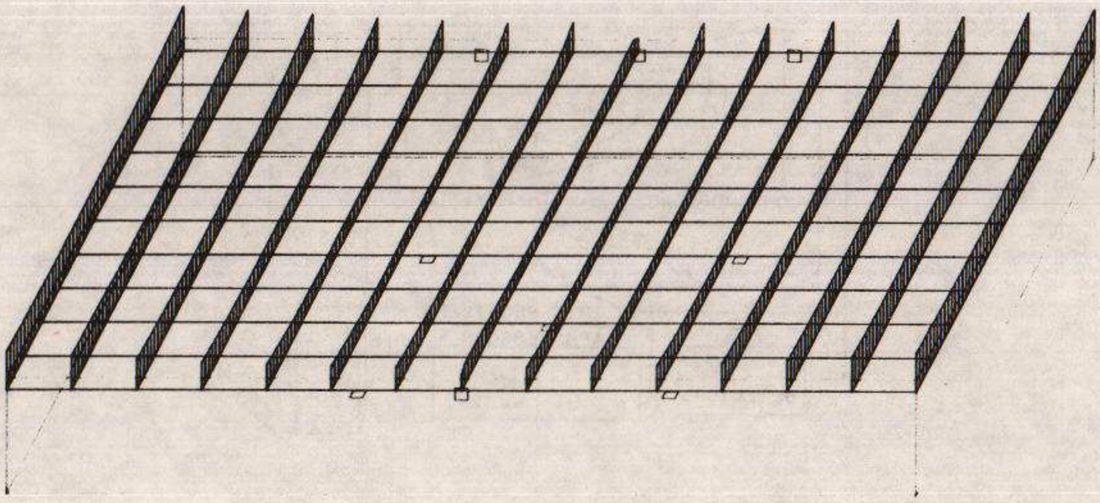

9 hydrophones

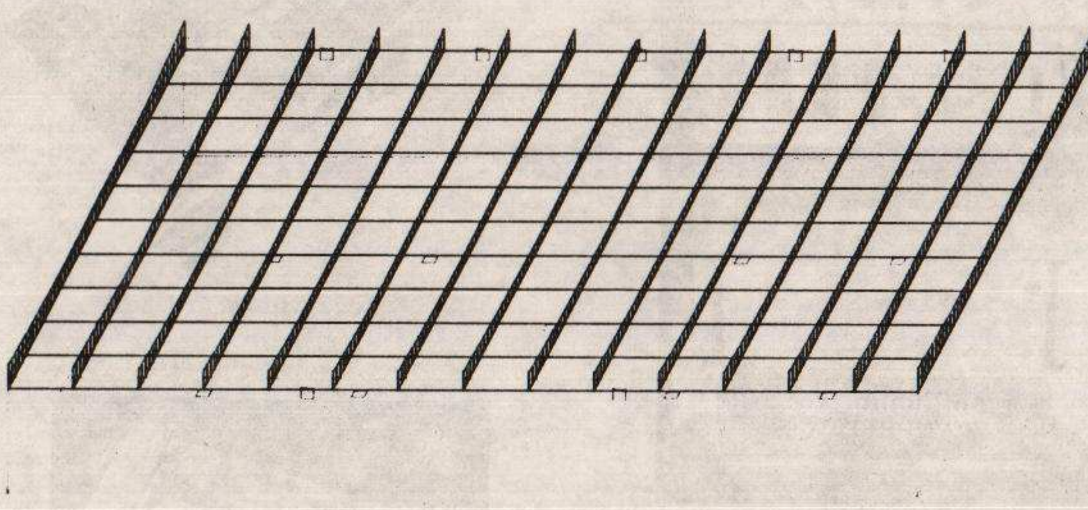

16 hydrophones

Figure 4. System precision versus xy position with pinger at 1 m depth. Squares equal total distance measurements precision and show hydrophone positions on walls and floor of tank. Total depth is 10 m.

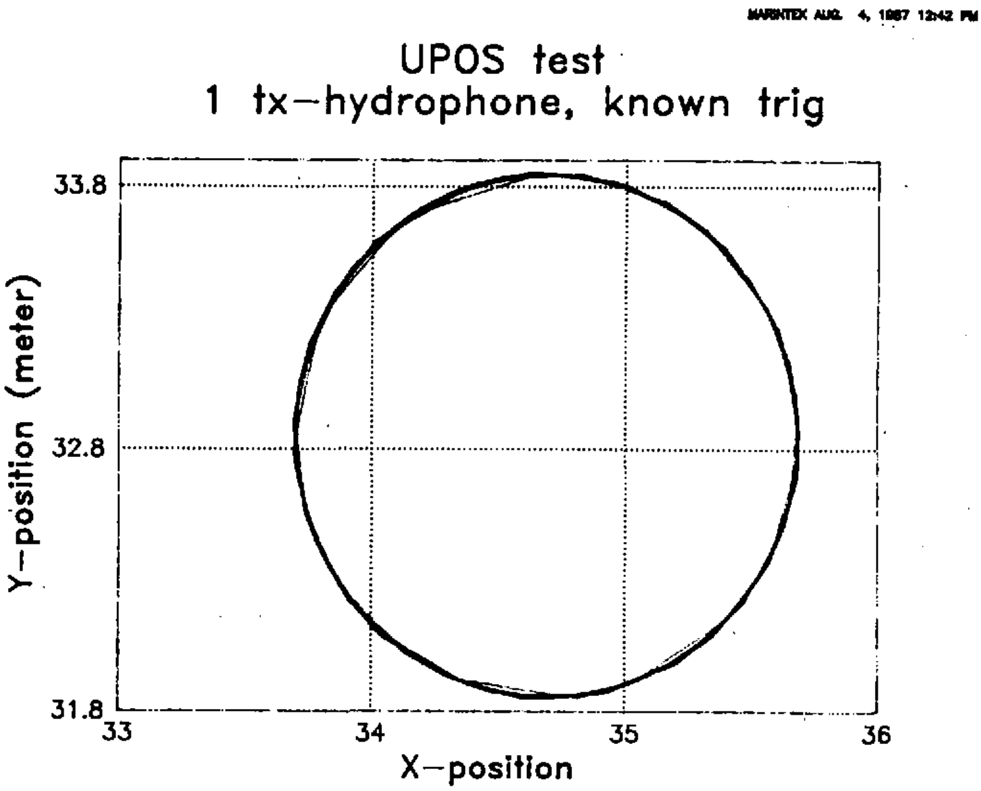

Figure 5.

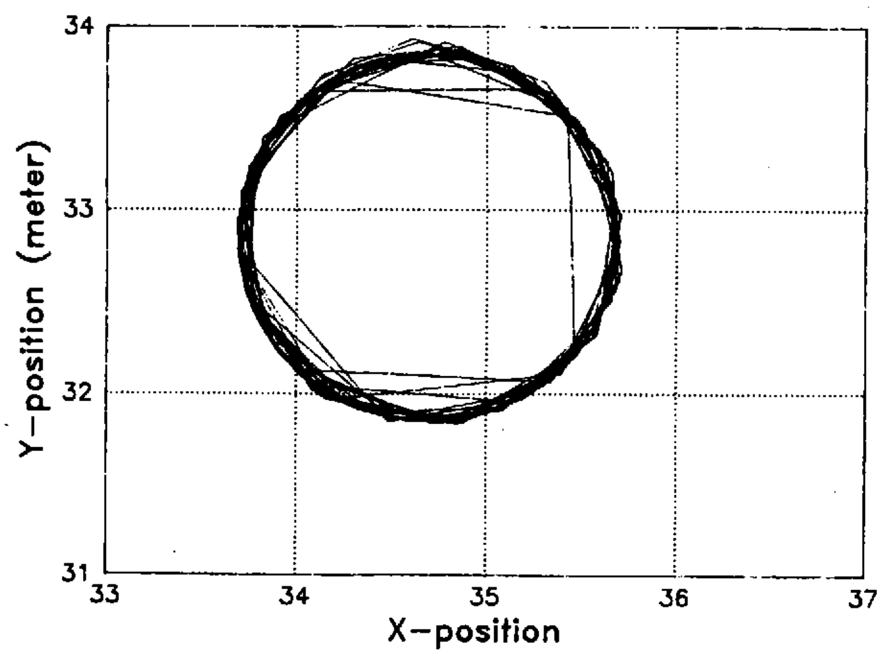

Figure 6.

Proceedings of the Institute of Acoustics

ACCURACY PREDICTION FOR DISTRIBUTED TRACKING SYSTEMS

A.J. Fenwick

SWS Computing Consultants Ltd, Leswalt by Stranraer, SW Scotland

INTRODUCTION

The results to be presented in this note are the outcome of a study which was begun at Thorn EMI, Naval Systems Division, aimed at producing better methods of assessing the accuracy of tracking systems. The study was prompted by the need to analyse the error performance of different range configurations during the preparation of proposals. The use of existing methods involved extensive and time consuming numerical calculations.

The purpose of a tracking range is to locate an object which may be moving, within a volume of water. The type of system under consideration here comprises a number of receivers, transmitters or transponders located at fixed and known positions. The distances between the object and those positions are measured and then converted into X,Y,Z position or range and bearing, by a suitable numerical transformation carried out by a computer. Distance may be found by measuring the time taken for pulses to travel between the object and the known positions, and then multiplying by the speed of sound.

Two key aspects of tracking range performance are the time to produce a fix, and its accuracy. The calculation time becomes important if the object is moving quickly. In underwater applications, however, speeds are low, the update rate does not need to be high and finding a computer which can handle the data collection and transformation tasks in real time should not be difficult.

A number of factors determine accuracy, some largely under the control of the designer, others uncontrollable and perhaps unpredictable. In the first category are the minimum increment in time, and the numerical precision of the algorithm. In the second are the true value of the speed of sound, and its variation from day to day and from place to place on the same day. The distribution of the datum positions throughout the water volume, and the accuracy with which they can be specified also affect accuracy. Ideally the distribution is controllable, but in practice it may be restricted, for example by features on the sea floor.

Accuracy may be assessed by modelling the errors in observed variables and applying the numerical transformations which convert travel time into the desired co-ordinates. Particular values may be assumed for the errors, in which case exact knowledge about performance under one set of conditions is gained, but a number of carefully chosen cases must be studied to form an overall picture.

Alternatively, the errors can be assigned appropriate statistical distributions, and average values and the scatter of fixing error found over a number of trials. As the error distributions will vary with the environmental conditions, this process must be carried out a number of times also. With either method, the amount of calculation required is considerable.

The method outlined in this note is to determine upper limits on the accuracy which can be achieved for known levels of errors in the data. The use of the method is demonstrated for a two dimensional tracking range with three datum positions, using a specific transformation of the distances, but the principles can be applied more generally.

MATHEMATICAL DISCUSSION

If the distance between a fixed point and a variable one is known, the variable point lies on circle whose centre is the fixed point. When the distances to several points are known, the unknown position is located by finding the intersection of circles centred at the known points. More than two distances must be known, as in general, two circles intersect twice, but if there are no measurement errors, three circles will intersect at a single point. Errors will shorten or lengthen the circle radii, and instead of three double intersections and one triple intersection, there will be six double intersections (see fig 1). The problem is to make an estimate of where the true position of the object is.

Let $(x_i, y_i), i = 1 .. 3$ be the known co-ordinates,

(x, y) be the unknowns,
t_i $i = 1 .. 3$ be the measured travel times, and let
c_i^1 $i = 1 .. 3$ be the speeds of sound along each path.

Then

$$(x - x_i)^2 + (y - y_i)^2 = (c_i t_i)^2 \quad i = 1 .. 3 \tag{1}$$

Solution
It is a fairly obvious first step in finding the unknown coordinates, to remove the squared terms in the unknowns by subtracting pairs of equations. Thus, taking the first and second equations, and the second and third equations,

$$(x_1 - x_2)x + (y_1 - y_2)y = 0.5(r_1^2 - r_2^2) + 0.5(d_2^2 - d_1^2) \tag{2a}$$

$$(x_2 - x_3)x + (y_2 - y_3)y = 0.5(r_2^3 - r_3^2) + 0.5(d_3^2 - d_2^2) \tag{2b}$$

where $r_i^2 = (c_i t_i)^2$ (3)

$$d_i^2 = x_i^2 + y_i^2 \tag{4}$$

For simplicity, choose the origin to be the circumcentre of the triangle. Then all the distances are equal and the second term on the right hand side of the equation disappears.

These equations are straight lines passing through intersections of pairs of circles and are the common chords of those circles. Note that any two pairs of equations from the set could be chosen, but that forming a third equation from the remaining pair gives no new information. The third line passes through the intersection of the other two.

When there are no measurement errors, the lines intersect at the triple circle intersection. Provided errors are small, the solution of the equations which gives the intersection of the chords is a good working estimate of the position of the object.

The chord equations can be represented in matrix form by

$$Ax = b$$

where A is the matrix of coefficients, x is the vector of unknowns and b is the vector containing differences of measured distances. The solution of these equations, which is the common chord estimate of position, is then given by

$$x = A^{-1}b$$

where A^{-1} is the inverse of A.

Allowing for errors in the data, the equations can be written

$$(A + E)y = b + f$$

where E is the matrix containing the errors in specification of datum positions, and f contains the errors in measurement of distance.

The error in the fix is the difference between the solutions of the ideal and actual equations

$$\begin{aligned} x - y &= A^{-1}b - (A + E)^{-1}(b + f) \\ &= (A + E)^{-1}(Ex - f) \qquad (5) \end{aligned}$$

ACCURACY ANALYSIS

The error performance of a tracking system can be specified in terms of the length of the error vector $x - y$ throughout the range coverage. Starting from equation 5, the upper limit for fixing error is found in terms of the norms of the input matrices and vectors expressing the measured values and their errors.

A vector norm is a generalised measure of length, and with it is associated a matrix norm, as discussed in [1]. There are many norms, but the appropriate one for this analysis corresponds to the usual definition of vector length,

$$||x|| = (x_1^2 + x_2^2)^{0.5}$$

The associated norm for a matrix A, $||A||$, is shown in [1] to be the largest eigenvalue of the the matrix A^TA.

Following the analysis given in [1], it can be shown that if the data errors are small, the relative error in a fix satisfies

$$||x - y||/||x|| \leqslant ||A||\,||A^{-1}||\,(||E||/||A|| + ||f||/||b||) \qquad (6)$$

The quantity $||A||\,||A^{-1}||$, known as the condition number of A, and written K(A), determines the sensitivity of the range to measurement errors. It is not dependent on any of those errors, but scales their effects. Range datum geometries with large condition numbers will be more sensitive to measurement error.

This inequality relating input and output error can be used to determine the performance of a tracking range. The condition number, and the position uncertainty term need only be calculated once, leaving just the effects of varying the distance measurement error to be considered in detail.

PERFORMANCE OF A 2-D RANGE WITH THREE DATUM POSITIONS

To demonstrate the use (6), first the condition number for a 2-D range with a triangular arrangement of datum positions will be found, then the effects of errors in the speed of sound and travel times will be investigated.

Condition Number

In the particular case under consideration, it is possible to relate the sensitivity to the properties of the datum triangle in an explicit way.

First, after calculating A^TA, it can be shown that its characteristic equation is

$$s^2 - (l_1^2 + l_2^2)s + (l_1 l_2 \sin(th))^2 = 0$$

where l_1 and l_2 are the lengths of two sides of the triangle

and 'th' is the included angle. The norm of A is the larger of the two solutions of this equation and the condition number is their ratio [1]. The roots can be expressed as the product of a length squared with a term depending only on the length ratio and the angle, and hence the condition number is independent of the size of the triangle, being affected only by its shape. Let

the ratio between the sides be $r = l_1/l_2$, then

$$||A|| = (l^2/2)[1 + r^2 + [(1 + r^2)^2 - (2r.\sin(th))^2]^{0.5}]$$

$$K(A) = [1 + r^2 + [(1 + r^2)^2 - (2r.\sin(th))^2]^{0.5}]^2/(2r\sin(th))^2 \quad (7)$$

Equation 7 is plotted for different values of 'r' and 'th' in figs 2A and 2B, and it can be seen that the condition number has a minimum of 1 for r = 1, th = 90. In this case, the datum triangle is right-angled and isoceles. When that shape is distorted, the condition number increases and the fixes are less accurate for a given set of measurements. Long narrow triangles show greater sensitivity to data errors than more symmetrical arrangements.

There will be in general, three condition numbers associated with a triangle, but only two if it is isoceles, and one if it is equilateral. For an isoceles right angled triangle, the two condition numbers are 1 and 6.85. For an equilateral triangle, the condition number is 3. With an arbitrary triangle, since the choice of equations to solve is arbitrary, it is better to choose the two equations which give the smallest condition number to take advantage of the lower sensitivity to error.

<u>Measurement Errors</u>

<u>Datum Position Error</u>. From the limit on relative error (6), it can be seen that errors in specifying datum positions induce a relative error in the fix which is constant over the range, and hence the absolute error increases away from the origin.

<u>Speed of Sound and Timing Error</u>. Allowing for a bias of dc in the speed of sound, and dt in the time measurements, the relative error in distance measurement is (dc/c + dt/t). The relative error in a fix induced by speed of sound error is also constant, whereas travel time error induces a relative fix error which decreases away from the origin.

These predictions are compared with the behaviour of the actual errors for an equilateral triangle in fig 3. The fix errors are plotted at points equally spaced throughout a square with the origin of co-ordinates at the intersection of diagonals. The error magnitude is assigned to one of sixteen bands represented by the characters 0 - 9, A - F, with '0' being the lowest.

Fig 3A shows the relative fix error for a bias of 1 in 10^3 in timing and as predicted, the error decreases away from the origin.

Fig 3B shows the absolute fix error for a bias of 1 in 1.5×10^3 in assumed speed of sound. This plot exhibits an error increasing away from the origin in proportion to range, which is also in agreement with the prediction.

ACCURACY PREDICTION FOR DISTRIBUTED TRACKING SYSTEMS

DISCUSSION

The analysis has shown that the effects of the various sources of input error can be separated, and for small errors, the contributions from datum position uncertainty, speed of sound and timing, add to-gether. The range datum geometry has been shown to affect sensitivity, and this has been quantified.

These results allow a quick assessment of the importance of the different errors, and first choices of range parameters may be made without extensive numerical computations. If follow-on calculations are required, this type of analysis can be used to direct attention to the more important cases and so improve the efficiency of a more detailed study.

REFERENCES

[1] James M. Ortega, 'Numerical Analysis', Academic Press, 1972

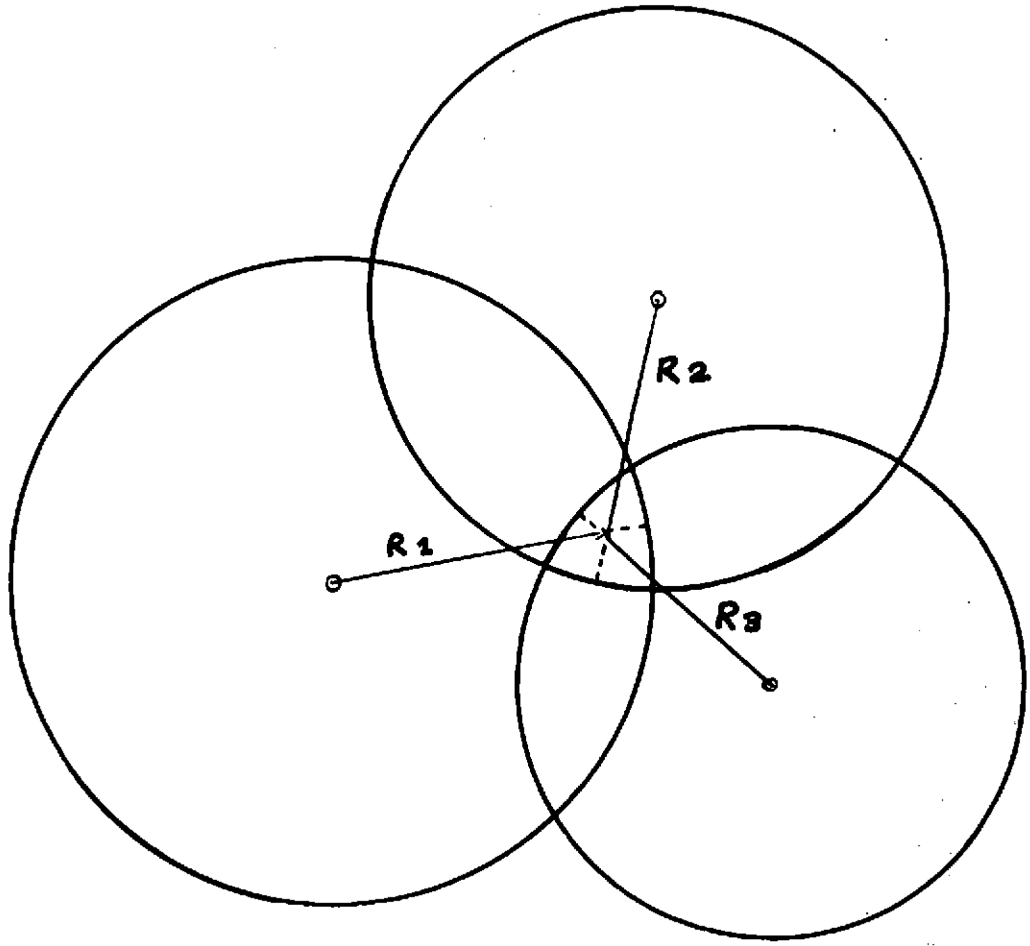

FIG 1 POSITION FIXING BY MEASURING DISTANCES

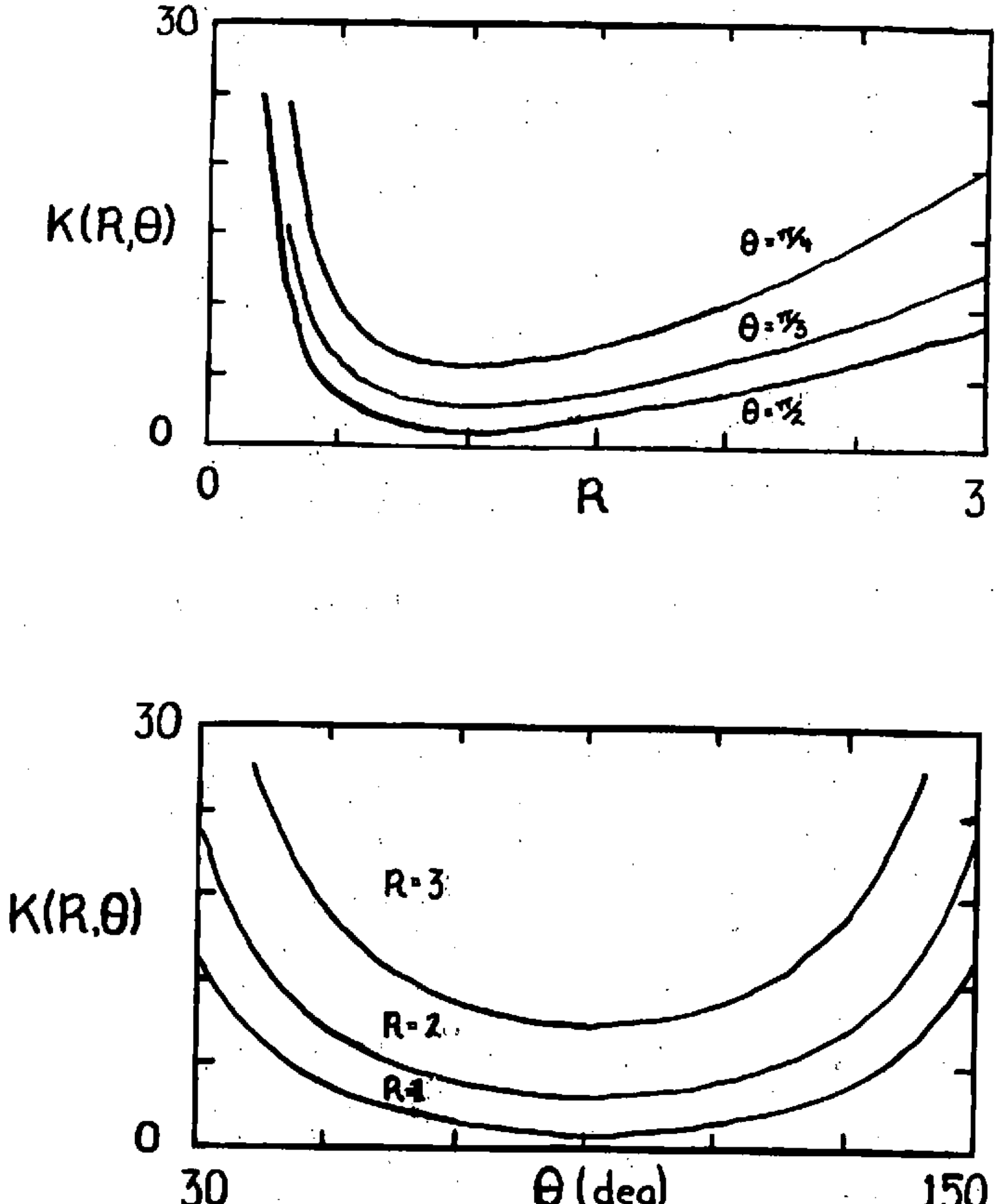

FIG 2 · EFFECT OF TRIANGLE SHAPE ON THE CONDITION NUMBER.

2	2	3	3	3	3	3	3	3	3	4	4	4	4	4	3	3	3	3	3	2
2	3	3	3	3	3	3	4	4	4	4	4	4	4	4	4	4	3	3	3	3
3	3	3	3	3	3	4	4	4	4	5	5	5	5	4	4	4	4	3	3	3
3	3	3	3	4	4	4	4	5	5	5	5	5	5	5	5	4	4	3	3	3
3	3	3	4	4	4	5	5	5	6	6	6	6	6	6	5	5	4	4	3	3
3	3	4	4	4	5	5	5	6	7	7	8	8	7	6	6	5	4	4	3	3
3	4	4	5	5	5	6	6	7	8	9	A	A	8	7	6	5	5	4	4	3
4	4	4	5	6	6	7	7	8	9	B	D	C	A	8	6	5	5	4	4	3
4	4	5	5	6	7	8	9	A	A	D	F	E	A	8	6	5	5	4	4	3
4	4	5	6	7	8	A	C	D	C	E	F	C	9	8	6	5	5	4	4	3
4	4	5	6	7	9	B	F	F	F	0	C	B	9	7	6	5	5	4	4	3
4	4	5	6	7	8	A	C	D	C	E	F	C	9	8	6	5	5	4	4	3
4	4	5	5	6	7	8	9	A	A	D	F	E	A	8	6	5	5	4	4	3
4	4	4	5	6	6	7	7	8	9	B	D	C	A	8	6	5	5	4	4	3
3	4	4	5	5	5	6	6	7	8	9	A	A	8	7	6	5	5	4	4	3
3	3	4	4	4	5	5	5	6	7	7	8	8	7	6	6	5	4	4	3	3
3	3	3	4	4	4	5	5	5	6	6	6	6	6	6	5	5	4	4	3	3
3	3	3	3	4	4	4	4	5	5	5	5	5	5	5	5	4	4	3	3	3
3	3	3	3	3	3	4	4	4	4	5	5	5	5	4	4	4	4	3	3	3
2	3	3	3	3	3	3	4	4	4	4	4	4	4	4	4	4	3	3	3	3
2	2	3	3	3	3	3	3	3	3	4	4	4	4	4	3	3	3	3	3	2

FIG 3A RELATIVE FIX ERROR FOR 1 IN 1000 TIMING ERROR

F	F	E	D	D	C	C	B	B	B	B	B	B	B	C	C	D	D	E	F	F
F	E	D	C	C	B	B	A	A	A	A	A	A	A	B	B	C	C	D	E	F
E	D	C	C	B	A	A	9	9	9	9	9	9	9	A	A	B	C	C	D	E
D	C	C	B	A	9	9	8	8	7	7	7	8	8	9	9	A	B	C	C	D
D	C	B	A	9	8	8	7	7	6	6	6	7	7	8	8	9	A	B	C	D
C	B	A	9	8	8	7	6	6	5	5	5	6	6	7	8	8	9	A	B	C
C	B	A	9	8	7	6	5	5	4	4	4	5	5	6	7	8	9	A	B	C
B	A	9	8	7	6	5	4	4	3	3	3	4	4	5	6	7	8	9	A	B
B	A	9	8	7	6	5	4	3	2	2	2	3	4	5	6	7	8	9	A	B
B	A	9	7	6	5	4	3	2	1	1	1	2	3	4	5	6	8	9	A	B
B	A	9	7	6	5	4	3	2	1	0	1	2	3	4	5	6	7	9	A	B
B	A	9	7	6	5	4	3	2	1	1	1	2	3	4	5	6	8	9	A	B
B	A	9	8	7	6	5	4	3	2	2	2	3	4	5	6	7	8	9	A	B
B	A	9	8	7	6	5	4	4	3	3	3	4	4	5	6	7	8	9	A	B
C	B	A	9	8	7	6	5	5	4	4	4	5	5	6	7	8	9	A	B	C
C	B	A	9	8	8	7	6	6	5	5	5	6	6	7	8	8	9	A	B	C
D	C	B	A	9	8	8	7	7	6	6	6	7	7	8	8	9	A	B	C	D
D	C	C	B	A	9	9	8	8	7	7	7	8	8	9	9	A	B	C	C	D
E	D	C	C	B	A	A	9	9	9	9	9	9	9	A	A	B	C	C	D	E
F	E	D	C	C	B	B	A	A	A	A	A	A	A	B	B	C	C	D	E	F
F	F	E	D	D	C	C	B	B	B	B	B	B	B	C	C	D	D	E	F	F

FIG 3B RELATIVE FIX ERROR FOR 1 IN 1500 SPEED OF SOUND ERROR

Proceedings of the Institute of Acoustics

SEISMIC STREAMER TRACKING, PAST, PRESENT AND FUTURE

C H Rodbourne and R J Sharp

DBE Technology, Aldershot, Hampshire, UK

INTRODUCTION

Early seismic surveys, primarily conducted for research, used a single towed acoustic source and a separate towed receiver. Signal processing was limited to analogue circuits providing a single trace, recording echos from the sea bottom and from the underlying geology. The quality of the data was extremely poor and provided little information for interpreting the structure.

By replacing the single receiver with a series of receivers at regular intervals (forming a streamer), a more complex picture could be produced. Whereas the single receiver produced a single trace corresponding to each point in the survey, the streamer produces a number of traces. All those traces, where the mid-points between the source and the receivers are co-incident, have effectively described the same physical point of the underlying structure. However, because the angle between the source, the mid-point and the receivers increases for receivers further along the streamer, their traces view the structure from different angles. This information is used to reconstruct a single improved trace from all those with a 'common mid-point' (CMP). The result, called the CMP stack, describes the underlying geology as if it were interrogated by a source and receiver positioned directly above the mid-point (at zero offset).

OBTAINING A CMP STACK

G is the gun, shot at intervals 1, 2 and 3.

A, B and C are individual receivers on the streamer.

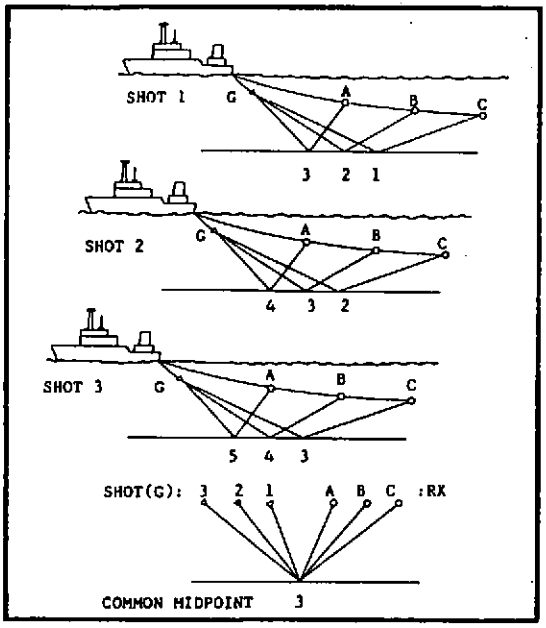

Traces from three shots with a common mid-point to form a gather.

In addition to producing an improved signal response, in the form of the CMP stack, these common mid-point traces (CMP gather) can be used to infer information about the velocity structure of the underlying rocks [1]. It has been demonstrated [2, 3] that the radius of curvature of the emerging wavefront reflected from an interface between two layers, as viewed by the traces in the CMP gather, is related to the difference in velocity between the layers.

Although these techniques, based around the concept of grouping traces into a CMP gather, have been accepted for use in traditional 2-D surveys (where a single section of the geologic structure is surveyed) they have not adapted well to the more rigorous demands of 3-D surveys where the whole of an area is surveyed and the resulting data analysed in every dimension.

Of particular concern is the accuracy with which the actual mid-point of each trace can be located. This is because the assumption that all the mid-points in a gather are coincident is not true. This is due to cable feathering (the streamer does not follow the line of path) and is referred to as mid-point scatter. Although a 2-D survey can ignore this problem with little effect on overall quality, 3-D surveys are much more sensitive to the problem. Furthermore it is necessary to ensure adequate coverage of the survey area in order to prevent spatial aliasing, which can only be achieved by the accurate location of every mid-point. The effects of mid-point scatter are reduced by re-grouping traces into gathers based on the actual locations of their mid-points (a procedure called binning) [4].

Effective binning and adequate coverage can only be achieved if mid-points can be accurately located. This, in turn, depends upon locating the acoustic sources and receivers accurately with respect to some known point (normally the survey vessel, which is itself located by satellite positioning and other navigation systems). This task has been complicated by the ever increasing complexity and diversity of the seismic acquisition hardware. Streamers are tending to become much longer, with three kilometres in general use and up to six kilometres for special cases. The number of streamers has also increased, with two as a standard but often more. In a recent advance one company has even employed twin streamers in a vertical configuration (over/under) in an attempt to improve quality and reduce weather down time [5].

In a modern seismic system the positions of the receivers along the streamer are determined from compass bearings recorded by units attached along the length of the streamer. The bearing information is collected by a computer system and applied to a sophisticated mathematical model of the streamer's shape. This ensures optimum use of the data whilst filtering out erroneous results. However compass systems do have some serious short comings. They are not effective in locating the start and attitude of the streamer with respect to the ship. Their effectiveness is reduced along the length of the streamer as well as at high latitudes. Finally their absolute accuracy is not sufficient to meet current requirements.

In the quest to improve upon the accuracy of compass based systems, it has become generally accepted that new positioning techniques must be employed to either replace or supplement the existing technology.

SEISMIC STREAMER TRACKING, PAST, PRESENT AND FUTURE

REQUIREMENTS FOR STREAMER POSITIONING

The complete positioning system should be capable of providing CMP locations to within ±5m or better. This accuracy should be maintained along the full length of the streamers which are generally between 1.5 and 3km but may extend to as long as 6km. The configuration of these streamers will be variable. A single streamer is seldom used for 3-D surveys with two or more being preferred. These streamers may typically be separated by 50m.

In order to achieve these requirements the functions of the positioning system can be divided into four. Positioning the front-end of each streamer, determining their overall shape, measuring the separation between each streamer, and positioning their ends.

Compass systems are adequate for fulfilling the second task, determining the streamer's shape, except at higher latitudes where they must be supplemented. Radio positioning can be used to track the tail buoy, although this still requires an assumption to be made about the position of the end of the streamer with respect to the tail buoy. Radio positioning has also been used for front end monitoring although this requires surface floats to be attached to the streamer tow cables which is not popular with many companies. Radio positioning also has many general drawbacks which does not make it suitable for stand alone operation.

The most promising approach to fulfilling some or all of the above tasks is acoustic positioning. Several systems have been developed and tested mainly for stand alone operation, and these are described below.

SIMRAD HPR

The Simrad system uses a narrow beam transducer which can track transponders/responders on airguns and on streamers. It is essentially a super short baseline technique relying upon the phase difference across a multiple element transducer to provide bearing information, and the transit time to provide range information. The narrow beam transducer is mounted on a shaft and penetrates the hull via a gate valve. The beam is electronically steered in the vertical plane and is mechanically rotated in the horizontal plane.

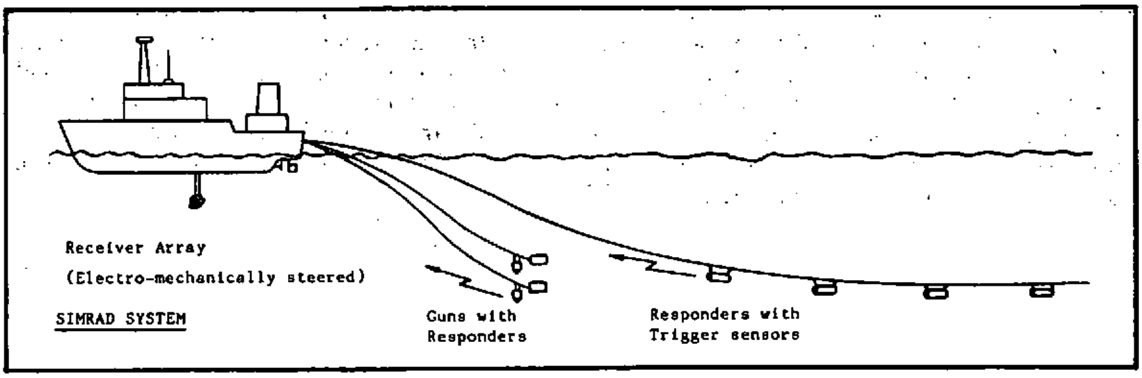

The system operates synchronously allowing the beam to be pointed to each airgun responder and then the streamer responders in turn, this sequence taking around 8 seconds for a 3000m maximum responder range which includes the time taken to track up to 6 gun responders. Each airgun responder is electrically connected to the onboard processing electronics which controls the output powers and provides the synchronised trigger. A control line in the streamer carries a coded signal which is detected by the clipped on responders (birds) causing them to transmit a synchronised signal. As no electrical connections are made between the streamer and responder, the latter are fitted with batteries [6].

A significant advantage of this system is its use of responders which improve the overall detection probability as no forward acoustic path is involved and there is no need to receive pulses in the poor signal to noise conditions close to the streamer at long ranges. Another benefit of responders is a reduction in the period of time to collect a data set as only single way pulse slant times are involved.

The Simrad system does have some inherent disadvantages which include the high bearing accuracy required to obtain results at the longer ranges. The claimed accuracy is 0.5° but to this must be added any installation tolerance which will create a bias. 0.5°is equivalent to 26m positional error at 3000m, this being well short of the performance being pursued by the survey companies. In the case of multiple streamers which are towed to one side of the towing vessel a major source of bearing inaccuracy arises from the non-isotropic nature of the medium in the horizontal plane due to the ship's wake. The resulting refraction causes the 'rays' to be bent and a corresponding error to occur in the bearing estimate. This poor acoustic environment also effects the range estimates as the speed of sound is very variable and difficult to determine. The Simrad system with its complex hull transducer station is relatively expensive and requires the ship to be specially fitted out.

OCEANO ALS

The Oceano system uses short baseline acoustic positioning techniques to position each of a pair of gun arrays which in turn position receiving elements in the streamer. The initial short baseline is formed by a pair of transducers penetrating the ship's hull in the fore-aft axis or athwartships which are used to provide ranges to acoustic modules fitted to each of the gun arrays. The acoustic modules which are cabled to the ship act as transmitters and are received by special hydrophones fitted inside the streamer sections as well as the hull mounted hydrophones. The acoustic modules therefore form a second baseline with respect to which the streamer hydrophones are positioned. All hydrophone signals are routed back to the onboard signal processor which times the pulse arrivals with respect to the initiating pulse and provides data to a computer for position calculations [7].

SEISMIC STREAMER TRACKING, PAST, PRESENT AND FUTURE

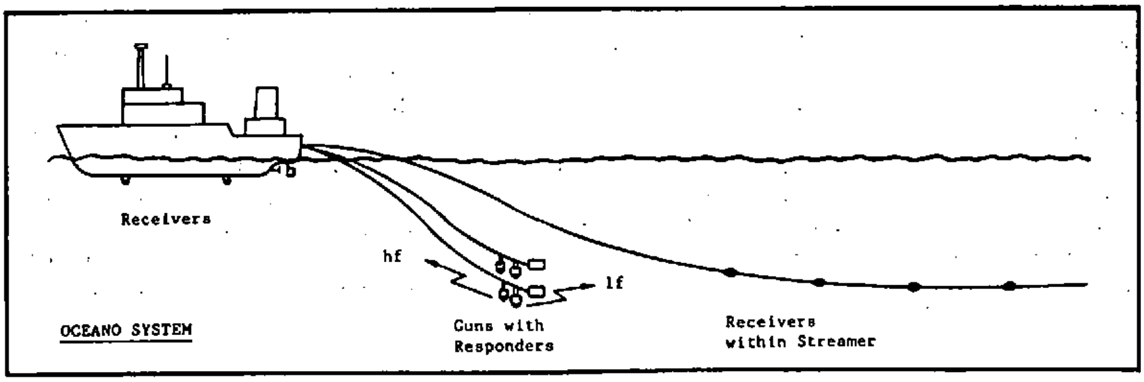

The Oceano system has advantages such as reduced dependance on acoustic paths through the wake (although at longer ranges this is still a potential problem) and simpler streamer deployment and recovery as no 'birds' are attached. The one way only acoustic path is also an advantage but the need to receive within the streamer cable is not ideal both in terms of the beam angle requirement and the higher noise environment aft of the ship. As for the Simrad system at the longer ranges (>1000m) small errors in range timing coupled to uncertainty in the value of the speed of sound will cause errors in excess of ±10m assuming that a 100m gun array baseline is used and its dimension is accurately known. Gun baseline measurement errors will further worsen the solution. In order to minimise baseline errors an additional pair of h.f. transducers are incorporated with the gun arrays. These higher frequency devices give greater timing resolution, hence improving the baseline estimate, but they do complicate the system. The system arrangement is such that it is not flexible.

DBE SST

DBE's current system uses its series 3000 multi-frequency control and telemetry equipment operating at around 30kHz, ie at the upper end of Simrad's band and between Oceano's l.f. and h.f. bands. The choice of operating frequency is difficult and is an inevitable compromise with the lower frequencies giving better propagation performance and the higher frequencies giving higher timing resolution and physically smaller devices for transmission.

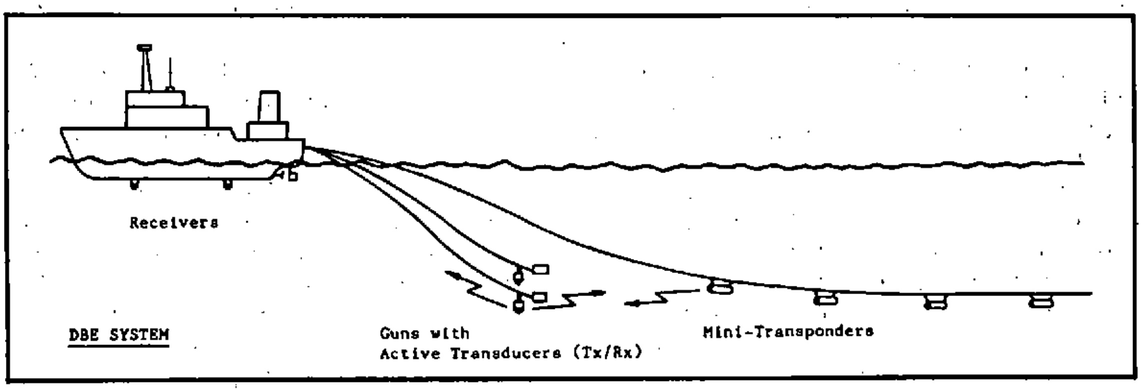

The DBE system is similar to Oceano's using a pair of transducers at known positions on the ship's hull to provide the initial short baseline from which are measured the positions of active transducers fitted to the gun arrays. (Active transducers are able to transmit as responders and receive as hydrophones). In order to obviate the need for specialised streamers the DBE 'birds' are mini transponders replying to the active transducer interrogation ping. Again the main disadvantages of this system are similar to those for Oceano's which are associated with the longer ranges and additionally the lower statistical reliability of two way pulse travel using transponders. The self contained independent hardware and compact size are advantages of the DBE system.

DBE INTEGRATED APPROACH

None of the systems considered meet all the outlined market requirements and therefore offer compromise solutions which will suit specific applications differently. The demand for higher and higher quality data from seismic surveys and for economy in producing them is reflected in the performance specifications for modern 3D seismic survey streamer positioning systems. Unfortunately the need to accurately locate streamers at longer ranges (>1000m) gives acoustic positioning systems a great deal of trouble. The disturbance of the acoustic medium due to the ship's wake and the firing of the guns results in range limited detection which is exacerbated by the short baseline giving increasing positional errors with increasing range. An added disadvantage of any system using these techniques is the relatively long frame time for each position fix. As time passes the current systems will find less and less favour with the survey companies who will look for an integrated approach using other sensors capable of providing better answers.

After consultations with Horizon Exploration who have previously used the DBE system and with Seismograph Services Limited who currently use a DBE system in a modified manner, DBE are developing their acoustic positioning system to provide coverage of the guns and the front-end of the streamers. This development work is being financially supported by the Offshore Supplies Office and will yield improvements which concentrate on providing the accurate location of the start of each streamer, an area of considerable uncertainty, whilst giving total flexibility to accommodate any reasonable streamer configuration. The output is intended to be integrated into a complete positioning system as well as providing an independent assessment of quality.

The system consists of a fixed short baseline attached to the hull of the ship, similar to previous systems. This baseline is used to locate an extended baseline of active transducers towed from the ship. These transducers can be attached to the gun frames or towed independently, and consist of an electronics unit with a separate detachable acoustic head that can be orientated to provide optimum cover. In addition, the transducer element is strengthened to withstand the repetive shock caused by the guns. An integral pressure transducer provides depth information to the on-board system. The software system uses this data to project all received ranges onto the horizontal plane, allowing the extended baseline to be towed below the guns and associated disturbance or altered should the transmission path be affected by water conditions, such as a thermocline.

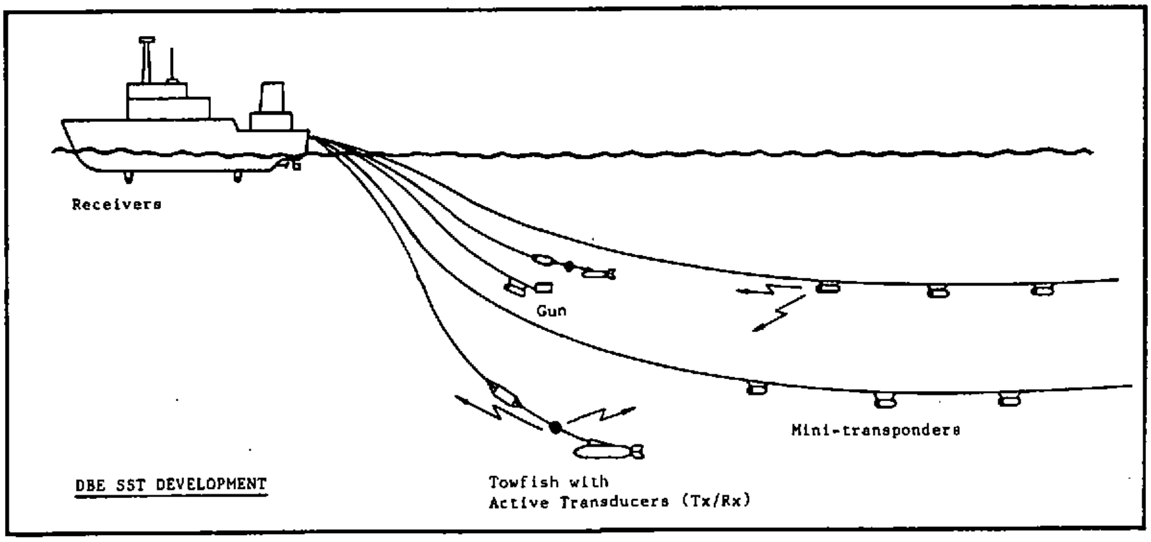

The extended baseline can range up to eight mini-transponders (modified to provide a streamlined shape and improved receiver characteristics) attached to any part of the system within a range of 1000m. As already discussed, it is not reasonable to expect a high degree of accuracy at ranges beyond 1000m.

All four transducers forming the two baselines, communicate their range data to the on-board equipment. Cycle time is obviously limited to the two-way travel time at maximum range, plus processing overheads. This is expected to be about three seconds, although it is more likely that a single cycle will be performed for each shot-point.

The processing will be performed by an IBM micro computer, attached to the dedicated hardware system controlling the subsea units. The software system, written in Ada for maximum reliability, is designed to combine data integrity with system flexibility. Processing will involve dynamic windowing, redundancy checks, data smoothing and statistical analysis. Checks are included to monitor the performance of each unit and raw data can be stored for later analysis. Processed data, in the form of three dimensional cartesian co-ordinates, referenced to a user defined co-ordinate space are transmitted to a remote host for integration into the complete positioning system. A high resolution graphics screen displays various data including a plan view of the system indicating actual positions and average positions.

THE FUTURE

The previous systems, intended to provide full positioning using acoustics, were not successful in this aim. Any acoustic system employing a short baseline or super short baseline technique suffers from a fundamental restriction in range which is limited further by poor or unusual weather conditions. Furthermore, DBE and others have experienced difficulties when mounting the baseline transducers in proximity to the guns. The operation of the guns stresses the units often causing premature failures and disturbs the water such that acoustic propagation is adversely affected, a point which is being addressed by the DBE system currently under development.

The system being developed by DBE is still a short baseline approach but recognises the above limitations and instead focuses on optimising performance within a useful range. However, in doing so it only addresses the task of positioning the front-end of the streamers. Any future developments should attempt to overcome the inherent range limitations of these techniques if they are to be successful in achieving all the requirements.

One approach, which has recently been investigated at DBE, is to form a long baseline of responder units attached along one streamer's length, and corresponding lines of receivers attached to the remaining streamers. By fixing the positions of the front end units (either by extending the system to two fixed units on the ship's hull, or by an independent means), the positions of adjacent units can be calculated down the whole length of the streamer. If more receivers than responders are placed on each streamer, then the additional data can be used to increase the accuracy and reliability of the position fixes.

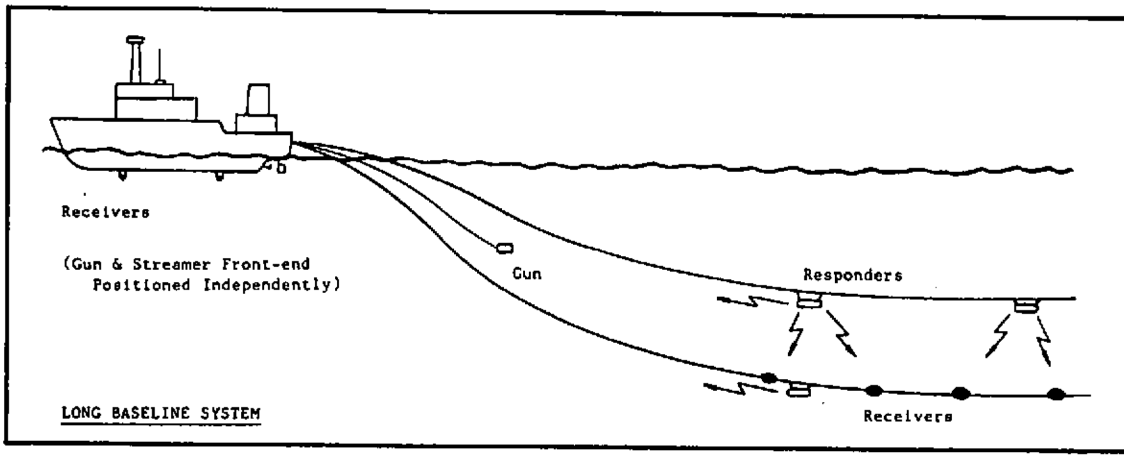

An additional feature of this design is the responder output waveform. Each unit can be programmed with a multi-frequency signature that ensures the highest probability of detection using a digital multi-frequency correlator. By changing this signature between cycles, the throughput rate can be drastically increased without interference from reverberations. This approach is believed to be necessary to ensure maximum availability of the system under all operating conditions. The recent use of over/under twin streamers to reduce weather downtime emphasises still further the need for systems to optimise their transmission techniques to combat the worsening acoustic environment.

To satisfy the last task for this system, to position the end of each streamer, the end responder can be replaced by an active transducer and a transponder attached to the tail buoy. This provides enough data to position the streamer ends with respect to the tail buoy, which is positioned with respect to the ship by other means such as microwave ranging or GPS (satelite).

SEISMIC STREAMER TRACKING, PAST, PRESENT AND FUTURE

SUMMARY

The basic requirement for any modern seismic streamer tracking system is to provide total positional information to better than 5m. All current systems in the field fall well short of providing this and changes in the performance of the acoustic elements of the system will not, in themselves, produce the necessary tracking improvement because of the fundamental nature of the problem - a poor acoustic environment near the sea surface behind the towing ship. There is therefore a need to design systems capable of accepting this limitation by tackling the problem in a different way acoustically and by integrating other sensors (eg depth, magnetic) to realise a total solution.

It should be noted that the need to identify the position of a streamer also exists for the military. Passive towed arrays are used to take advantage of the low transmission loss of low frequency sound, generated by vessels, for detection, classification and tracking purposes. The beamforming techniques used which take advantage of the long acoustic aperture of the towed array, also need to know the position of all elements in the array. Although military operational requirements demand covert (ie silent) techniques, some of the proposed commercial techniques previously described are being evaluated for use in performance assessment trials. The spin-off from this type of work will be of direct value to solving the seismic streamer tracking problem.

REFERENCES

[1] TANER, M T AND F KOEHLER, Velocity Spectra - Digital Derivation of Velocity Functions. Geophysics 34 p859, 1969.

[2] O'BRIEN, P N S AND A L LUCAS, Velocity Dispersion of Seismic Waves. Geophysical Prospecting 19, p1, 1971.

[3] SHAH, P M Use of Wavefront Curvature to Relate Seismic Data with Subsurface Parameters. Geophysics 38, p812, 1973.

[4] JAKUBOWICZ, H AND R BENSON, A Flexible Approach to the Stacking and Quality Control of 3-D Data. (In print).

[5] Article from the Oilman, August 1987, p56.

[6] Simrad HPR Streamer and Airgun Tracking System - Technical Leaflet C1544E, May 1984.

[7] COOK PL Principles and Approaches for Towed Array Tracking, International Seminar on Subsea Acoustics, Bergen, Norway, 1986.

Proceedings of the Institute of Acoustics

AMPLITUDE MODULATED CONTINUOUS EMISSION ACOUSTIC RANGING TECHNIQUE

A.K.T. Lee (1), J. Lucas (1) and L.E. Virr (2)

(1) Department of Electrical Engineering and Electronics, University of Liverpool, P.O.Box 147, Liverpool L69 3BX.
(2) Admiralty Research Establishment, Experimental Diving Unit, Vernon, Portsmouth PO1 3ER.

INTRODUCTION

A wide range of sonar systems now exists, operating at acoustic carrier frequencies of up to 700kHz, and covering distances from a few metres to many kilometres, and for purposes which include navigation, detection, location and classification of underwater objects and echo-sounding [1].

In the majority of sonar systems, target discrimination is achieved by using the pulse/echo technique whereby the range to any particular target can be estimated from the echo-return time and the speed of sound in water. In order to achieve accuracy closely spaced targets, short pulse lengths and consequently wide bandwidth systems are required with the attendant penalty of noise susceptibility.

An alternative to the conventional pulse/echo technique for which a high degree of range resolution is claimed is the use of a frequency modulated carrier, range being calculated from the frequency difference between transmitted and returned signals. Such systems present major problems however, and complex circuitry is required for their realization in hardware.

A need was identified for a simple ranging system capable of accurate measurement of distance to a single target underwater, for example the sea-bed, ship's hull etc., one possible application being use for altitude control of a remotely operated vehicle (ROV). This paper describes such a system, in which a carrier is amplitude modulated at selected modulating frequencies and transmitted continuously and range is calculated from the phase difference between transmitted and received signals. Accuracy is ultimately limited by the accuracy of phase shift measurement at the carrier frequency.

CONCEPT OF THE RANGEFINDING TECHNIQUE

This ranging technique is based on the linear phase delay of the received signal with respect to the transmitted signal due to the finite time taken by the wave front to travel from the transmitter to the receiver via the reflecting surface [2]. In the present system, in addition to the carrier frequency f3, two low frequency sinusoidal signals at f1 and f2 are used to modulate the carrier sequentially. The phase shift of the modulating frequency with the longest wavelength gives the first approximation to the range, and the phase shift of the second frequency with a shorter wavelength gives a more accurate measure of the range when considered together with the phase information given by the first approximation. Use of this approximate range information enables accurate estimation of range from the carrier phase shift. Ultimate accuracy is determined by the acoustic carrier frequency in the present system 40kHz corresponding to range accuracy of $\pm$1mm assuming approximately $\pm$10 degree accuracy in phase shift measurement at the carrier frequency. In order to avoid measurement ambiguities, f3/f2 and f2/f1 should not exceed, say, 10. The carrier amplitude modulated by the lowest frequency modulating signal, f1, is transmitted and the phase difference between the modulating signal and the received signal at f1 after demodulation recorded. The approximate range is given by:

$$R1 = \frac{1}{2} \left(\frac{\phi_1}{360} \right) \lambda_1 \qquad (1)$$

The value of R1 measured at the longest wavelength is only approximate because a large displacement has to be made for a small change of phase angle, and a small displacement is difficult to measure accurately. In order to obtain a more accurate reading, the shorter modulating wavelength λ_2 is used (where $\lambda_1/\lambda_2<10$). The shorter modulating wavelength enables greater accuracy in range measurement. While greater accuracy can be achieved at the shorter wavelength λ_2, it is necessary to ascertain the number of complete wavelengths (N2) contained in the total path length from the transmitter to the receiver. If the first approximation given by R1 is used as a first indication of the range, the integer number of wavelengths N2 of the shorter wavelength signal λ_2 enclosed in R1 is given by:

$$N2 = \mathrm{Int} \left\{ \frac{\lambda_1}{\lambda_2} \times \frac{\phi_1}{360} \right\} \qquad (2)$$

The total number of wavelengths N2 plus the fractional phase change ϕ_2 (< 360) of the shorter wavelength signal gives:

$$R2 = \frac{1}{2} \left(\frac{\phi_2}{360} + N2 \right) \lambda_2 \qquad (3)$$

The value of R2 is a more accurate measure of the displacement. Greatest accuracy is achieved by using the phase shift of the carrier itself (ϕ_3) at frequency f3, following the same procedure where the integer number N3 of wavelength enclosed in R2 is given by:

$$N3 = \mathrm{Int}\left\{ \frac{\lambda_2}{\lambda_3} \left(\frac{\phi_2}{360} + N2 \right) \right\} \qquad (4)$$

Thus range R3 is:

$$R3 = \frac{1}{2} \left(\frac{\phi_3}{360} + N3 \right) \lambda_3 \qquad (5)$$

A difficulty in evaluating N2 and N3 may arise due to the inaccuracy of measuring R1 and R2 respectively. Whenever the conditions R1 $\simeq N2 \lambda_2$ or R2 $\simeq N3 \cdot \lambda_3$, equations (2) and (4) may cause N2 or N3 to be incorrect by 1 integer. In order to overcome the problem, the algorithm used incorporates a simple check to establish the correct N2 or N3 value. N2 is taken as $\{\mathrm{Int}(\frac{\lambda_1}{\lambda_2} \cdot \frac{\phi_1}{360} \pm 1)\}$, whichever gives R2 nearest to R1. Similarly N3 is taken as $\{\mathrm{Int}[\frac{\lambda_2}{\lambda_3}(\frac{\phi_2}{360} + N2) \pm 1]\}$, whichever gives R3 nearest to R2. If the transmitter and the receiver are adjacent, then the distance (D) of an object is given by D = R/2.

CIRCUIT IMPLEMENTATION

The block diagram of the rangefinder circuit is given in figure 1. The sinusoidal frequencies used in this rangefinder were generated by two RS8038 waveform generator ICs [3]. One RS8038 was permanently tuned to generate the carrier (nominally 40kHz), and the other one generated one or other of the modulating signals (nominally 400Hz or 4kHz) as required by switching in the appropriate timing resistors through analogue switches. The amplitude modulation was performed by an analogue multiplier RS1495 used as a balanced modulator. The carrier and the modulating signals are generated simultaneously from the two RS8038 devices, and fed to the inputs of the analogue multiplier. The modulation index was set to < 1 by adjustment of the amplitude of the modulating signals by using the dc offset at the input to the multiplier. The AM signal at the output of the multiplier is amplified and used to drive the transmitting transducer, separate transducers being used for transmission and reception. For the present (initial) experiments, custom built transducers were not used as one of the objectives was to establish optimum design criteria with regard to mechanical and electro-acoustic features and operating frequencies.

The demodulator circuit comprises a differential amplifier and an envelope detector. The differential amplifier is used to eliminate any common mode noise present at the output of the receiving transducer. The envelope detector is a diode circuit followed by a 4th-order active bandpass filter. Two sets of 4th-order bandpass filters are required, tuned to the two modulating signal frequencies (i.e. nominally 400Hz and 4kHz), the appropriate filter being switched in by reed relays when required.

The ranging technique requires accuracy of phase measurement. A phase comparison measurement technique was designed to measure the phase difference of two sinusoidal waves inputs over a wide range of frequencies. The principle of operation is demonstrated in figure 2. The two sinusoidal signals are converted into square waves, and the rising edges of the two square waves used to modulate the "on" time of the Q output of a D-type flip-flop. The Q output of the D-type flip-flop thus gives a rectangular pulse train with pulse width corresponding to the phase difference between the sinusoidal signals. The rectangular pulse is integrated to produce a dc output proportional to the pulse width, providing a convenient input to the microprocessor. The simple phase comparator described above was used to measure phase shifts between 0 - 180 degree, and a second D-type flip-flop, with the transmitted and received signals connected to the "D" and clock inputs respectively, was used to provide additional "lead/lag" information to enble phase shift measurements in the range 0 - 360 degree.

RESULTS
Preliminary experiments were carried out in air using commercially available (identical) transmitting and receiving transducers at a carrier frequency of 40kHz, with modulating frequencies of 400Hz and 4kHz. For the in-air experiments, receiver "bandwidth" was minimized by mechanical means and the ranging system used to scan a number of objects at distances up to 5m. Since this distance could be considerably greater than half wavelength at the lowest modulating frequency, (i.e. 40cm at 400Hz), the system was used to measure increments in range of not greater than 40cm). Figure 3 shows the variation of phase shift at the modulating and carrier frequencies with the transmitting and receiving transducers facing each other. Figure 4 shows the results obtained when the ranging system was used, with transducers side-by-side, to scan the edge of a box-shaped object against a flat baseplate. Regions of uncertainty are evident corresponding to the edge of the object. Figure 5 shows the results of scanning a "V" preparation with 45 degree angled sides weld joint using the carrier frequency alone (40kHz) for which ultimate range modulation (in air) is 4mm. The correlation between acoustic scan and the actual "V" shape is evident.
In-water experiment to date have been limited by available transducers and, as stated earlier, one objective of the

initial experiments was to determine optimum design criteria. The system was mounted on a buoy, with transmitter and receiver transducers pointing downwards beneath the water surface. After initial "calibration" experiments the same arrangement was used in a large 10m diameter tank with adjustable water "depth" (actually achieved by varying the depth of a wooden floor of approximately the same diameter as the tank). Figure 6 shows the floor depth as recorded by the ranging system as a function of actual depth. Figure 7 shows the results obtained when the system was used to scan a large box-shaped object.

CONCLUSIONS

System effective for measuring distance accurately to large flat surface, e.g. sea-bed. Application for depth, height monitoring, height control of ROV.

Further experiments will determine transducer requirements and optimum operating frequencies for useful sea-bed type measurements.

References

[1] L.E. Virr, 'Role of electricity in subsea intervention', IEE Proc., Vol 134, PtA, No.6, 547-76, (1987)
[2] F.G. Stremler, 'Introduction to communication systems', Addison-Wesley Publishing Company, London.
[3] RS Components Data Catalogue and Information Notes, P.O.Box 12, Stockport, Cheshire SK4 2JT
[4] J. Blitz, 'Fundamental of ultrasonics', Butterworths, London.

Acknowledgements

One of the author (A.K.T. Lee) wishes to thank ARE (EDU) for the granting of the studentship to allow him this work to be undertaken.

AMPLITUDE MODULATED CONTINUOUS EMISSION ACOUSTIC RANGING TECHNIQUE

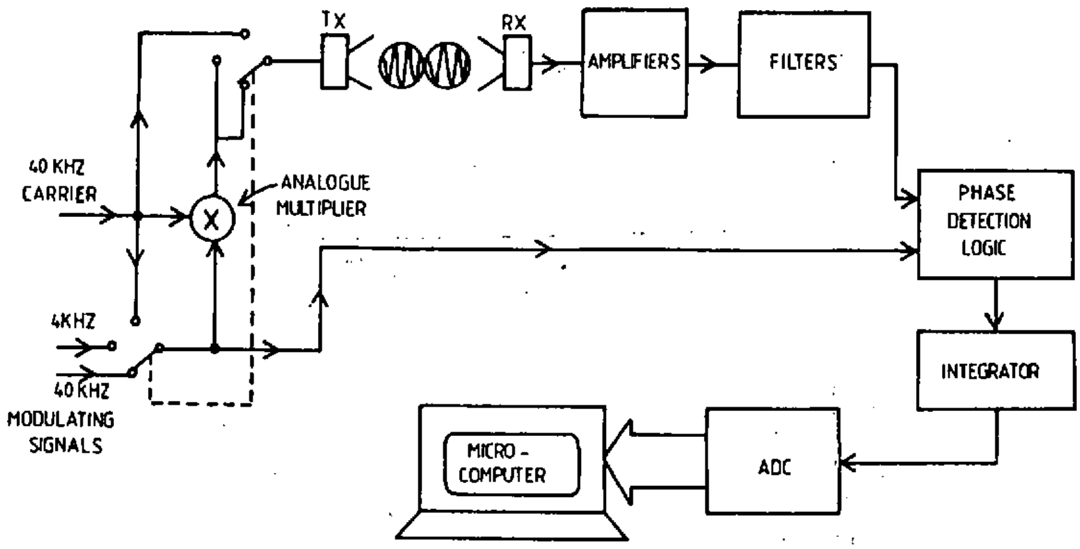

FIGURE. 1.

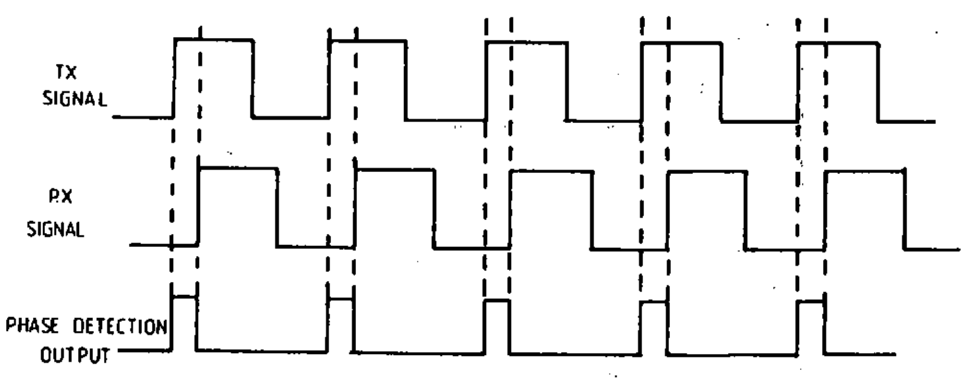

FIGURE. 2.

AMPLITUDE MODULATED CONTINUOUS EMISSION ACOUSTIC RANGING TECHNIQUE

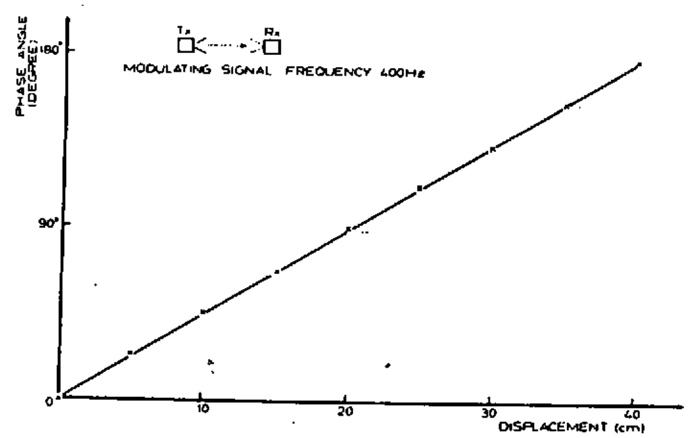

FIGURE. 3.(a).

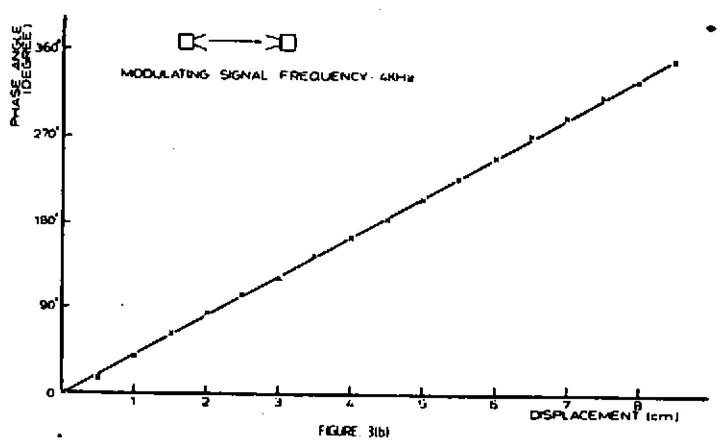

FIGURE. 3(b)

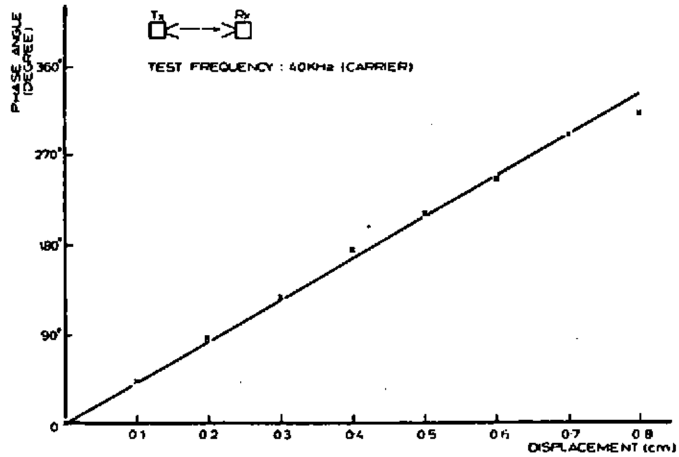

FIGURE. 3(c)

AMPLITUDE MODULATED CONTINUOUS EMISSION ACOUSTIC RANGING TECHNIQUE

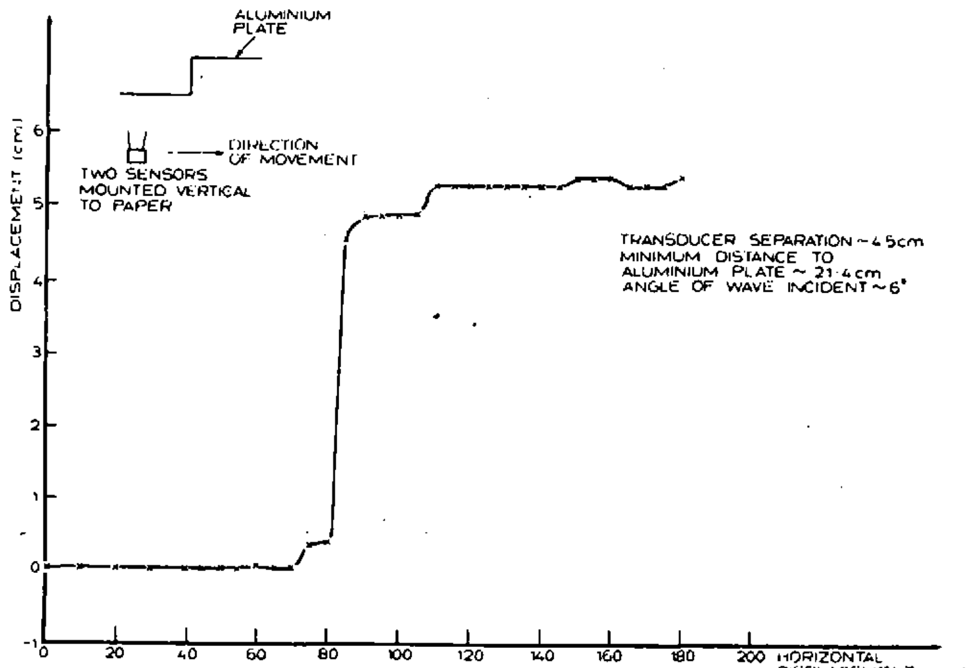

FIGURE 4

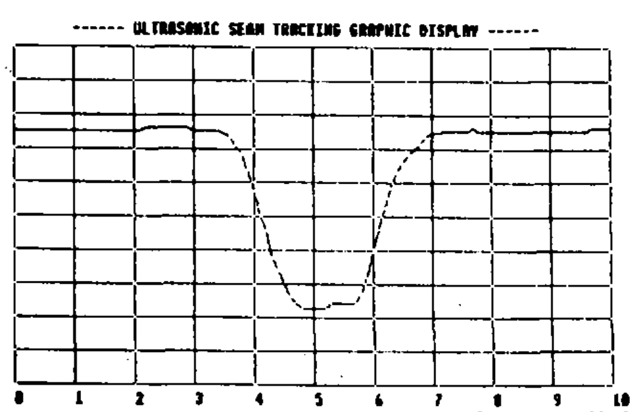

Vertical displacement: 0.4mm/DIV
Metal thickness: 2mm

FIGURE. 5.

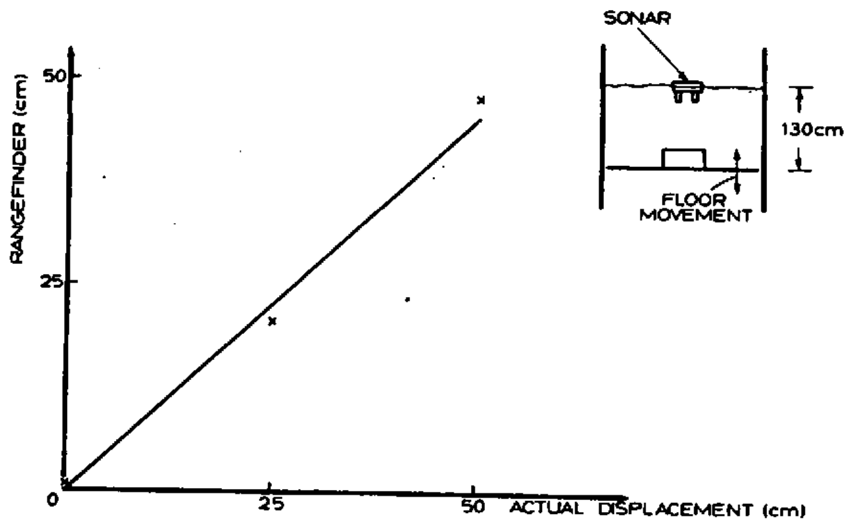

FIGURE. 6.

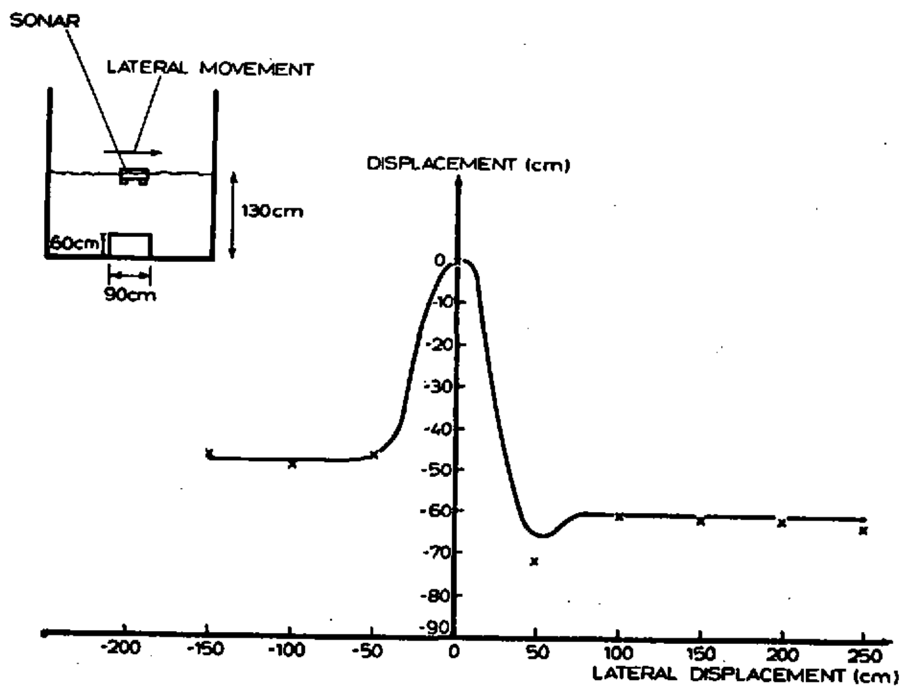

FIGURE. 7.

Proceedings of the Institute of Acoustics

THE PREDICTED PERFORMANCE OF AN UNDERWATER NAVIGATION SYSTEM BASED ON A CORRELATION LOG

P. Atkins and B. V. Smith

Department of Electronics and Electrical Engineering,
University of Birmingham, P.O. Box 363, Birmingham B15 2TT

INTRODUCTION

Acoustic velocity sensors may be successfully used as part of an integrated underwater navigation system. Considerable improvements may be achieved in the the accuracy of the velocity estimate by using bottom referenced systems compared to water-mass referenced systems such as electromagnetic logs.

The traditional acoustic method of obtaining a velocity estimate is by the use of a Doppler log. A suitable compromise must usually be made between good Doppler discrimination and large operational ranges. Correlation logs [1] are a possible alternative to the Doppler log and are in general less affected by secondary disturbances such as temperature variations in the water-mass.

The performance of the correlation log is primarily determined by the transducer geometry. The accuracy of the velocity estimate will also be related to the observation distance allowed to obtain an estimate of the correlation function of the backscattered acoustic field. The large integration distances that are required to obtain velocity estimates make the correlation log an ideal sensor for measuring the elapsed distance of a vessel travelling at a near constant velocity and heading.

ESTIMATION OF THE SPATIAL CORRELATION FUNCTION

Both spatial and temporal correlation logs operate by estimating the position of the spatial cross-correlation function with respect to time. The resolution of this estimate will therefore be determined by the spatial separation and the effective signal-to-noise ratio of the spatial correlation function.

The form of the spatial covariance function will, for most operating conditions, be determined by the geometry of the acoustic projector. For example, the form of the spatial covariance function assuming small slopes for the bottom irregularities and a circular projector may be predicted as [2,3]:

$$\overline{V_1 V_2^*} = W^2 \int_0^1 D^2rt \; x(1-x^2) \; J_o(dkx) \, dx \qquad (1)$$

where $Drt = \dfrac{2J_1(kax)}{(kax)}$, the directivity function of the projector

THE PREDICTED PERFORMANCE OF AN UNDERWATER NAVIGATION SYSTEM BASED ON A CORRELATION LOG

and W is a constant
x is an integration variable
J_o, J_1 are Bessel functions
k is the wave number
d is the spatial separation of two receivers
a is the projector radius

This function is derived by analytic techniques whereas the measured function is obtained from stochastic signals and will therefore only approach the predicted value as the observation distance approaches infinity. Predicted normalised spatial covariance functions are shown in figure 1 for three circular projectors with diameters of 10mm, 20mm and 30mm, which are operating at a frequency of 150kHz.

Jenkins and Watts [4] show that the covariance of an estimated covariance function may be approximated by :

$$Cov[Cxx(u_1),Cxx(u_2)] \simeq \frac{1}{D}\int_{-\infty}^{\infty} \gamma xx(r)\gamma xx(r+u_2-u_1) + \gamma xx(r+u_2)\gamma xx(r-u_1)\, dr \qquad (2)$$

where Cxx is the estimate of the covariance function
γxx is the theoretical covariance function
u_1, u_2 are spatial lags

This approximation is only valid if the observation distance, D, is large. This assumption will be valid for a practical correlation log where the observation distances are typically of the order of tens of metres. The spatial lag terms u_1 and u_2 are also assumed to be small.

By equating the lag terms u_1 and u_2 the variance of the estimated covariance function may be obtained.

$$Var[Cxx(u)] \simeq \frac{1}{D}\int_{-\infty}^{\infty} \gamma xx^2(r) + \gamma xx(r+u)\gamma xx(r-u) \quad dr \qquad (3)$$

This equation shows that the variance of an ensemble of covariance estimates is inversely proportional to the observation distance, D. The normalised variance of the theoretical function described by equation (1) is shown with respect to the spatial offset from the peak of the function in figure 2. The cases for the three different projector diameters are shown in this figure.

Figure 2 effectively provides an estimate of the normalised noise error power at a particular spatial separation from the peak of the spatial covariance function. However, a correlation log operates by attempting to measure the position of the peak of the estimated function. This estimate of the position of the peak will also depend on the correlation of the noise power across the function. Assuming that the peak of the estimated covariance function lies at a point $u_1 = 0$ then the covariance of the noise power may be obtained by :

THE PREDICTED PERFORMANCE OF AN UNDERWATER NAVIGATION SYSTEM BASED ON A CORRELATION LOG

$$\mathrm{Cov}[Cxx(0),Cxx(u)] \approx \frac{1}{D}\int_{-\infty}^{\infty} 2.\gamma xx(r)\gamma xx(r+u)\ dr \qquad (4)$$

This may be plotted with respect to the spatial separation u for varying projector dimensions, as shown in figure 3. It will be noticed that the noise power in the estimate of the spatial covariance function is highly correlated across the likely areas of interest. A comparison of figures 1 and 3 shows that the width of the noise covariance function is greater than the equivalent width of the spatial covariance estimate.

From a knowledge of the variance and the covariance parameters, the uncertainty in the estimate of the position of the peak of the function may be calculated. Assume that the theoretical peak of the spatial covariance function lies at a point u=0. The probability that the measured peak lies at, or beyond, a point, u, may be found by estimating the probability that Cxx(u) is greater than Cxx(0), remembering that Cxx(0) and Cxx(u) are measured functions and are assumed to have normally distributed statistics associated with them. This may be calculated by :

$$p_e(u) = \int_{\infty}^{\infty}\int_{Cxx(u)}^{\infty} p(Cxx(0)).p(Cxx(u)|Cxx(0))\ \ dCxx(0)\ dCxx(u)$$

where $p(Cxx(u) >= Cxx(0)) = p_e(u)$

For a normal bivariate distribution this may be shown to be equal to :

$$p_e(u) = \frac{1}{\sqrt{2.\pi.\mathrm{Var}(Cxx(0))}}\int_{-\infty}^{\infty}(1 - \mathrm{erf}(Yo))\ \exp^{\frac{-(x - \gamma(0))^2}{2.\mathrm{Var}(Cxx(0))}}\ dx$$

where

$$Yo = \sqrt{\frac{K11.x^2}{2.(K11.K22 - K12^2)}}\left[1 - \frac{K12}{K11} + \frac{K12}{K11}.\ \gamma(0) - \gamma(u)\right]$$

and
$$K11 = \mathrm{Var}(Cxx(0))$$
$$K22 = \mathrm{Var}(Cxx(u))$$
$$K12 = \mathrm{Cov}(Cxx(0),Cxx(u))$$

The results of numerical calculations of $p_e(u)$ are plotted in figure 4 for three projector diameters and observation distances, D, of 1m and 10m. The probability $p[Cxx(u) >= Cxx(0)]$ diminishes very rapidly with the spatial displacement, u. The results can be seen to be highly dependent on the observation distance, D.

The statistics of an ensemble of estimates of the peak of the spatial covariance function are likely to be normally distributed with a mean equal to that of the theoretical position of the peak. The value of u equivalent to one standard deviation may be derived by setting $(1 - p_e(u))$ equal to 0.683, this is justified as the variance of the estimate is highly correlated across the region of interest.

THE PREDICTED PERFORMANCE OF AN UNDERWATER NAVIGATION SYSTEM BASED ON A CORRELATION LOG

Figure 5 shows the required observation distance, D, plotted with respect to the value of the standard deviation of the estimated position of the peak.

RESOLUTION OF THE VELOCITY ESTIMATE

Both temporal and spatial correlation logs operate by measuring the displacement of the spatial covariance function with respect to time. In the case of the temporal correlation log this displacement is fixed whereas in the case of a spatial correlation log this separation may fall anywhere within a pre-defined range of values.

Assume that the separation of the spatial covariance function is defined as S and that the uncertainty of this estimate is given by ΔS. The accuracy of the system may then be defined as $\Delta S/S$. The spatial uncertainty ΔS is equivalent to one standard deviation associated with the estimate of the peak of the spatial covariance function. In a practical situation the size of the transducer housing will be limited. This places a limit on the separation, S, and on the maximum update rate in terms of the distance travelled for a given accuracy. A typical transducer housing would be of the order of 75mm for a commercial vessel and 300mm for a small, survey-orientated submersible. The maximum transducer separation would typically be of the order of 25mm less than the housing dimensions. Figure 6 shows the expected accuracies with respect to distance travelled of a device with transducer separations of 25mm and 250mm and projector diameters of 10mm and 20mm.

Figure 6 shows the required observation distance to obtain a specified accuracy and shows the importance of using large receiver transducer separations to obtain high accuracies. Practical sonar correlation logs would normally use a pulsed transmitter when ranges in excess of a few metres are required. A sampled version of the acoustic backscattered field is therefore used in obtaining the estimate of the covariance function. The sampling efficiency may be defined as the transmit pulse duration divided by the pulse repetition period. This sampling efficiency would typically be in the range 10% to 20%, resulting in the actual distance travelled by the vessel being between five and ten times the observation distance predicted in figure 6.

LIMITATIONS ON THE RECEIVER TRANSDUCER SEPARATION

A limit is imposed on the maximum value of receiver transducer separation by the velocity and the depth separation (altitude) of the vessel. The spatial covariance function moves at a rate $2\bar{v}$ away from the reference receiver, where $\bar{v}$ is the velocity of the vessel. Equating this to the transducer separation, S, and time:

$$S = 2\bar{v}t$$

Typically, the time t would be of the order of half the transmit pulse period. The transmit pulse period is in turn limited to a value of the order of half the two-way propagation time. i.e.

transmit pulse period = $\frac{z}{c}$

where z is the depth separation
c is the velocity of propagation

Therefore

$$S <= \frac{v.z}{c}$$

This places a severe limitation on the accuracy of the device at low speeds and in shallow water. Under these conditions, the effective receiver separations must be reduced to compensate. The spatial correlation log has the inherent ability to do this because of its multi-element array structure, such a device will have a very poor accuracy performance under such conditions.

A typical minimum depth with respect to speed trade-off is shown in figure 7. This shows the performance bounds for a number of transducer separations when using a 10mm diameter projector. The predicted accuracy performance for an observation distance of 10m is shown in brackets for comparison. A correlation log will not be able to operate with the defined accuracy in the region enclosed by the ordinates and the performance bound.

OTHER PERFORMANCE LIMITING FACTORS

The above discussion of the predicted performance of a correlation log is based on the spatial characteristics of the acoustic backscattered field. A number of other performance limiting factors must also be considered.

Electrical system noise will affect all the channels used by the correlation log. This will be uncorrelated from channel to channel and will be bandlimited. In a practical system the signal-to-system noise ratio will be large. The time period required for the vessel to travel the required observation distance between velocity updates will ensure that a large number of independent samples are incorporated into the process and hence the effects will be negligible.

Acoustic noise will consist of two components. An uncorrelated noise component will be received, the primary source being flow noise. A partially correlated noise signal will be received from isotropic noise sources and reverberation. Increasing the pulse repetition period may be required to remove the effects of reverberant signals.

The design of the receiver elements may introduce a summation of correlated components caused by the large number of linear paths that may be drawn from one finite sized receiver element to another. This effect may cause significant errors when the vessel is moving with excessive transverse velocities.

THE PREDICTED PERFORMANCE OF AN UNDERWATER NAVIGATION SYSTEM BASED ON A CORRELATION LOG

The most significant performance limiting factor has been found to be due to returns from the wake of the vessel. In general, the wake of the vessel will be moving at a greater differential velocity with respect to the vessel than that of the sea bed. The wake frequently contains significant levels of aeration and therefore has a large target strength. A simple projector could place a sidelobe pointing to the wake with an attenuation of only 13dB with respect to the main lobe. Significant quantities of information obtained from the wake could thus be processed causing a large error in the velocity estimate with respect to the sea bed.

COMPARISON OF THE PREDICTED AND MEASURED RESULTS

A two axis temporal correlation log has been constructed and field tested [5,6]. The results of a number of track plots obtained by integrating the output of this device with respect to heading are shown in figure 8. The vessel was timed through two theodolites aligned normally to the expected track of the vessel, this provided an estimate of the actual velocity of the vessel. Figure 8 shows two sets of tracks caused by windage and a current acting on the vessel as it steered to a constant heading.

Figure 9 shows an expanded view of the end of the tracks complete with 1% error bounds. The standard deviation-to-mean percentage evaluated over eleven runs was measured as 0.64%. No parameters are available for the likely timing errors in these measurements caused by the manual identification of the position of the vessel. When related to the velocity of the vessel this represents a timing error of about 1.6s, probably limited by the human reaction time of initiating and terminating a run.

The correlation log used for these measurements incorporated a projector of dimension 10mm and a receiver separation of 28.28mm. Velocity estimates were obtained at intervals of approximately 60m. Assuming that a sampling efficiency of 10% was used then the actual observation distance was of the order of 6m. Figure 5 indicates that the predicted error in determining the peak of the spatial covariance function would be of the order of 0.34mm for this observation distance. This corresponds to a value for the predicted accuracy for a single velocity estimate of the order of 1.2%. Fifteen such velocity estimates would be obtained within a single track as shown in figure 8. Assuming a normal distribution of errors, it would be expected that the standard deviation-to-mean ratio of the elapsed distance would be of the order of 0.31%. It can be seen that the predicted and measured performances of the correlation log are of the same order.

CONCLUSIONS

A number of performance limiting criterion have been illustrated for a correlation log. It is the view of the authors that the performance of a correlation log may be accurately predicted from a knowledge of the geometry of the transducer and a value of the observation distance. A high signal-to-noise ratio has been assumed throughout, as this is readily obtained in practice.

THE PREDICTED PERFORMANCE OF AN UNDERWATER NAVIGATION SYSTEM BASED ON A CORRELATION LOG

A comparison has been made between the predicted performance and the measured performance of a correlation log. The measured and predicted results were found to agree closely.

ACKNOWLEDGEMENTS

The design, manufacture and testing of the two-axis, temporal correlation log referred to in this paper was funded by the Admiralty Research Establishment. The authors are indebted to the staff of ARE for their help throughout.

REFERENCES

[1] Dickey, F.R. Jr and Edward, J.A.: 'Velocity Measurement Using Correlation Sonar', IEEE Position Location and Navigation Symposium, San Diego, 6-9 November 1978, pp 255-264.

[2] Smith, B. V.:'A Study of the Influence of Spatial Correlations on the Performance of Correlation Logs'. Departmental Memorandum No. 498. Department of Electronics and Electrical Engineering. University of Birmingham.

[3] Atkins, P. and Smith, B. V.:'Simulation of Acoustic Backscattering from a Random Surface using Optics', Acoustics '86, Salford, April 1986, Proc. Inst. of Acoustics, Vol. 8, Pt. 3, pp 155-164.

[4] Jenkins G.M. and Watts D.G.: 'Spectral Analysis and its Applications', Holden-Day.

[5] Atkins, P. and Smith, B. V.:'High Accuracy Two-Axis Velocity Measuring Device', IERE Conference - Electronics for Ocean Technology, March 1987, Publication No. 72, pp77-82.

[6] Atkins, P. and Smith, B. V.:'The Optimal Extraction of Velocity Information from a SONAR Correlation Log', Microprocessing and Microprogramming 21 (1987) pp161-170

THE PREDICTED PERFORMANCE OF AN UNDERWATER NAVIGATION SYSTEM BASED ON A CORRELATION LOG

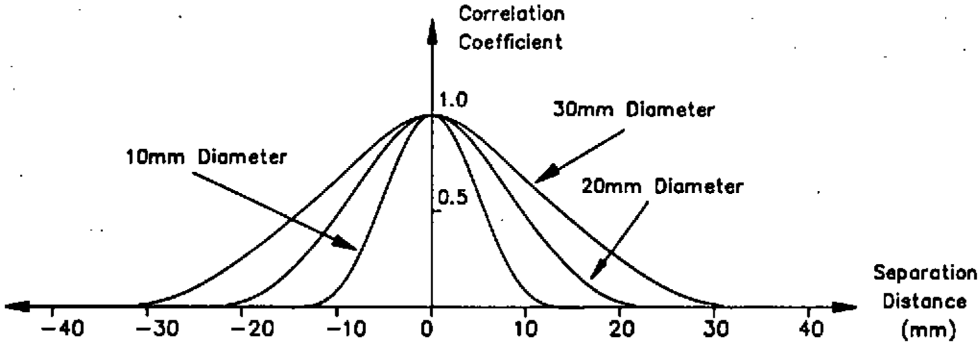

Figure 1 : Predicted Spatial Correlation Functions for Three Circular Projectors

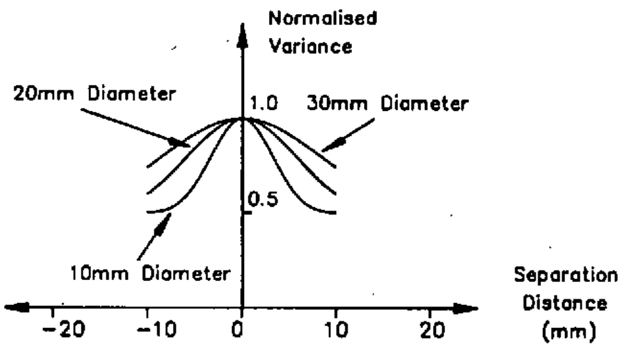

Figure 2 : Predicted Normalised Variance of the Spatial Correlation Function

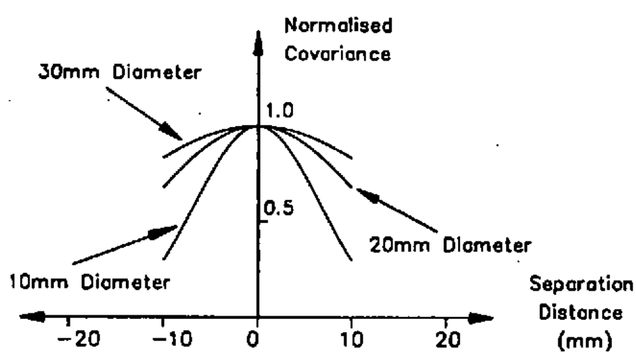

Figure 3 : Predicted Normalised Covariance of the Spatial Correlation Function

THE PREDICTED PERFORMANCE OF AN UNDERWATER NAVIGATION SYSTEM BASED ON A CORRELATION LOG

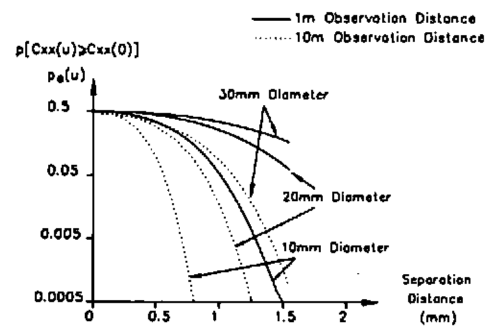

Figure 4 : Probability, $p_e(u)$, that $Cxx(u) \geq Cxx(0)$

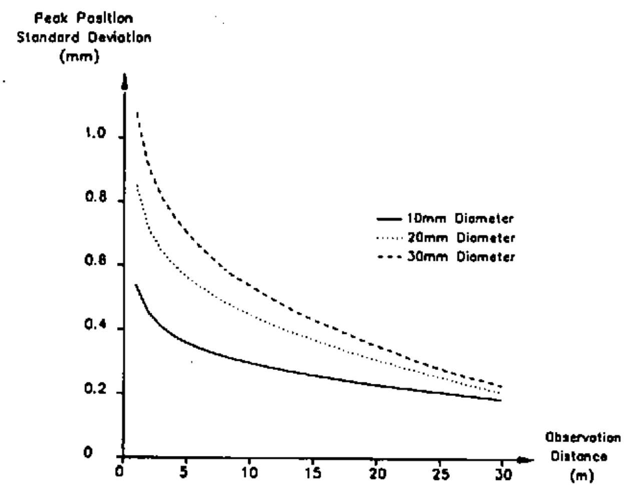

Figure 5 : Standard Deviation of the Peak Estimate with respect to the Observation Distance

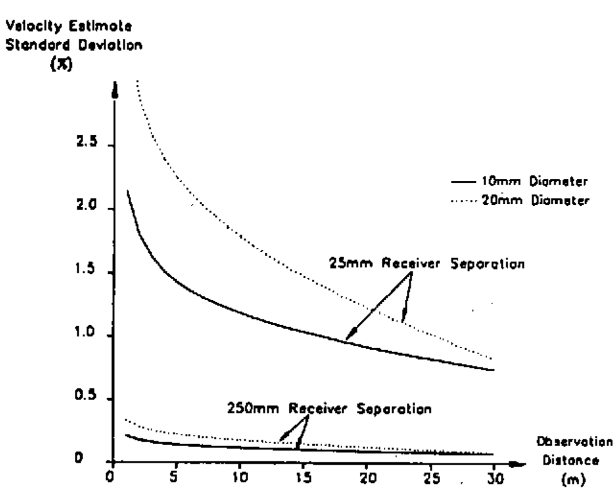

Figure 6 : Predicted Percentage Error in the Velocity Estimate

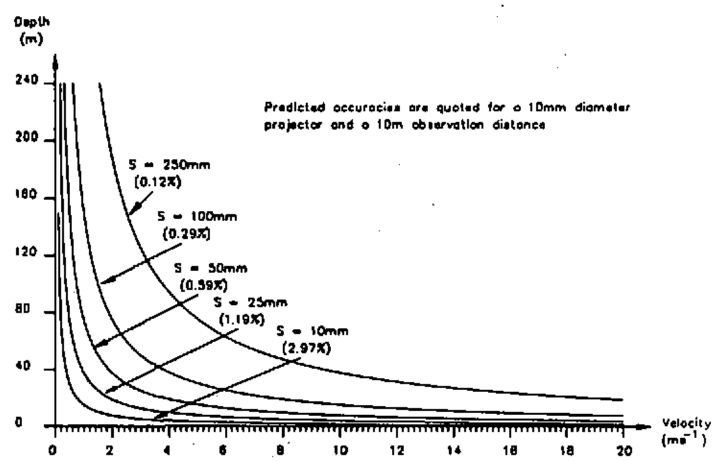

Figure 7 : Minimum Speed and Depth Bounds with respect to Receiver Separation

THE PREDICTED PERFORMANCE OF AN UNDERWATER NAVIGATION SYSTEM BASED ON A CORRELATION LOG

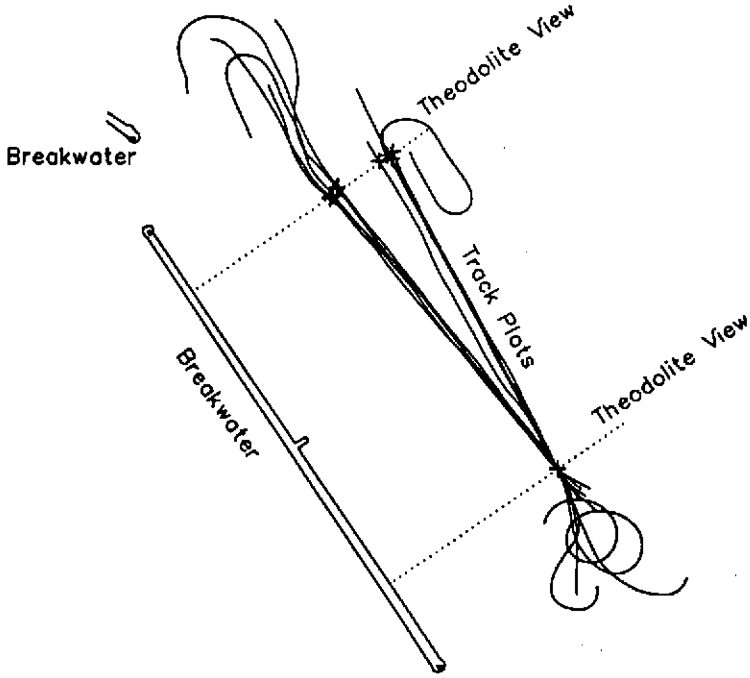

Figure 8 : Predicted Track Plots of Vessel

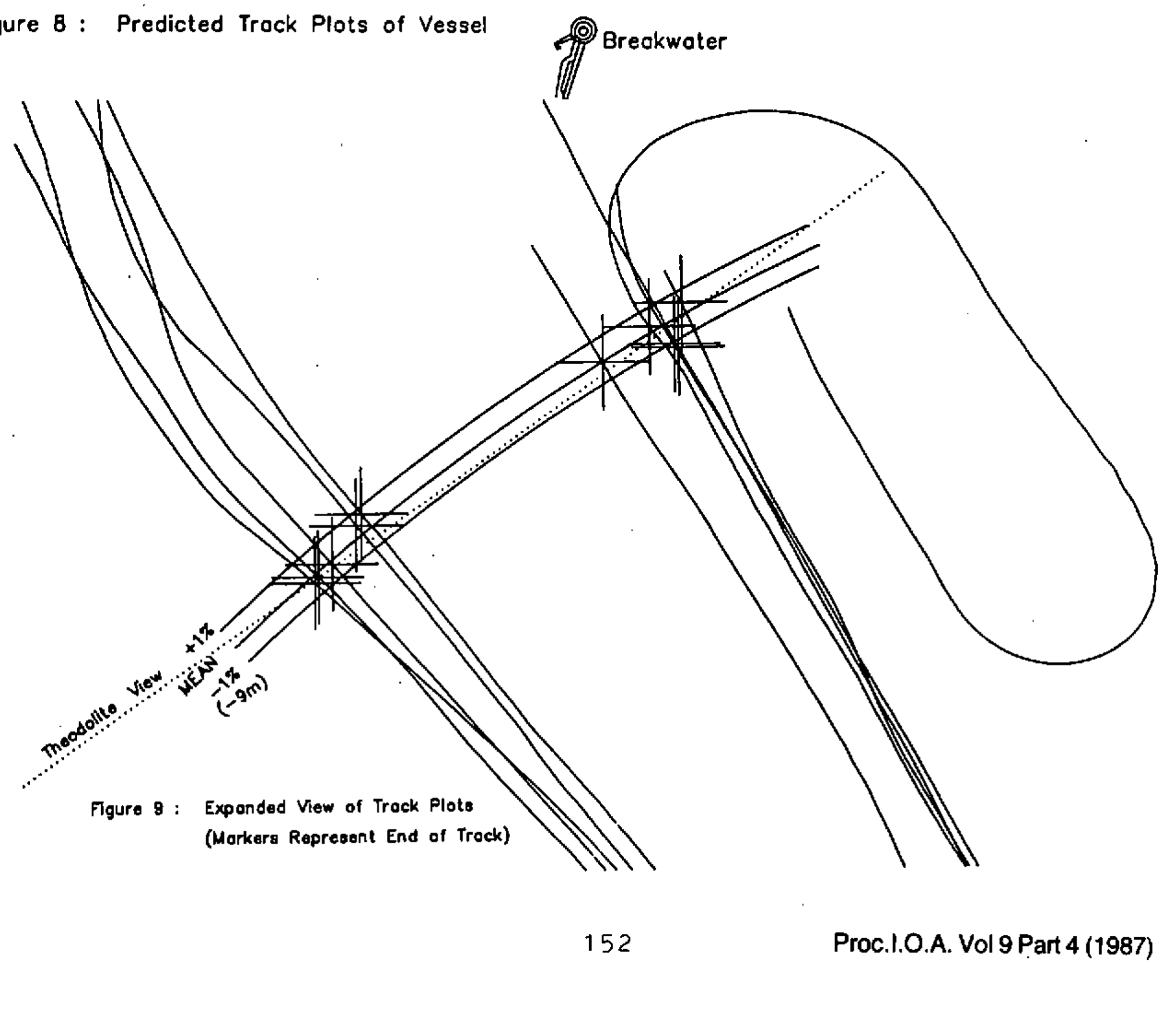

Figure 9 : Expanded View of Track Plots
(Markers Represent End of Track)

Proceedings of the Institute of Acoustics

AN EXPERIMENTAL ACOUSTIC TEMPORAL CORRELATION LOG FOR SHIP NAVIGATION

S. K. Hole, W. Forsythe, B. Woodward

Dept. of Electronic & Electrical Engineering, University of Technology, Loughborough, Leicestershire.

ABSTRACT

Acoustic Doppler logs have generally replaced traditional speed logs on board merchant ships, but their operation is far from ideal. Consequently, increasing interest has been shown in the acoustic correlation log which promises to overcome some of the deficiencies of the Doppler log. Advantages of it include bottom tracking the velocity to a greater depth than a Doppler log and much simpler transmitting and receiving array design.

The transducer arrangement is similar to the conventional echo sounder, where the pulses are transmitted vertically downwards. It is possible to operate the log in pulsed mode to great depths.

In shallow water a CW mode can be engaged, which permits a correlation log to be implemented easily at low cost and is ideal for navigation in shallow coastal waters, rivers and estuaries. It is this mode which is primarily under investigation and the subject of this paper. The paper describes work undertaken at LUT in implementing a CW correlation log in a water tank for the velocity measurement of a tracked platform.

INTRODUCTION

This paper describes work undertaken in the design and development of a temporal correlation log for the measurement of a ship's velocity. Initial experiments were carried out in a laboratory tank by measuring the velocity of a tracked platform. The platform runs in a straight line, horizontally across one side of the tank on two tracked girders approximately 300 mm above the water surface. Two stepper motors provide the motive force to drive it under computer control; this gives it a precisely known velocity.

The equipment is comprised of three parts, a projector/hydrophone array, a rack-mounted sonar and a microcomputer for control, which is interfaced to it as shown in Figure 1. The projector/hydrophone array is attached to the platform so that its propagation axis is in line with the tank's length and so that echoes are received from the end wall. This allows echoes to be received from the far field of the array at an effective range of approximately 8m (the tank's length). The transducers, with a 23^{o} half power beamwidth, are operated at their resonant frequency of 218 kHz.

The sonar rack houses all the electronics for the processing of the sonar signals, namely a transmitter, a dual-channel amplitude demodulating receiver and a digitiser. The transmitter is comprised of a stable reference oscillator feeding an external power amplifier via an attenuator which sets the transmitted continuous wave power level. The amplifier drives the projector located on the submerged transmitting/receiving array. The received echoes are picked up by the two hydrophones and are fed to the dual-channel receiver where they are amplified and detected. The two output voltage levels corresponding to the amplitude of the received signals are then digitised and passed to a microcomputer for processing.

A control program written in PASCAL configures the system as required. Parameters can be changed by choosing options from a Menu-driven user interface. Digitised samples can be stored on disc for later analysis, so that a comparison between different signal processing algorithms can be made.

THEORY

The temporal correlation log relies on the time delay measurement between signals received from two hydrophones H1 and H2 travelling inline with the velocity vector $\underline{V}$ of interest. If the hydrophone vector separation is $\underline{d}$ and the time delay measurement is T, then velocity vector $\underline{V}$ is given by

$$\underline{V} = \underline{d}/2T$$

as explained below.

In order to measure the time delay both received signals should be identical for perfect correlation; this is known as waveform invariance and is the basis of correlation velocity measurement. De-correlation occurs when the two signals are not identical, but a time delay measurement is still possible.

Dickey[1] described an aircraft navigator based on a continuous wave correlation radar. In the present work his explanation for identical signal reception is applied to a sonar system, shown in Figure 2, comprising two identical hydrophones H1 and H2 separated by a distance vector $\underline{d}$, and a projector P located midway between them. On a ship both the hydrophones and projector point vertically downwards. They move forward with a velocity $\underline{V}$, and the projector transmits a cw signal. Let the received signals on H1 and H2 be r1(t) and r2(t) respectively, and their detected envelope from the receivers be R1(t) and R2(t). Consider a point scatterer S at time t1, lying in a position where it intercepts the transmitted beam. Then the path length of the ray from P to the scatterer and back to H1 is PS+SH1. Later at time t2 when all three transducers have moved forward a distance $\underline{d}/2$, it can be seen that the new ray length from P to S and back to H2(PS+SH2) is identical to the first. Therefore the contribution of S to the signals r1(t1) and r2(t2) is the same, because it has the same amplitude and phase due to the same ray length. Now consider an infinite number of point scatterers, each one contributing to the two echoes received at H1 at time t1 or H2 at time t2. It is therefore possible to say $r1(t1) \simeq r2(t2)$ is valid, which shows that the received signal r2(t) is a delayed version of r1(t) by an amount t2-t1=T. We can therefore say that

$$\underline{V}T = \underline{d}/2$$

or

$$\underline{V} = \underline{d}/2T$$

which is the correlation log equation. The two detected envelopes R1(t) and R2(t) are described by

$$R1(t) = A1\left|r1(t) + n1(t)\right|_{LPF}$$

$$R2(t) = A2\left|r2(t) + n2(t)\right|_{LPF}, \quad r1(t+T) = r2(t)$$

where A1 and A2 are the gain factors of the receivers. Both the received signals r1(t) and r2(t) have additive noise n1(t) and n2(t) respectively, which may be background noise from the water or receiver noise. Figure 3 shows typical received envelopes.

The time delay measurement T is obtained by cross-correlating R1(t) and R2(t) after they have been quantised. Both the received signals r1(t) and r2(t) have additive noise n1(t) and n2(t) respectively, which may be background noise from the water or receiver noise. Figure 3 shows typical received envelopes.

The time delay measurement T is obtained by cross-correlating R1(t) and R2(t) after they have been quantised. Both R1(t) and R2(t) are quantised to 8-bit resolution, which should be sufficient provided there is no loss of accuracy during the correlation process. The quantisation noise is uncorrelated and will tend to cancel out in the correlation averaging process. However, the additive noise n1(t) and n2(t) may be correlated, and analysis is required for correlation in low signal-to-noise ratios. The reader is referred to Watts [2] for an analysis of amplitude quantisation with respect to correlation.

THE SYSTEM

The system comprises three main components as previously mentioned, a projector/hydrophone array, a rack mounted sonar and a microcomputer, as shown in Figure 1. The task of the microcomputer, which is an IBM PC-compatible model with an MSDOS operating system, is to control the sonar and to process the data received from it. Communication with it is by using 32 bytes of the input/output bus to read and write to peripheral registers; 16 bytes exist in the rack and the other 16 on the expansion card which plugs into the computer. A ribbon cable links the computer to the sonar which decodes the input/output bus for use. Figure 4 shows a block diagram of the sonar.

The main programming language for the system is PASCAL. Assembler is used in the interrupt handling routine, which is invoked when the analogue-to-digital converters have completed a conversion. The two 8-bit words read from the converters are stored in two arrays. The main program can then access these values and process them accordingly.

Projector/Hydrophone Array

The transducer array consists of a projector and two hydrophones, all of which are identical in construction and interchangeable. They consist of half-wavelength resonant piezoelectric elements, which give maximum efficiency for both projector and hydrophones. They are mounted in the array backplane and their relative positions are variable.

The individual elements are 20 mm-diameter piezoelectric ceramic discs made of PZT-4, with a 200 kHz nominal centre frequency. Each one is mounted in its own housing to ensure electrical isolation between the projector and hydrophones. The elements are air-backed, mounted in low density syntactic foam for support. This is enclosed in a circular Nylatron housing and unloaded epoxy resin is used as the acoustic window and also to seal the units. This arrangement gives a minimum possible separation of 50 mm between any pair of transducers when they are mounted in the array backplane. Locking clamps enable the transducers to be moved apart and re-clamped, thereby permitting a maximum separation between two transducers of 350 mm. This permitted different hydrophone separations and different hydrophone-to-projector separations to be used to study the effect of projector location on the correlation function.

During calibration it was found that the complete transducers were nearly identical, each with a resonant frequency of 218 kHz, a Q of 35 and a -3dB beamwidth of 23°. The first sidelobes were found to be 20 dB down on the main lobe.

Tests taken in the water tank revealed negligble crosstalk between the projector and hydrophones. The isolation was found to be at least -90dB for all hydrophone positions.

Ray path analysis of the tank using the projector hydrophone beamwidth shows that valid echoes are received over the central portion of the track. Echoes received when the platform is within 1.5 m of the tank's two sides are not analysed; only those received during a travelling distance of 2.5m over its central position are used. Pulsed transmissions verify that multiple echoes do occur but these diminish by the sixth one, where they are lost in the background reverberation. There is some decorrelation between the two received signals because of this and the problem is currently being investigated.

Dual Channel Amplitude Demodulation Receiver

The purpose of the receiver is to boost the two hydrophone signals r1(t) and r2(t) to acceptable levels, to detect them and to generate their envelopes R1(t) and R2(t). The phase of the carrier is not important in this application. Each channel of the receiver consists of four parts (1) a high input impedance low-noise pre-amplifier, (2) a bandpass filter, (3) an envelope detector, and (4) a low-pass filter, as shown in Figure 5.

The pre-amplifier and bandpass filter have a combined voltage gain of 100 (+40dB). The bandpass filter removes excess pre-amplifier noise and eliminates extraneous signals, such as self-noise, from around the carrier frequency. This is an active resonant type based on an operational amplifier design. The centre frequency is tuned to 218 kHz and the bandwidth is approximately 20 kHz.

The envelope detector consists of a precision rectifier based on two operational amplifiers and has a voltage gain of 4 (+12dB) before detection. The output at this stage is now dc coupled, so offset voltages become important and an offset null capability is present. The low-pass filter boosts the video signal up to full scale range (+10v) and attenuates any residual carrier. The filter is a third order type with a corner frequency of 4 kHz.

The video output from the receiver has a full scale range of +10v dc; the corresponding input for this is 6.25 mV at 218 kHz.

The two video signals R1(t) and R2(t) feed the inputs to the digitiser.

Digitiser

The purpose of the digitiser is to quantise the two video channels to 8-bit resolution and to pass the two values to the micro computer at a given sampling frequency.

A programmable sequencer is used to generate the timing waveforms at 8-bit resolution and to pass the two values to the micro computer at a given sampling frequency.

A programmable sequencer is used to generate the timing waveforms at 8 different sampling frequencies ranging from 100 Hz to 4 kHz. The design is based on a ROM look-up table to generate the signals to control the sample-and-hold amplifiers and the analogue-to-digital converters. Once a conversion has been completed an interrupt is generated to the microcomputer, which then reads the values from the two ADCs and stores them in memory for later processing.

Stepper Motor Interface

The two stepper motors on the platform are driven by two drive cards running in parallel. The cards only need a Direction and Step signal to operate. The Direction signal is obtained by writing to a latch from the computer. A programmable interval timer (PIT) is configured as both a programmable frequency generator and a counter. This allows the Step pulse frequency to be variable in order to alter the motor speed, but it only sends a certain number of pulses to control the platform displacement. Once configured the PIT is entirely automatic in operation and the computer can carry out other tasks.

Carrier Generation

A sinewave at around 218 kHz is required to drive the projector at its resonant frequency. A 218.750 kHz signal is derived from a 14.0 MHz quartz oscillator by dividing its output frequency by 64 with a binary counter. The signal is Low-pass filtered to remove harmonics and obtain a sinewave. It is fed through a programmable attenuator to set the power level at the projector. Its output is buffered to drive an external power amplifier which powers the projector.

RESULTS AND CONCLUSIONS

Individual components of the system have been tested and they work satisfactory. They are currently undergoing integration, and system performance tests are presently being carried out. So far results from the sonar seem to be in accordance with expectations. At present only a rudimentary analysis of digitised echoes is being carried out. Correlation signal processing algorithms are being developed and it is intended that they should perform in real time, with the velocity measurement taken over a variety of platform speeds.

Analysis of the echoes for decorrelation effects due to the finite size of the tank is required. Ideally these should be compared with results obtained from open water and it is anticipated that open water trials will take place early in 1988. The system performance can then be analysed from a moving platform in an open expanse of water.

ACKNOWLEDGEMENTS

The authors would like to thank the UK Science and Engineering Research Council (SERC) and S.G. Brown Ltd for funding the research work.

REFERENCES

[1] F. R. Dickey, Jr., 'The Correlation Aircraft Navigator, a Vertically Beamed Doppler Radar', Proceedings of the National Conference on Aeronautical Electronics, 463-466, May 1958.

[2] D. G. Watts, 'A General Theory of Amplitude Quantization with Applications to Correlation Determination', Proceedings IEE, Vol.109, Part C, 209-218, (1962).

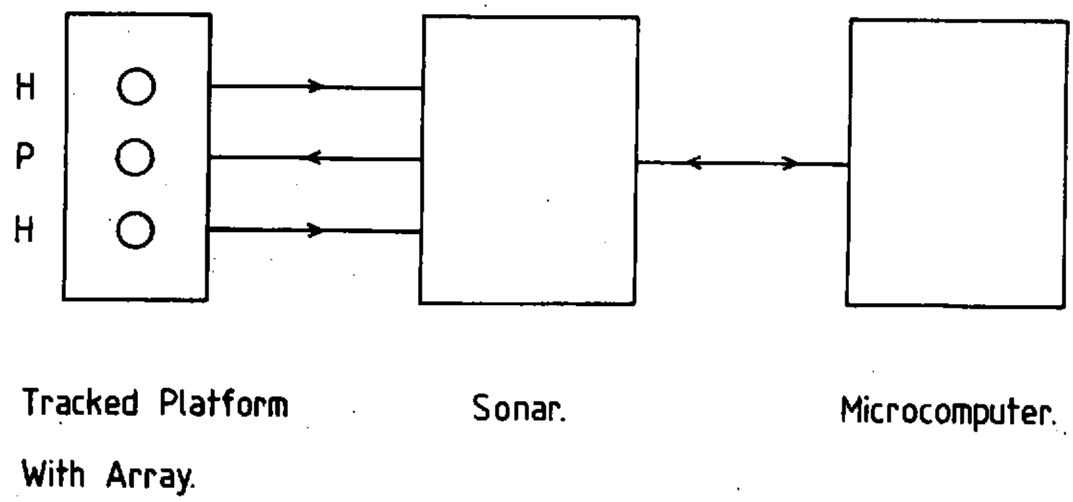

Figure 1 The System's Main Components.

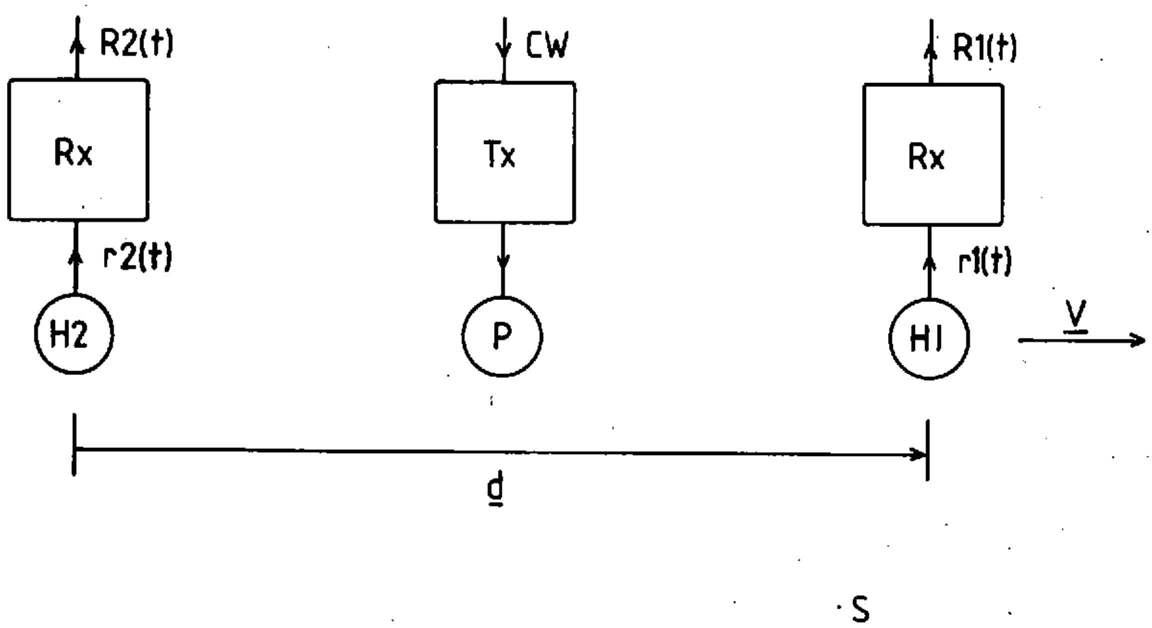

Figure 2 Array Geometry For Waveform Invariance.

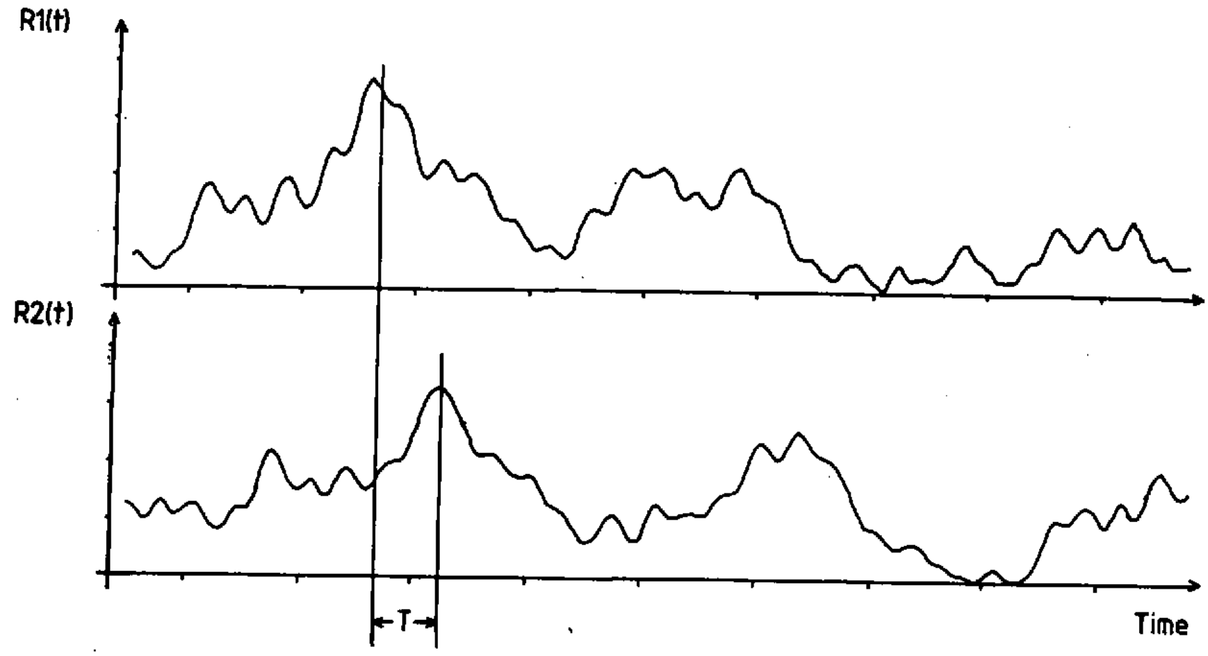

Figure 3 Typical Receiver Output Signals.

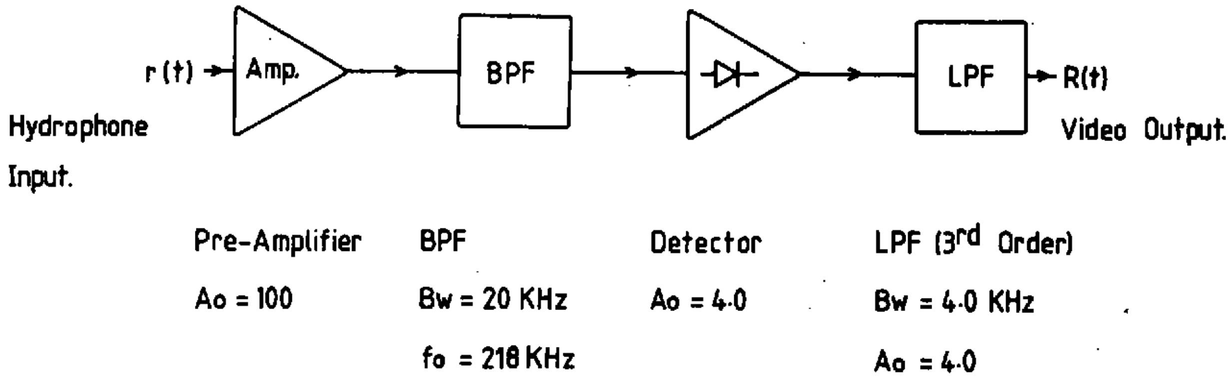

Figure 5 Receiver Block Diagram (One Channel).

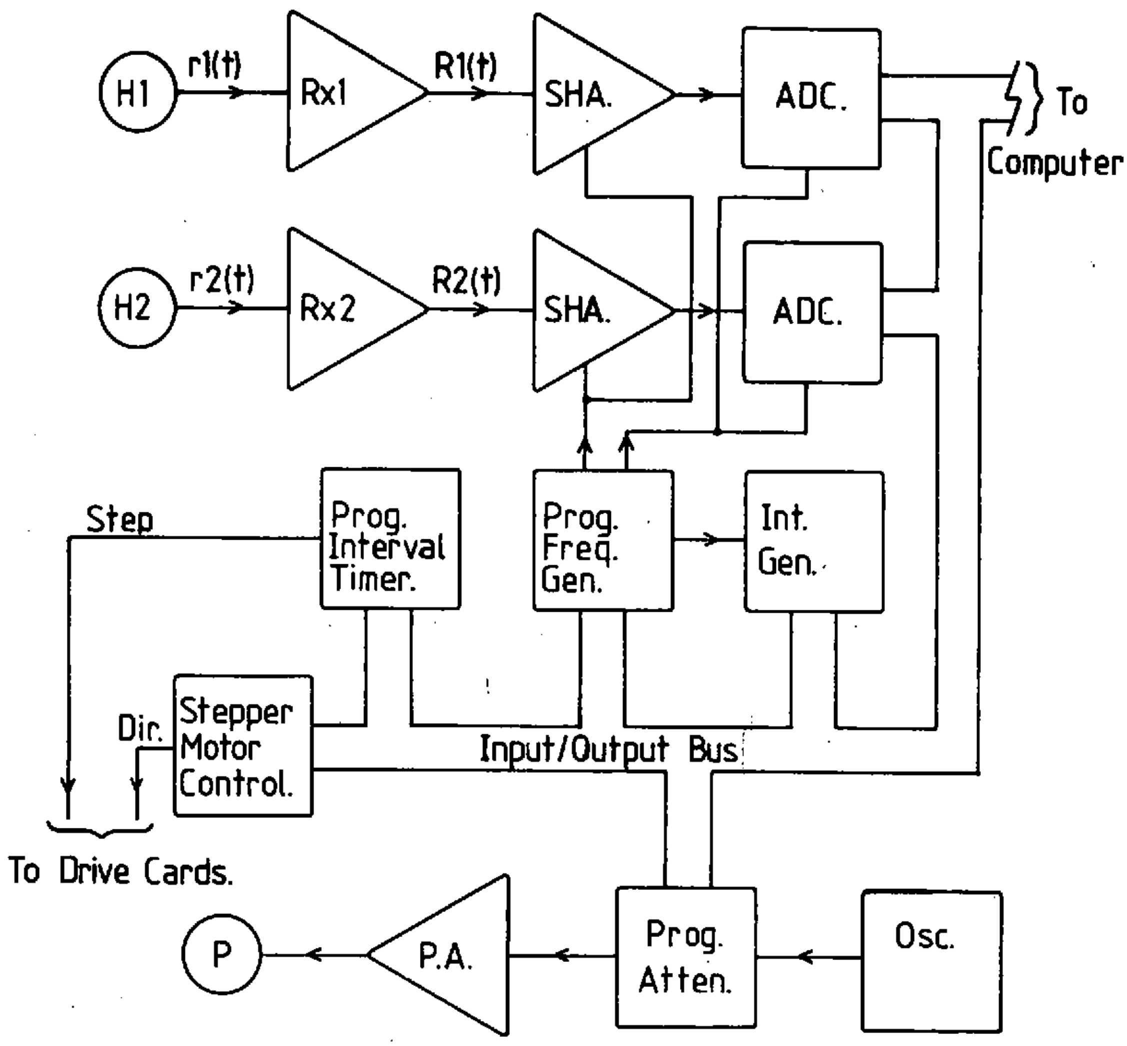

Figure 4 Sonar Block Diagram.

Author Index

List of Authors

P.R. Atkins
Department of Electronics and Electrical Engineering
University of Birmingham
P.O. Box 363
Birmingham
B15 2TT

S.C. Bateman
Dept. of Electronic and Electrical Engineering
University of Technology
Loughborough
Leicestershire
LE11 3TU

R. Coates
Electronic Engineering Sector
School of Information Systems
University of East Anglia
Norwich
NR4 7TJ

D.M.F. Chapman
Institute of Sound and Vibration Research
University of Southampton
Southampton SO9 5NH
(on loan from
Defence Research Establishment Atlantic
Nova Scotia
Canada)

H. Davidson
Department of Electrical and Electronic Engineering
University of Newcastle upon Tyne
Newcastle
NE1 7RU

R.M. Dunbar
Dept. of Electrical and Electronic Engineering
Heriot-Watt University
Edinburgh
EH1 2HT

A. Falahati
Dept. of Electronic and Electrical Engineering
University of Technology
Loughborough
Leicestershire
LE11 3TU

A.J. Fenwick
South West Scotland Computing Consultants Ltd
Lochnaw Workshop Centre
Lochnaw Castle
Leswalt-by-Stranraer
Wigtownshire
DG9 0RW

C. H. Flewellen
Institute of Oceanographic Sciences
Deacon Laboratory
Wormley
Godalming
Surrey

W. Forsythe
Dept. of Electronic and Electrical Engineering
University of Technology
Loughborough
Leicestershire
LE11 3TU

B.K. Gazey
Dept. of Electronic and Electrical Engineering
University of Birmingham
P.O. Box 363
Birmingham
B15 2TT

P.J. Hanna
Division of Chemical and Physical Sciences
Deakin University
Victoria 3217
Australia

S.K. Hole
Dept. of Electronic and Electrical Engineering
University of Technology
Loughborough
Leicestershire
LE11 3TU

A.G.J. Holt
Department of Electrical and Electronic Engineering
University of Newcastle upon Tyne
Newcastle
NE1 7RU

E. Hermanowicz
Telecommunication Institute
Technical University of Gdansk
ul. Majakowskiego 11/12
80-952 Gdansk
Poland

J. Jaffe
Woods Hole Oceanographic Institution
Woods Hole
MA 02543
USA

S.A.S. Jones
Thorn EMI Electronics Ltd
Naval Systems Division
Albert Drive
Sheerwater
Woking
Surrey
GU21 5RU

A.K.T. Lee
Department of Electrical Engineering and Electronics
University of Liverpool
P O Box 147
Liverpool
L69 3BX

J. Lucas
Department of Electrical Engineering and Electronics
University of Liverpool
P O Box 147
Liverpool L69 3BX

R.L. Mansfield
Dept. of Electronic and Electrical Engineering
University of Birmingham
P.O. Box 363
Birmingham
B15 2TT

P. Mullholland
Department of Electrical and Electronic Engineering
University of Newcastle upon Tyne
Newcastle
NE1 7RU

R.D. Peden
Division of Chemical and Physical Sciences
Deakin University
Victoria 3217
Australia

C.H. Rodbourne
Engineering Department
DBE Technology Group PLC
Eastern Road
Aldershot
Hampshire
GU12 4TD

M. Rojewski
Telecommunication Institute
Technical University of Gdansk
ul. Majakowskiego 11/12
80-952 Gdansk
Poland

G.H. Sandsmark
University of Trondheim
Norwegian Institute of Technology
N-7034 Trondheim
Norway

R.J. Sharp
Engineering Department
DBE Technology Group PLC
Eastern Road
Aldershot
Hampshire
GU12 4TD

B.V. Smith
Department of Electronic and Electrical Engineering
University of Birmingham
P.O. Box 363
Birmingham
B15 2TT

A. Solstad
Elektronikklaboratoriet ved NTH
N-7034 Trondheim
Norway

G.Vavik
Continental Shelf and Petroleum Technology Research A/S (IKU)
P.O. Box 1883
Jarlesletta
N-7001 Trondheim
Norway

L.E. Virr
Admiralty Research Establishment
Experimental Diving Unit, Vernon
Portsmouth
PO1 3ER

P. Walmsley
Thorn EMI Electronics Ltd
Naval Systems Division
Albert Drive, Sheerwater
Woking
Surrey
GU21 5RU

P.A. Willison
Electronic Engineering Sector
School of Information Systems
University of East Anglia
Norwich
NR4 7TJ

B. Woodward
Dept. of Electronic and Electrical Engineering
University of Technology, Loughborough
Leicestershire
LE11 3TU